Title: Resonant non-Gaussianity

Date: Mar 16, 2010 11:00 AM

URL: http://pirsa.org/10030037

Abstract: Two of the most exciting observables in the cosmic microwave background (CMB) radiation, which could deeply impact our picture of the early universe, are non-Gaussianity and tensor modes. A potential detection of tensor modes can be explained in terms of a model of large field inflation. Theoretical considerations suggest that a symmetry should be invoked in order to protect the flatness of the inflaton potential and hence an axion enjoying a shift symmetry is a natural candidate. As main example, I will present a model of inflation in string theory based on axion monodromy. Non-perturbative effects typically correct the axion potential leading to small sinusoidal modulations on top of an otherwise flat slow roll potential. It can be shown analytically that a resonance between the oscillations of the background and the oscillations of the curvature fluctuations is responsible for the production of an observably large non-Gaussian signal. An explicit expression for the shape of this resonant non-Gaussianity will be presented. There is essentially no overlap between this shape and the local, equilateral, and orthogonal shapes, and in fact resonant non-Gaussianity is not captured by the simplest version of the effective field theory of inflation. Hopefully the analytic expression for resonant non-Gaussianity will be useful to further observationally constrain this class of models.

Resonant non-Gaussianity

based on

Flauger & E.P.

arXiv:1002.0833 (hep-th)

and

Flauger, McAllister, E.P., Westphal & Xu

arXiv:0907.2916 (hep-th)

Enrico Pajer

Cornell University, Ithaca

Perimeter

Mar 2010

Outline

1. Motivations
2. The model: inflation from axion monodromy
3. Non-Gaussianity in the bispectrum
4. Summary and conclusions

Cosmological data

We are living in the golden age of observational cosmology:

Cosmological data

We are living in the golden age of observational cosmology: COBE goes to Stockholm,

Cosmological data

We are living in the golden age of observational cosmology: COBE goes to Stockholm, WMAP has measured the CMB with percent accuracy...

and now Planck: the satellite, launched on May 2009, finished the first full sky map (95%) on Feb 14th!

The picture emerging from the data

- Inflation does not solve the horizon and flatness problem but can arguably alleviate it. It provides a mechanism that shifts in the past the initial condition problem.

The picture emerging from the data

- Inflation does not solve the horizon and flatness problem but can arguably alleviate it. It provides a mechanism that shifts in the past the initial condition problem.
- Neverless it is a spectacular model to generate cosmological perturbations.
- So far the simplest models of inflation is compatible with the data [see e.g. WMAP7] , i.e. small, scale-invariant but slightly red tilted, Gaussian, adiabatic primordial curvature perturbations.

Exciting signatures in the sky

Obervables that could deeply impact our picture of the early universe:

- Tensor modes:

Exciting signatures in the sky

Obervables that could deeply impact our picture of the early universe:

- Tensor modes:
  - Detectable in the T anisotropies or in the polarization of the CMB. Current bound on the tensor-to-scalar ratio: $r < .20$ [WMAP7+SN] .
  - A detection would support inflation and determine the high scale (order GUT) where it took place.

Exciting signatures in the sky

Obervables that could deeply impact our picture of the early universe:

- Tensor modes:
  - Detectable in the T anisotropies or in the polarization of the CMB. Current bound on the tensor-to-scalar ratio: $r < .20$ [WMAP7+SN] .
  - A detection would support inflation and determine the high scale (order GUT) where it took place.
- non-Gaussianity:
  - Detectable e.g. in the three-point function of T perturbations. Current bounds are of the order a percent (shape dependent).
  - A detection would rule out the simplest class of models (a slowly rolling single canonically normalized field).

Tensor modes and the Lyth bound

- The detection of tensor modes, e.g. in the B-mode polarization, would fix the scale of inflation close to the GUT scale.

Tensor modes and the Lyth bound

- The detection of tensor modes, e.g. in the B-mode polarization, would fix the scale of inflation close to the GUT scale.
- Measuring tensor modes puts a lower bound on the range of variation of the inflaton [Lyth 98]

$$\frac{\Delta\phi}{M_{pl}} > \sqrt{\frac{r}{0.01}}$$

Tensor modes and the Lyth bound

- The detection of tensor modes, e.g. in the B-mode polarization, would fix the scale of inflation close to the GUT scale.
- Measuring tensor modes puts a lower bound on the range of variation of the inflaton [Lyth 98]

$$\frac{\Delta\phi}{M_{pl}} > \sqrt{\frac{r}{0.01}}$$

- In a fundamental theory a flat potential over a superplanckian distance is hard to control, e.g. η-problem.

Tensor modes and the Lyth bound

- The detection of tensor modes, e.g. in the B-mode polarization, would fix the scale of inflation close to the GUT scale.
- Measuring tensor modes puts a lower bound on the range of variation of the inflaton [Lyth 98]

$$\frac{\Delta\phi}{M_{pl}} > \sqrt{\frac{r}{0.01}}$$

- In a fundamental theory a flat potential over a superplanckian distance is hard to control, e.g. η-problem.
- This is the main motivation to consider axion monodromy inflation

Schematically

Tensor modes	$\Rightarrow$	High scale	$\Rightarrow$	Large field	$\Rightarrow$	more UV-sensitive

UV-sensitivity

- EFT approach: learn about higher scales studying UV-sensitive observables.

UV-sensitivity

- EFT approach: learn about higher scales studying UV-sensitive observables.

UV-sensitivity

- EFT approach: learn about higher scales studying UV-sensitive observables.
- Inflation is a UV-sensitive mechanism. Schematically

$$V(\phi) = \frac{1}{2}m^2\phi^2 + \sum_n \lambda_n \frac{\phi^n}{M_{pl}^{n-4}}$$

UV-sensitivity

- EFT approach: learn about higher scales studying UV-sensitive observables.
- Inflation is a UV-sensitive mechanism. Schematically

$$V(\phi) = \frac{1}{2}m^2\phi^2 + \sum_n \lambda_n \frac{\phi^n}{M_{pl}^{n-4}}$$

- Within string theory and supergravity many models suffer from an η-problem.

UV-sensitivity

- EFT approach: learn about higher scales studying UV-sensitive observables.
- Inflation is a UV-sensitive mechanism. Schematically

$$V(\phi) = \frac{1}{2}m^2\phi^2 + \sum_n \lambda_n \frac{\phi^n}{M_{pl}^{n-4}}$$

- Within string theory and supergravity many models suffer from an η-problem.
- We need to invoke a symmetry, e.g. shift symmetry.

Axion monodromy

Two difficulties for large field models in a UV theory

- Space: $\Delta\phi > M_{pl}$ is often impossible (e.g. brane inflation)

Axion monodromy

Two difficulties for large field models in a UV theory

- Space: $\Delta\phi > M_{pl}$ is often impossible (e.g. brane inflation)
- Flatness: $\epsilon, \eta \ll 1$ is rare (e.g. η problem)

Axion monodromy

Two difficulties for large field models in a UV theory

- Space: $\Delta\phi > M_{pl}$ is often impossible (e.g. brane inflation)
- Flatness: $\epsilon, \eta \ll 1$ is rare (e.g. η problem)

Axion monodromy addresses both [(Silverstein & Westphal)(1+McAllister)]

- Invoke a shift symmetry on a "angular" field

Axion monodromy

Two difficulties for large field models in a UV theory

- Space: $\Delta\phi > M_{pl}$ is often impossible (e.g. brane inflation)
- Flatness: $\epsilon, \eta \ll 1$ is rare (e.g. η problem)

Axion monodromy addresses both [(Silverstein & Westphal)(1+McAllister)]

- Invoke a shift symmetry on a "angular" field
- The symmetry is broken in a controlled way inducing a monodromy.

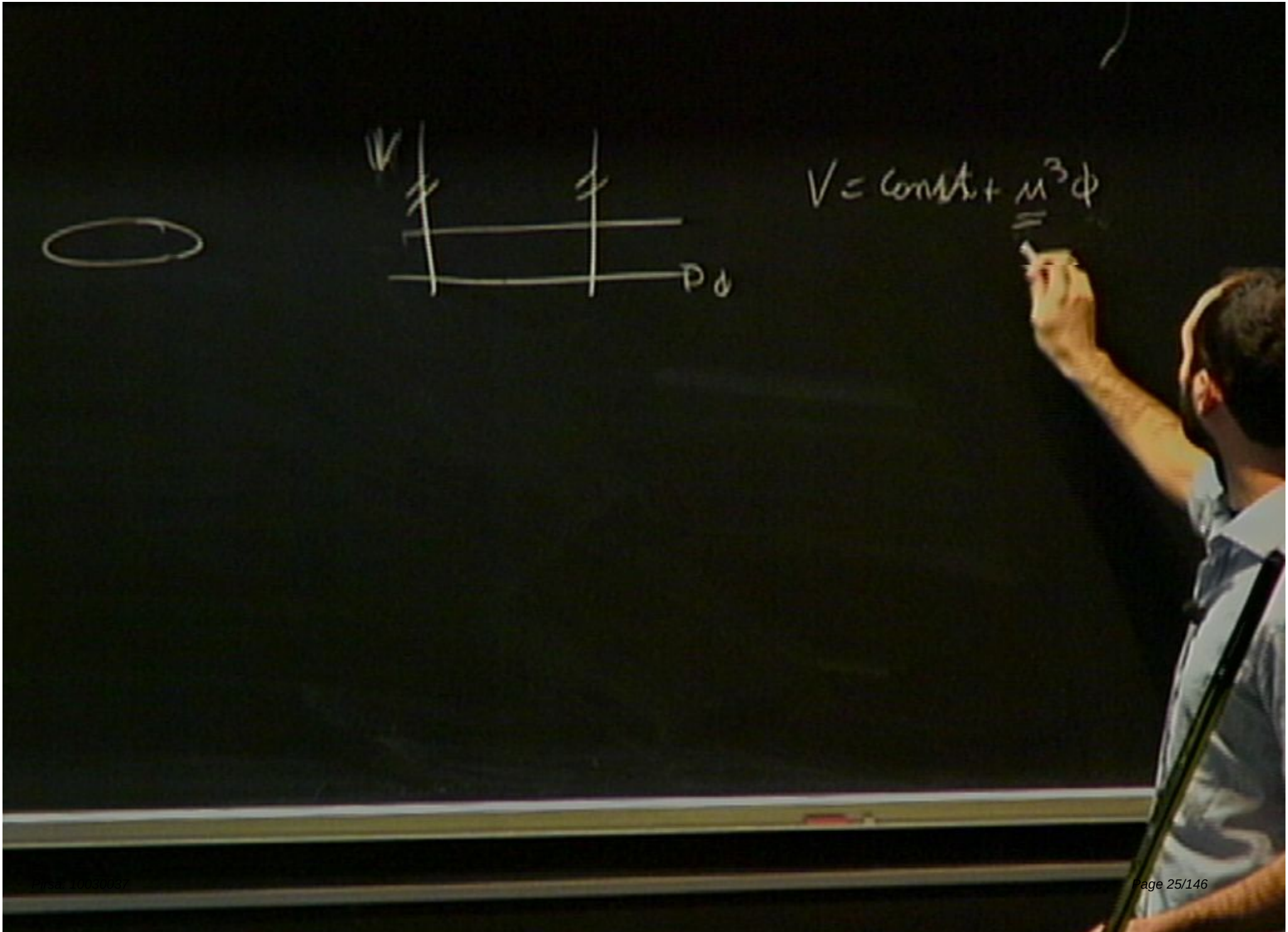
V
ϕ
$V = \text{const.} + \mu^3 \phi$

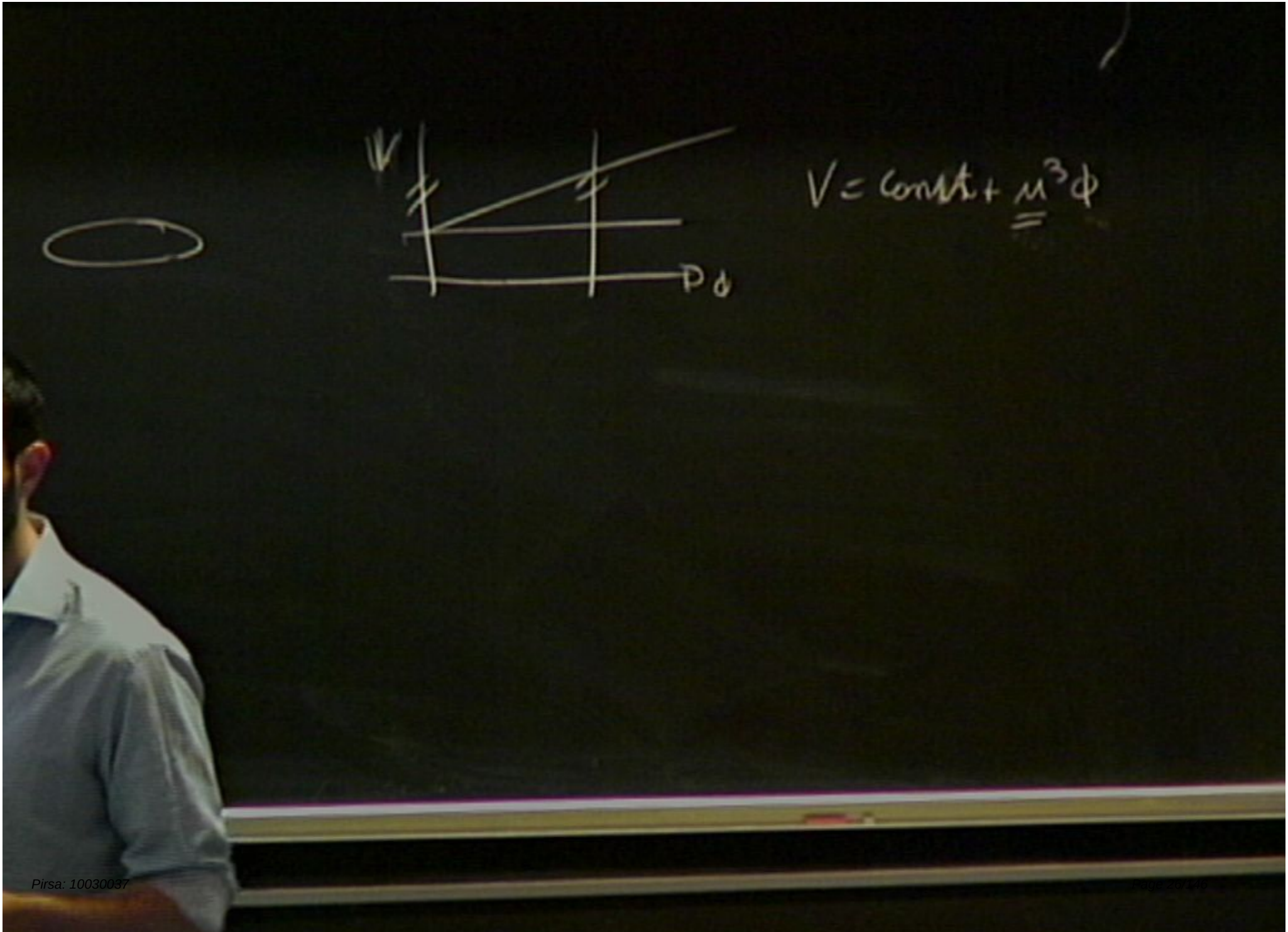

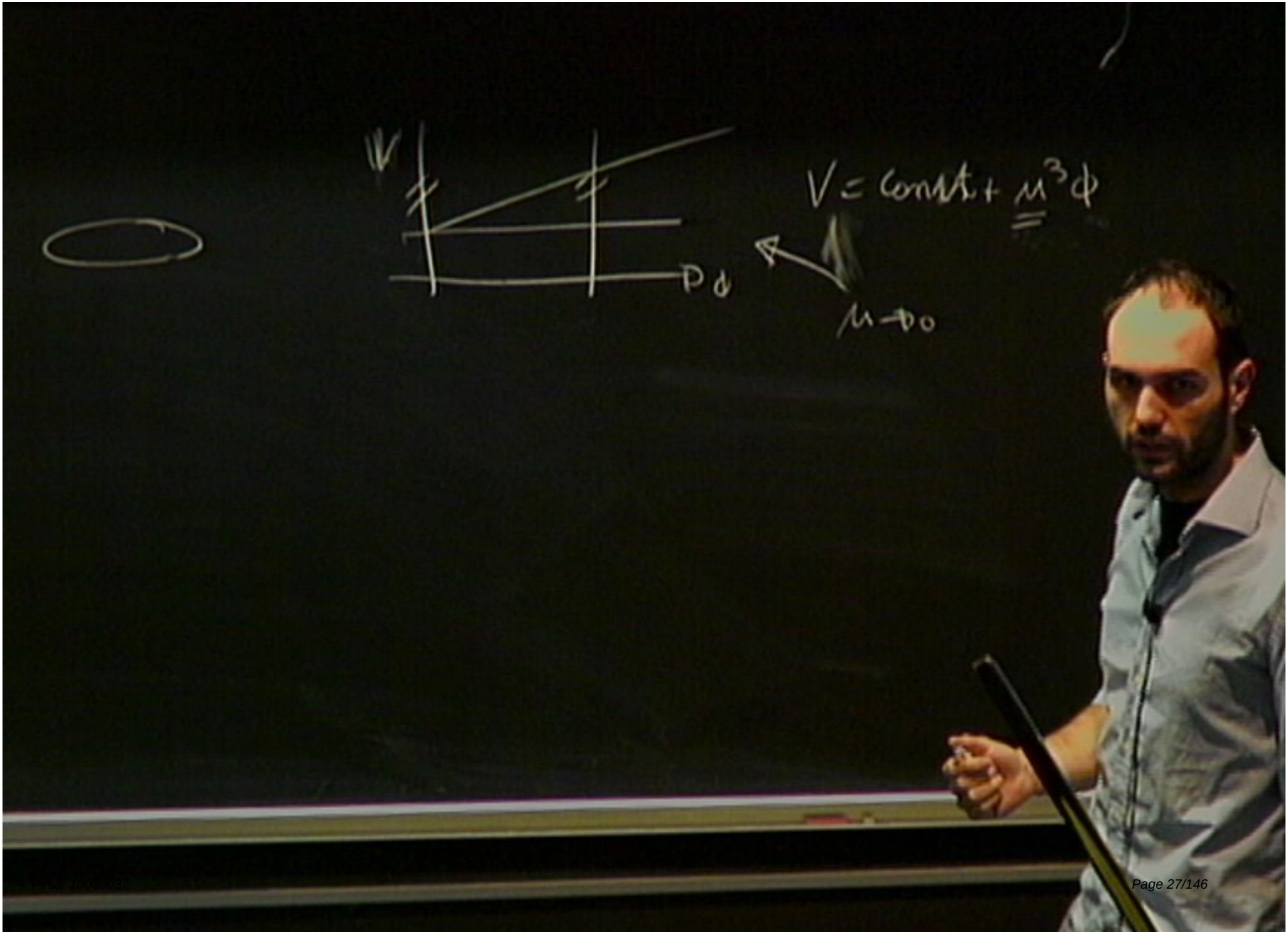
V
ϕ_0
$V = \text{const.} + \mu^3 \phi$
$\mu \to 0$

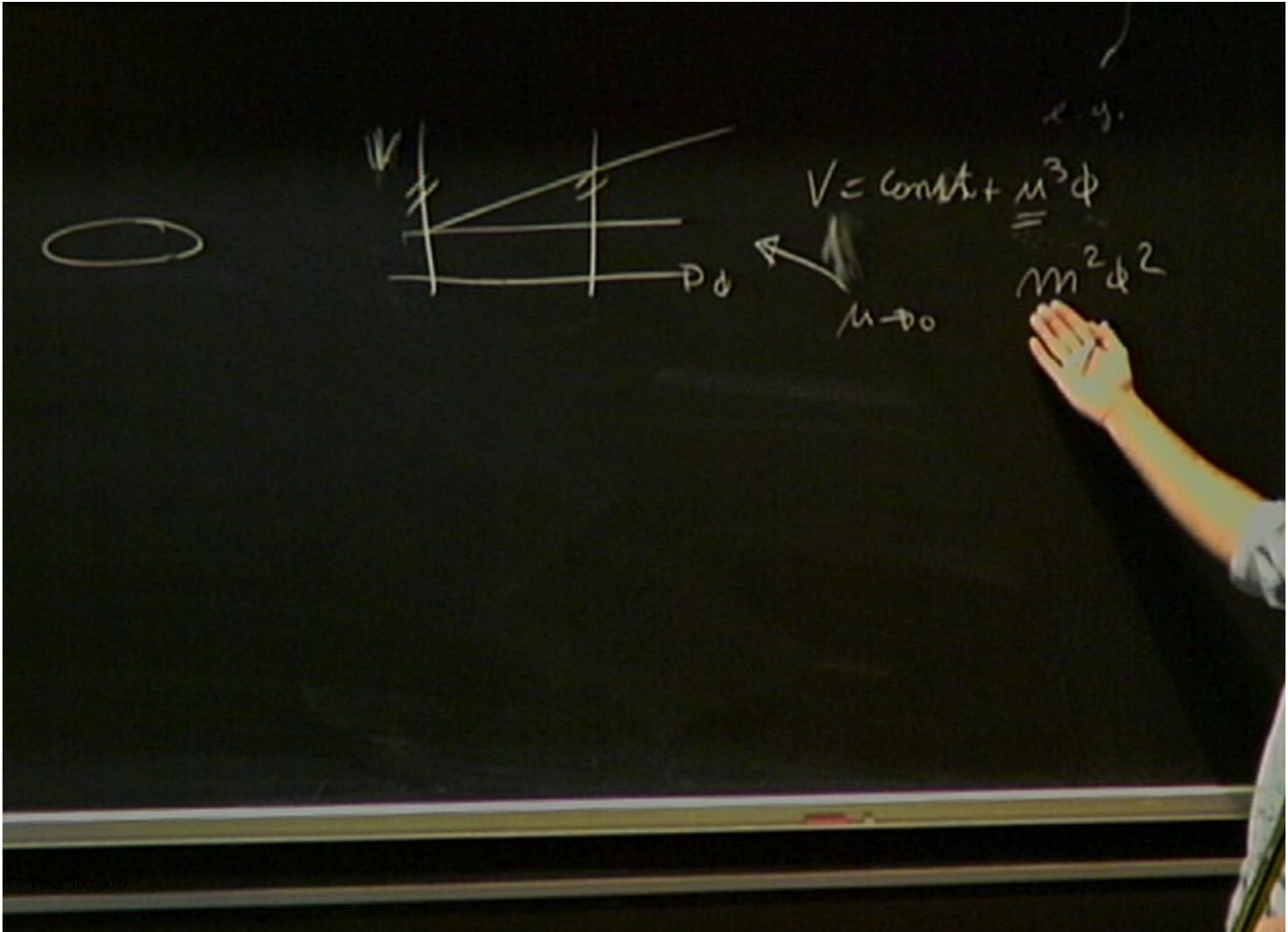
V
ϕ_0
$V = \text{Const.} + \mu^3\phi$
$\mu \to 0$
$m^2\phi^2$

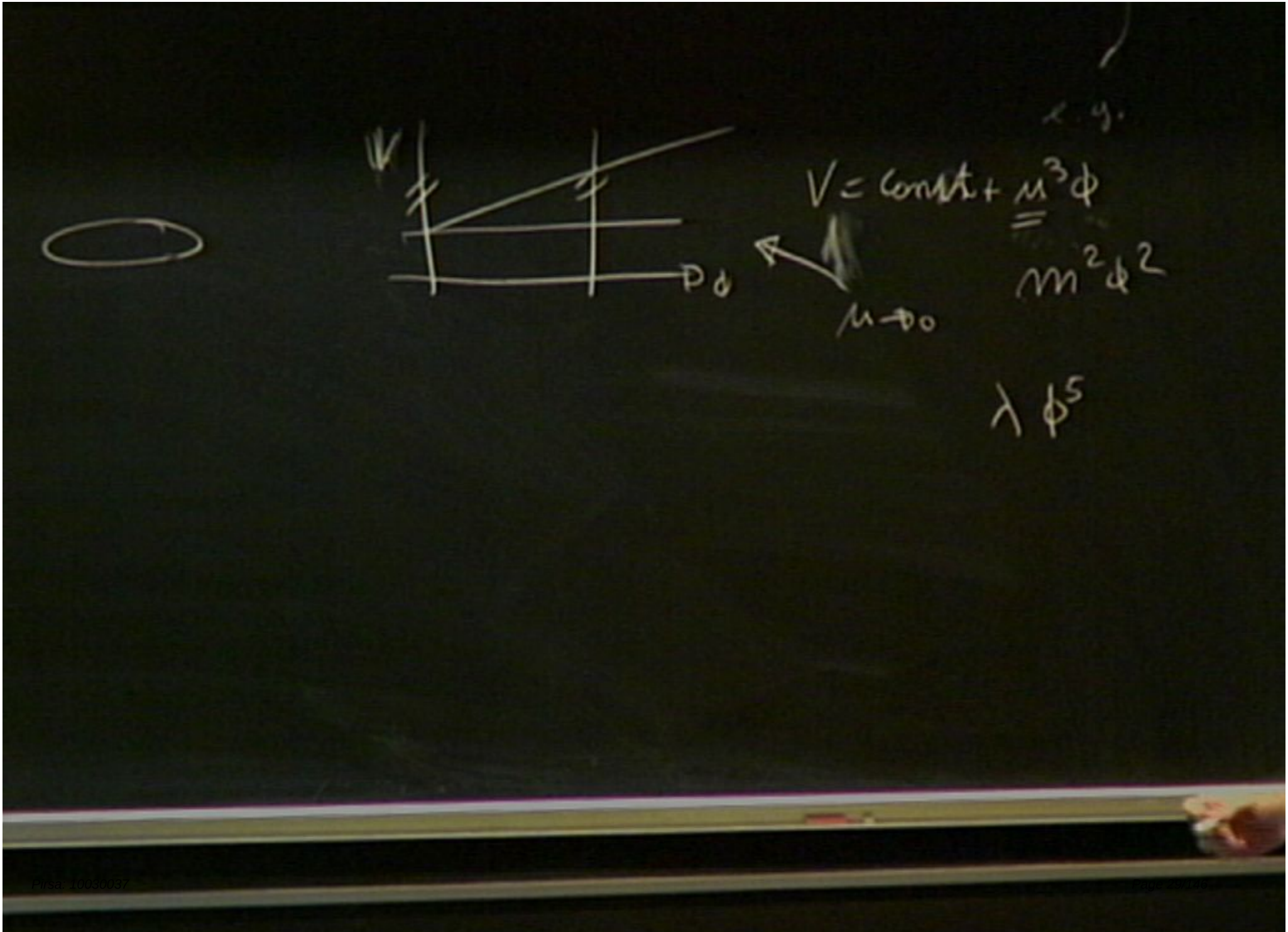

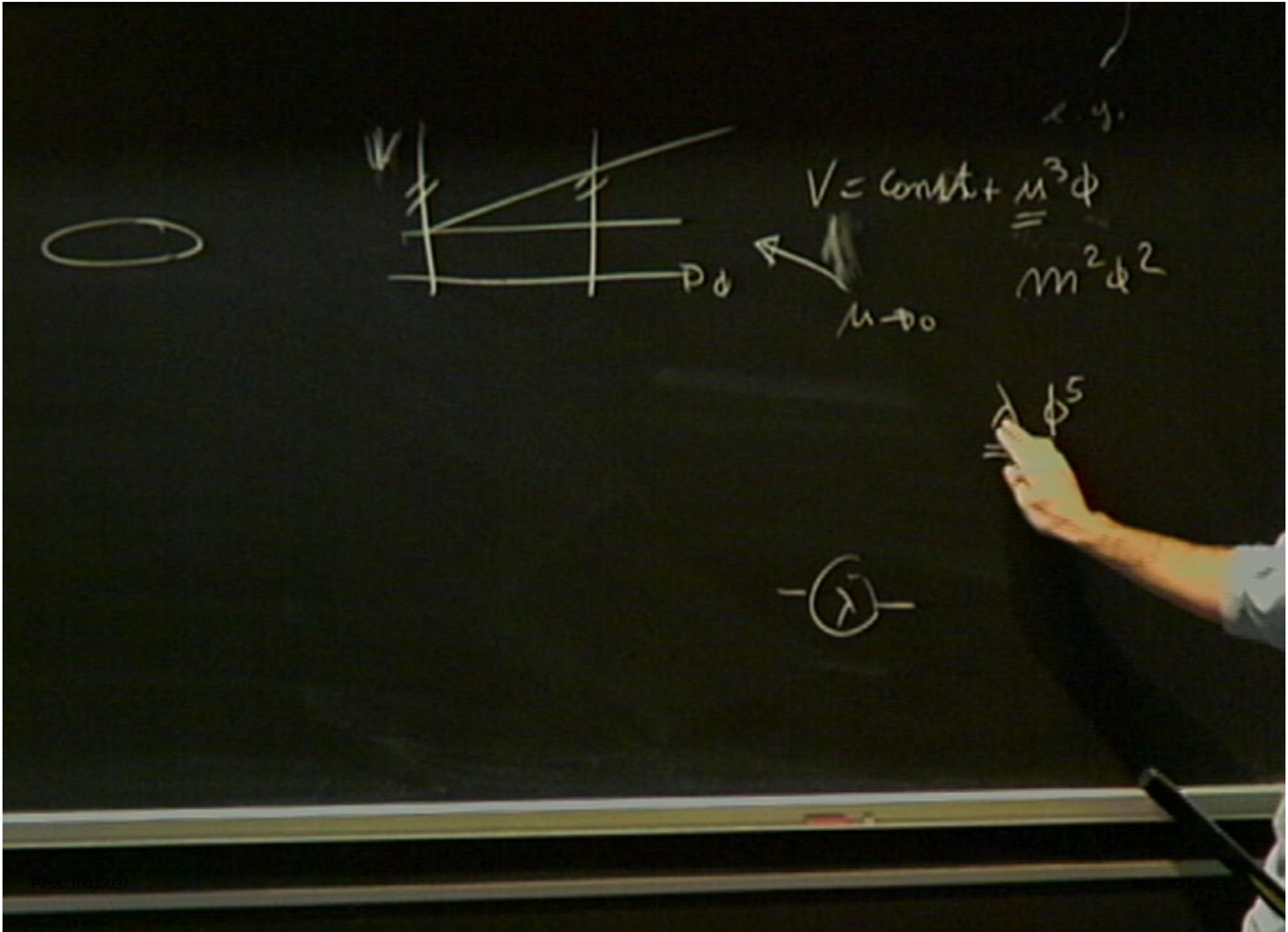
V
ϕ_0
$V = \text{Const.} + \mu^3 \phi$
$\mu \to 0$
$m^2 \phi^2$
$\lambda \phi^5$
λ

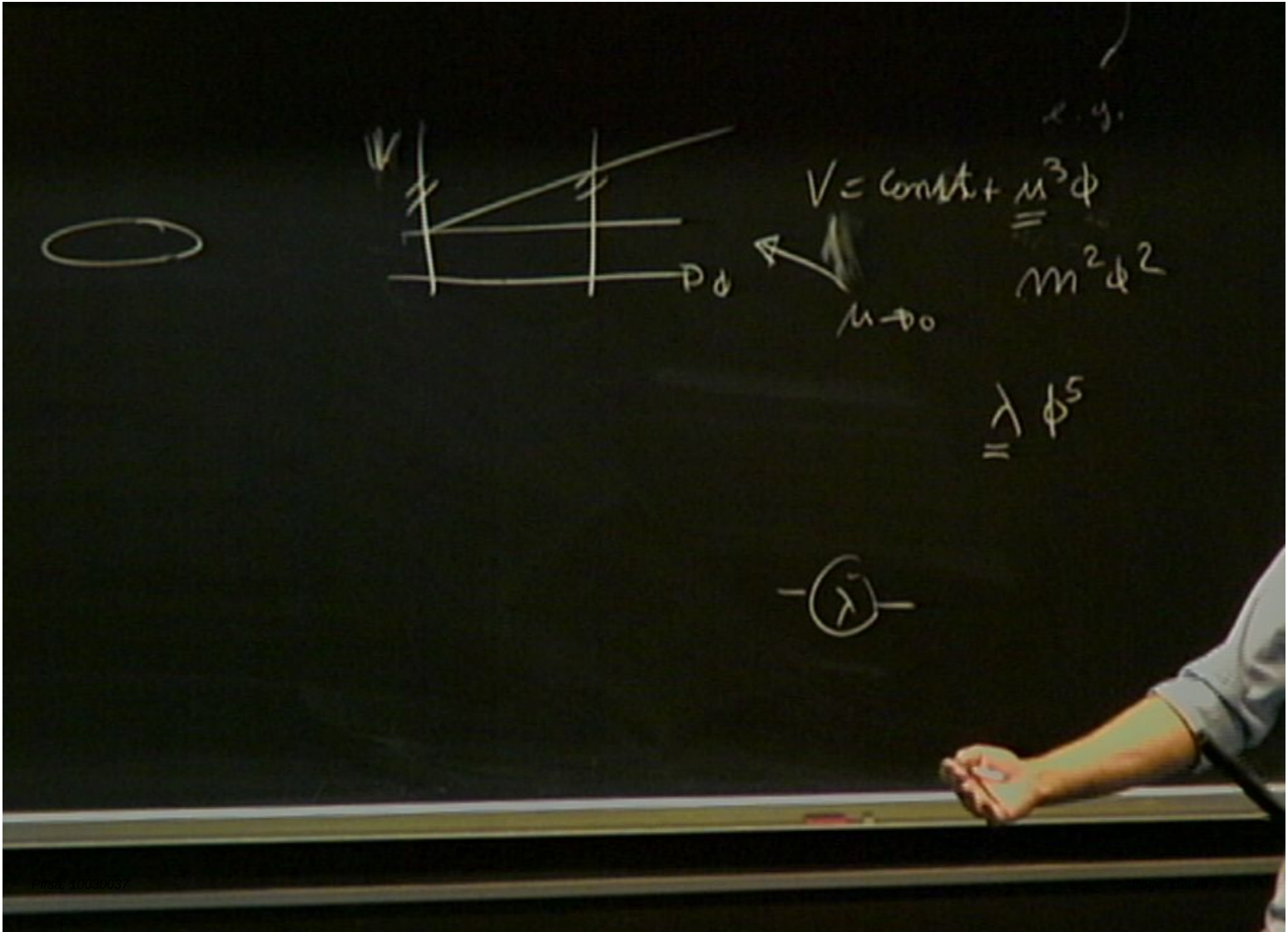
V
ϕ_0
$V = \text{Const.} + \mu^3 \phi$
$= m^2 \phi^2$
$\mu \to 0$
$= \lambda \phi^5$
λ

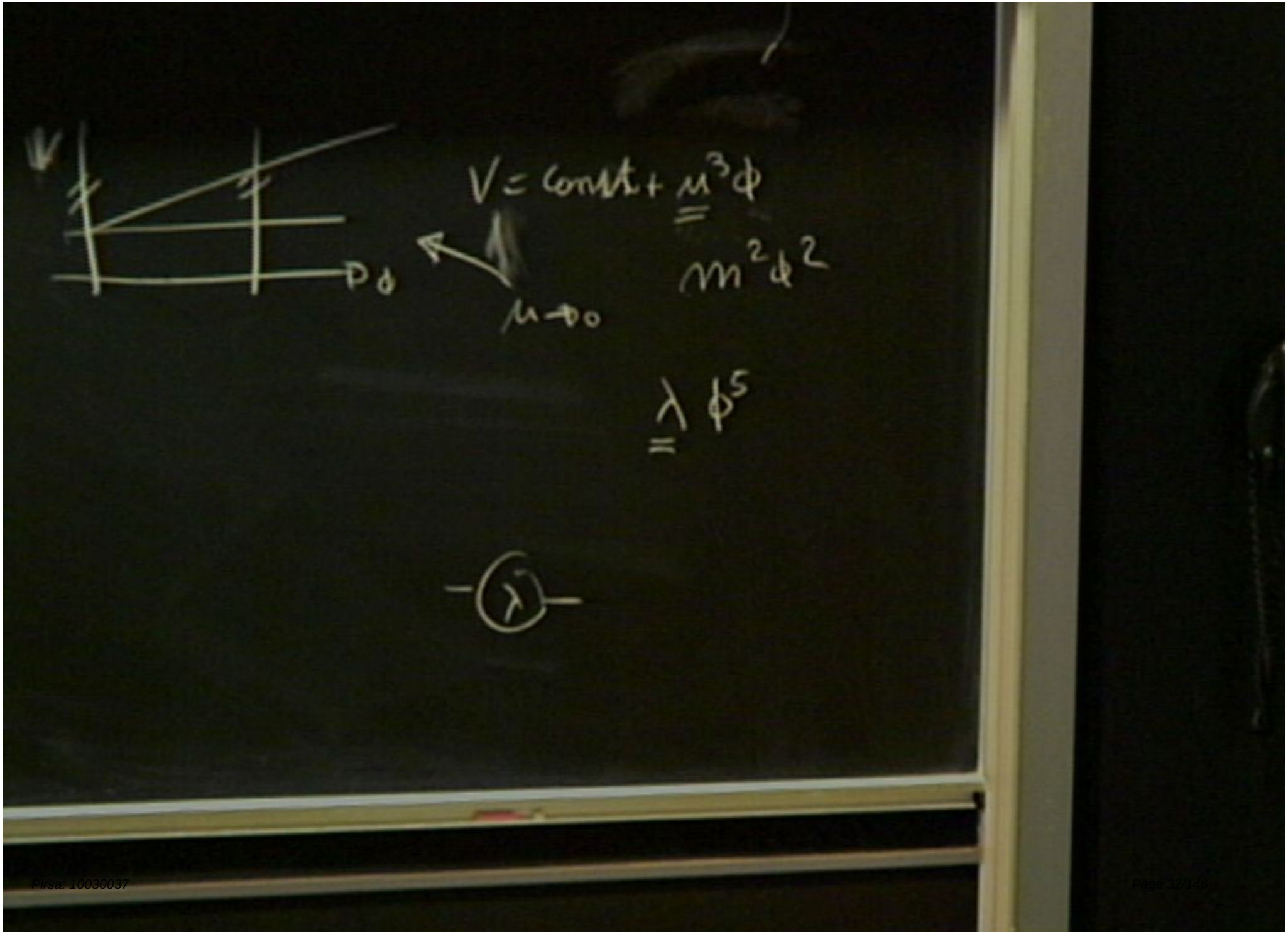
V
ϕ_0
$V = \text{const} + \mu^3 \phi$
$\mu \to 0$
$m^2 \phi^2$
$\lambda \phi^5$
λ

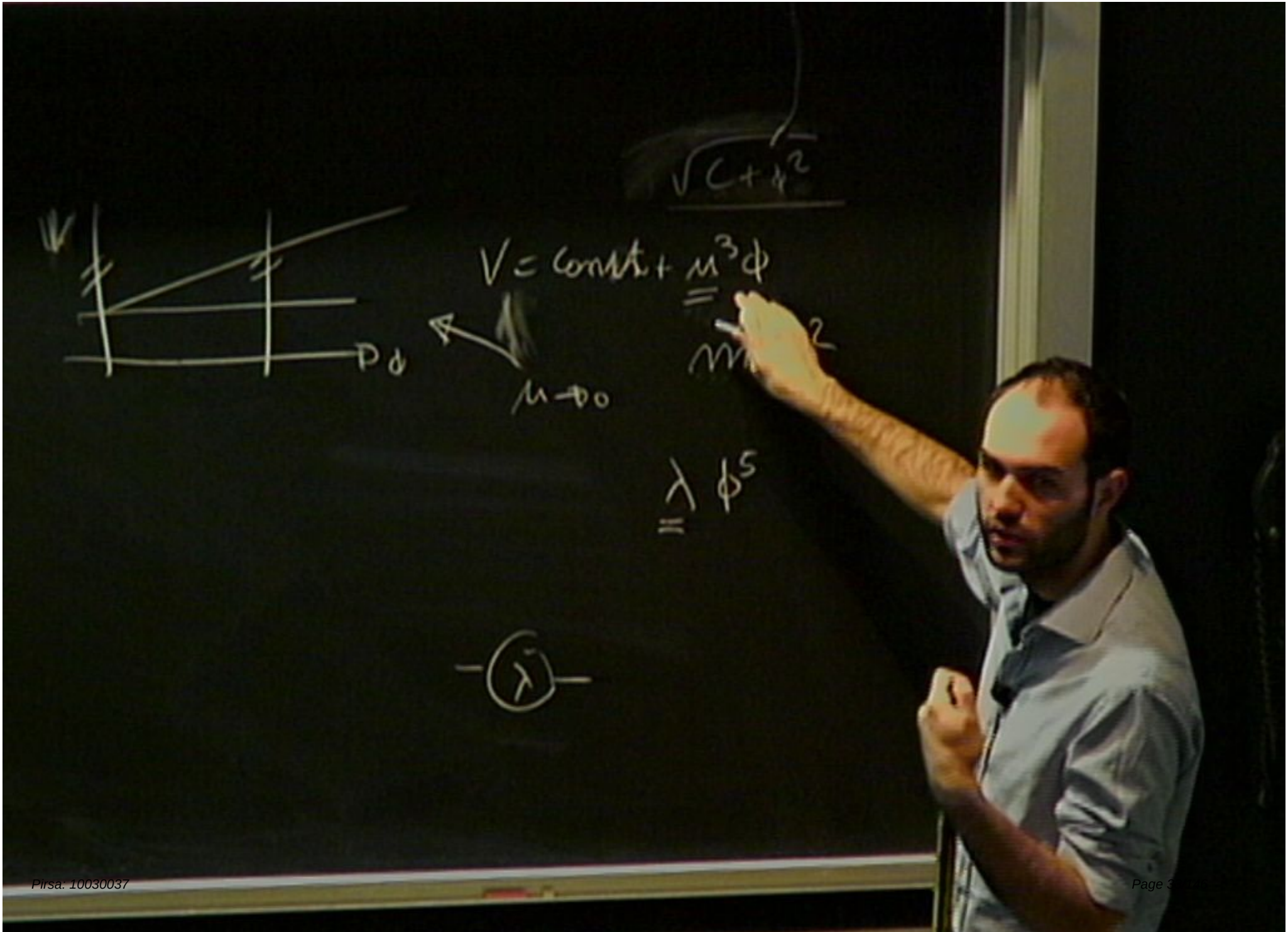
$\sqrt{C+\phi^2}$
$V = \text{const.} + \mu^3\phi$
$= \lambda\phi^5$
$\mu \to 0$
λ

Axion monodromy

Two difficulties for large field models in a UV theory

- Space: $\Delta\phi > M_{pl}$ is often impossible (e.g. brane inflation)
- Flatness: $\epsilon, \eta \ll 1$ is rare (e.g. η problem)

Axion monodromy addresses both [(Silverstein & Westphal)(1+McAllister)]

- Invoke a shift symmetry on a "angular" field
- The symmetry is broken in a controlled way inducing a monodromy.
- This enlarges the field space and provides the potential for inflation.

Generically non-perturbative effects generate modulations.

Axions in field theory

- Axions are scalar fields with only derivative couplings and might arise e.g. from the breaking of a $U(1)$ symmetry [Peccei & Quinn 77]
- They enjoy a continuous shift symmetry at all orders in perturbation theory

$$\phi(x) \to \phi(x) + \text{constant}$$

Axion in string theory

String theory seen from a low energy 4D observer has in general many axions:

- Model independent axions, e.g. dualizing $B_{\mu\nu}$ or $C_{\mu\nu}$. Model dependent axions from integrating a p-form over a p-cycle of the compact manifold

Axion in string theory

String theory seen from a low energy 4D observer has in general many axions:

- Model independent axions, e.g. dualizing $B_{\mu\nu}$ or $C_{\mu\nu}$. Model dependent axions from integrating a p-form over a p-cycle of the compact manifold

Axion in string theory

String theory seen from a low energy 4D observer has in general many axions:

- Model independent axions, e.g. dualizing $B_{\mu\nu}$ or $C_{\mu\nu}$. Model dependent axions from integrating a p-form over a p-cycle of the compact manifold.
- The shift symmetry is valid at all order in perturbation theory so it can ensure the flatness of the inflaton potential.
- The shift symmetry is broken non-perturbatively, e.g by world-sheet or brane instantons. Periodic modulations.

Axion in string theory

String theory seen from a low energy 4D observer has in general many axions:

- Model independent axions, e.g. dualizing $B_{\mu\nu}$ or $C_{\mu\nu}$. Model dependent axions from integrating a p-form over a p-cycle of the compact manifold.
- The shift symmetry is valid at all order in perturbation theory so it can ensure the flatness of the inflaton potential.
- The shift symmetry is broken non-perturbatively, e.g by world-sheet or brane instantons. Periodic modulations.

Modulation are generic

Flat potential $\Rightarrow$ Shift symmetry $\Rightarrow$ Axions $\Rightarrow$ non-perturbative modulations

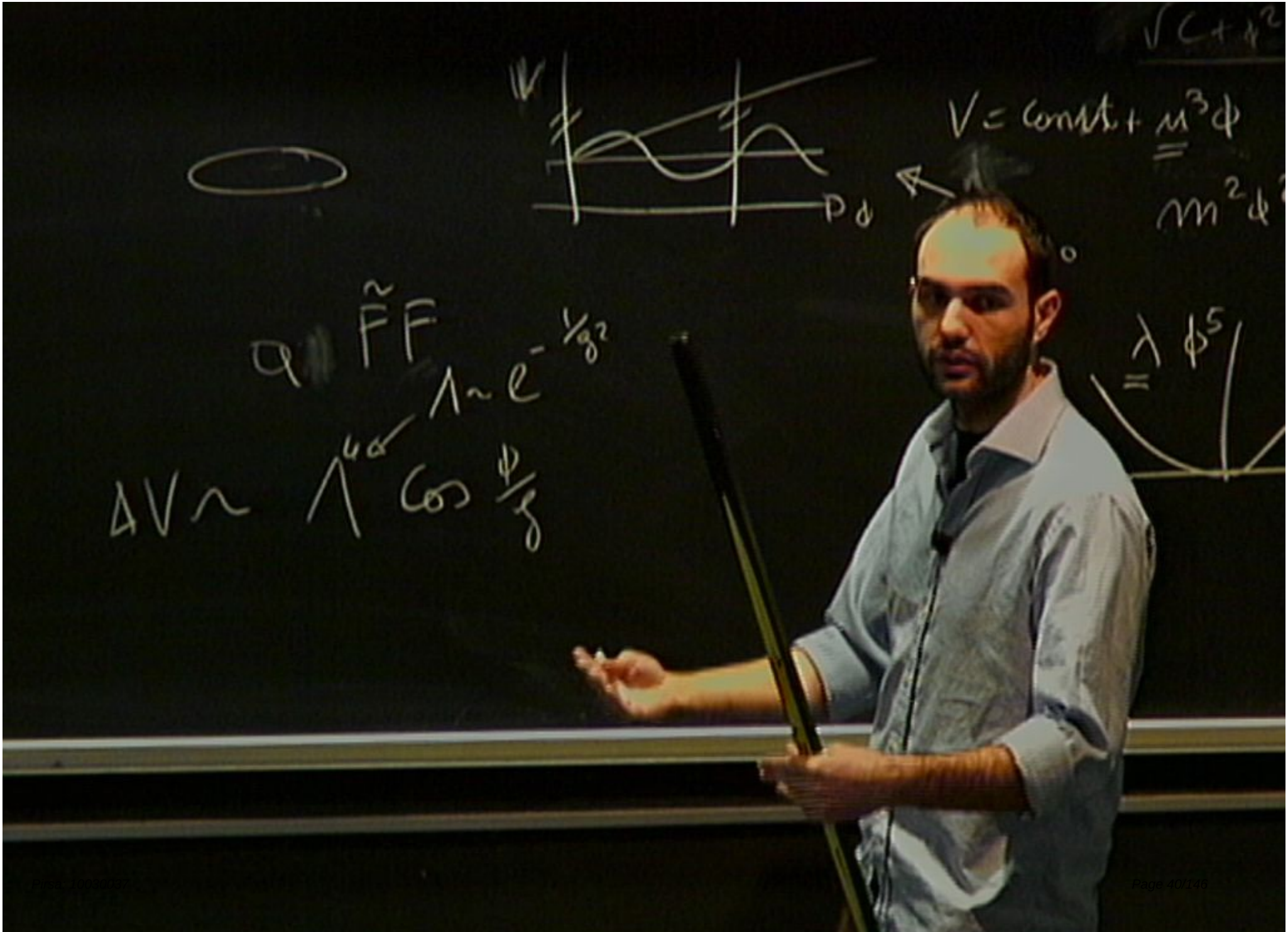
V
p_ϕ
$V = \text{const.} + \mu^3 \phi$
$m^2 \phi^2$
$\lambda \phi^5$
$\tilde{F}F$
$\Lambda \sim e^{-1/g^2}$
$\Delta V \sim \Lambda^4 \cos \frac{\phi}{f}$

A cartoon of the model

We consider Type IIB (orientifolds) because moduli stabilization is more developed.

- In the $N = 1$, 4D effective theory there is an axion $c(x)$ coming from 10D C_2 integrated over a two-cycle Σ_2
- Wrapping a 5-brane over Σ_2 induces a potential for $c(x)$ (world-sheets with boundary).

A cartoon of the model

We consider Type IIB (orientifolds) because moduli stabilization is more developed.

- In the $N = 1$, 4D effective theory there is an axion $c(x)$ coming from 10D C_2 integrated over a two-cycle Σ_2
- Wrapping a 5-brane over Σ_2 induces a potential for $c(x)$ (world-sheets with boundary).

A cartoon of the model

We consider Type IIB (orientifolds) because moduli stabilization is more developed.

- In the $N = 1$, 4D effective theory there is an axion $c(x)$ coming from 10D C_2 integrated over a two-cycle Σ_2
- Wrapping a 5-brane over Σ_2 induces a potential for $c(x)$ (world-sheets with boundary).
- If the 5-brane is a warped region, the potential leads to viable inflation (COBE normalization)
- The moduli stabilization á la KKLT does not spoil the shift symmetry.

Linear potential for the inflaton

The shift symmetry can be broken in the presence of boundaries.

Consider a D5-brane wrapped on a two-cycle Σ.
The DBI action

$$-T_5 \int d^6x e^{-\Phi} \sqrt{\det\left(G^{ind} + B^{ind}\right)}$$

Linear potential for the inflaton

The shift symmetry can be broken in the presence of boundaries.

Consider a D5-brane wrapped on a two-cycle Σ.
The DBI action

$$-T_5 \int d^6x e^{-\Phi} \sqrt{\det\left(G^{ind} + B^{ind}\right)}$$

The shift $a(x) \to a(x) + \text{const}$ of $a(x) = \int_\Sigma B_2$ stores some potential energy.

$$V(b) = T_5 \sqrt{L^4 + a^2} \sim T_5 a \quad \text{for large } a$$

This generates the linear inflaton potential (and break SUSY). COBE normalization and control require to red-shift T_5

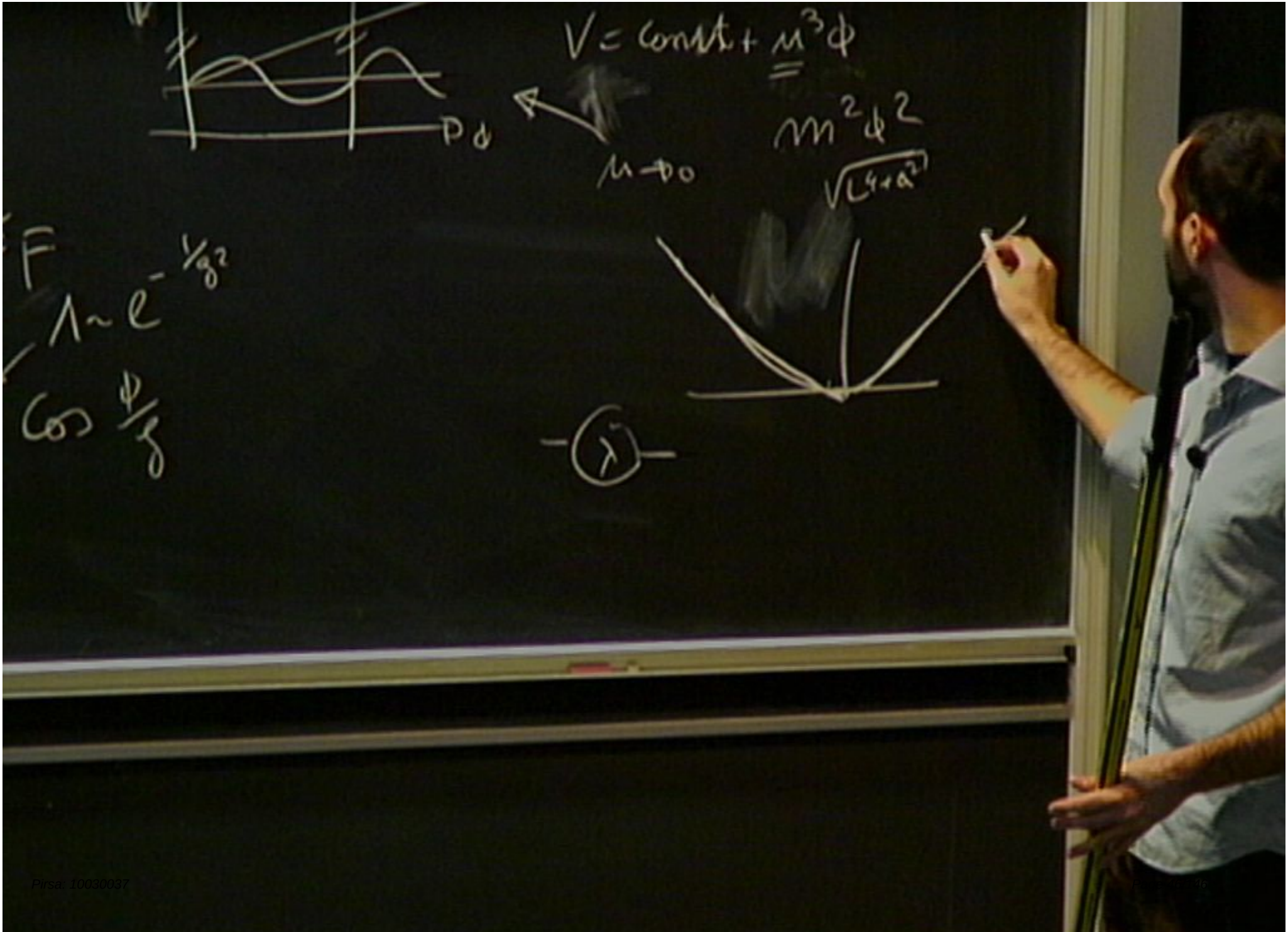

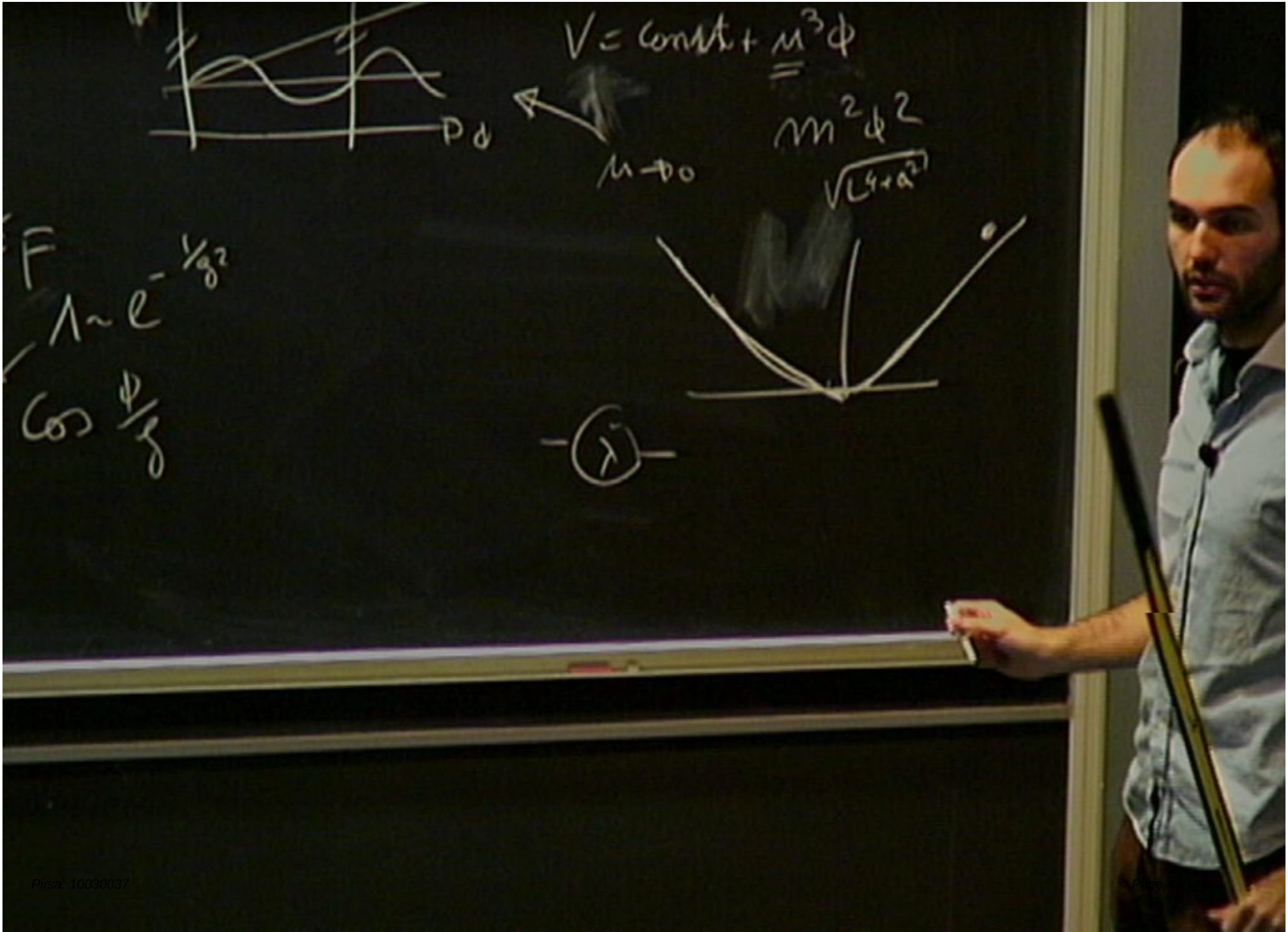
V = Const. + μ³ φ
m² φ²
μ → 0
λ

Linear potential for the inflaton

The shift symmetry can be broken in the presence of boundaries.

Consider a D5-brane wrapped on a two-cycle Σ.
The DBI action

$$-T_5 \int d^6x e^{-\Phi} \sqrt{\det\left(G^{ind} + B^{ind}\right)}$$

The shift $a(x) \to a(x) + \text{const}$ of $a(x) = \int_\Sigma B_2$ stores some potential energy.

$$V(b) = T_5 \sqrt{L^4 + a^2} \sim T_5 a \quad \text{for large } a$$

This generates the linear inflaton potential (and break SUSY). COBE normalization and control require to red-shift T_5

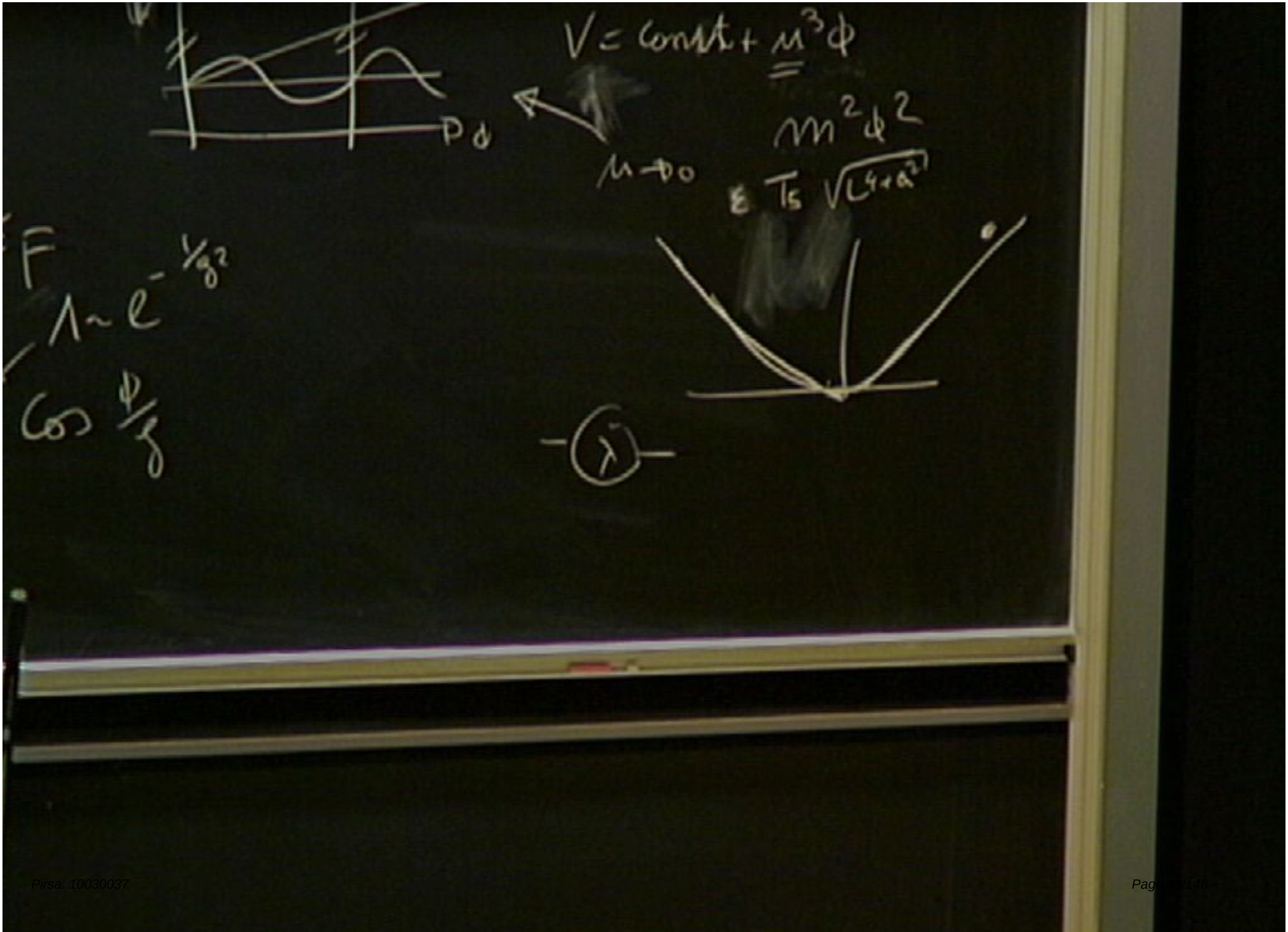
V = const + μ³φ
m²φ²
μ→0
F
Λ ~ e^{-1/g²}
cos φ/g
λ

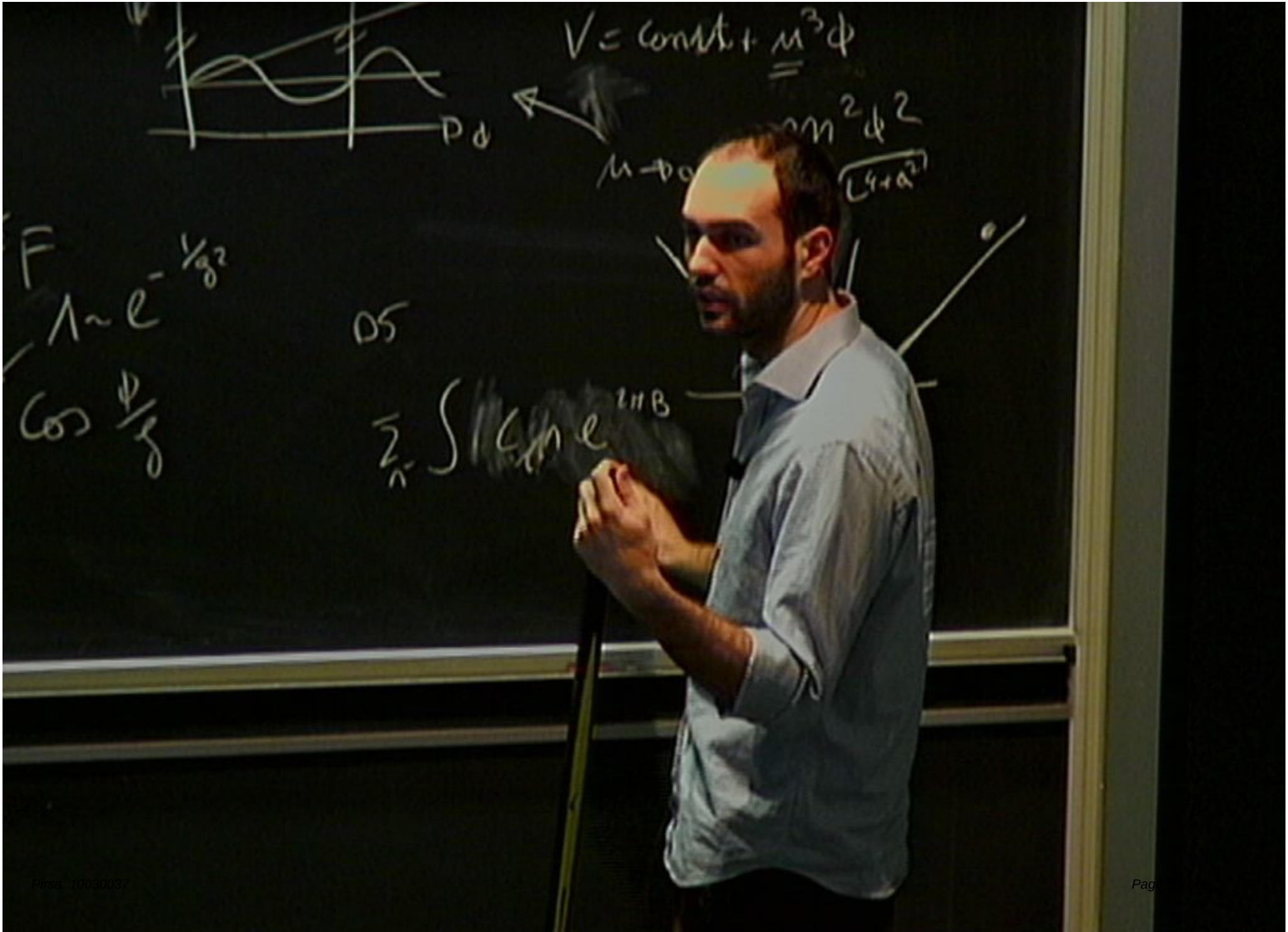
V = Const. + m³ φ
Pd
05

Linear potential for the inflaton

The shift symmetry can be broken in the presence of boundaries.

Consider a D5-brane wrapped on a two-cycle Σ.
The DBI action

$$-T_5 \int d^6x e^{-\Phi} \sqrt{\det\left(G^{ind} + B^{ind}\right)}$$

The shift $a(x) \to a(x) + \text{const}$ of $a(x) = \int_\Sigma B_2$ stores some potential energy.

$$V(b) = T_5 \sqrt{L^4 + a^2} \sim T_5 a \quad \text{for large } a$$

This generates the linear inflaton potential (and break SUSY). COBE normalization and control require to red-shift T_5

The effective potential

Inflation is driven by a real scalar field with potential

$$V(\phi) = \mu^3 \phi + b\mu^3 f \cos\left(\frac{\phi}{f}\right)$$

Linear potential for the inflaton

The shift symmetry can be broken in the presence of boundaries.

Consider a D5-brane wrapped on a two-cycle Σ.
The DBI action

$$-T_5 \int d^6x e^{-\Phi} \sqrt{\det\left(G^{ind} + B^{ind}\right)}$$

The shift $a(x) \to a(x) + \text{const}$ of $a(x) = \int_\Sigma B_2$ stores some potential energy.

$$V(b) = T_5 \sqrt{L^4 + a^2} \sim T_5 a \quad \text{for large } a$$

This generates the linear inflaton potential (and break SUSY). COBE normalization and control require to red-shift T_5

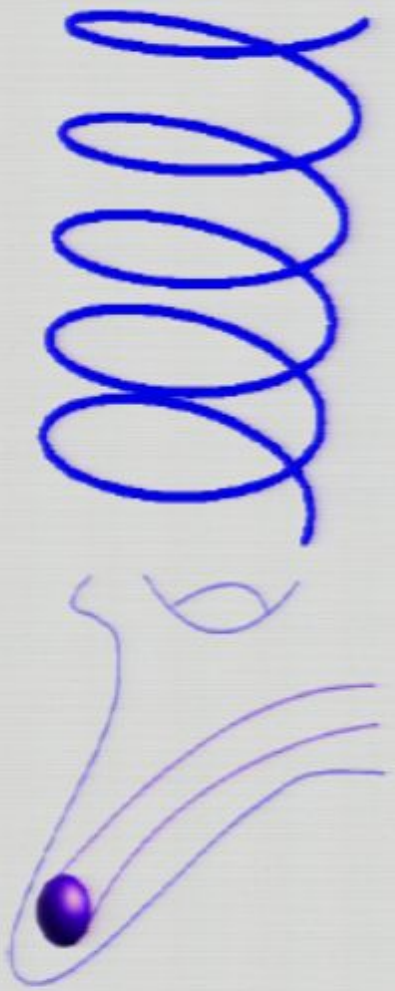

The effective potential

Inflation is driven by a real scalar field with potential

$$V(\phi) = \mu^3 \phi + b\mu^3 f \cos\left(\frac{\phi}{f}\right)$$

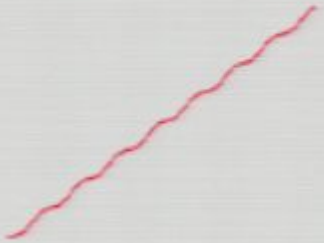

The effective potential

Inflation is driven by a real scalar field with potential

$$V(\phi) = \mu^3\phi + b\mu^3 f \cos\left(\frac{\phi}{f}\right)$$

- $b < 1 \Rightarrow$ monotonic potential
- $\phi \gg M_{pl}$ gives large-field inflation. With $\mu = 6 \cdot 10^{-4} M_{pl}$ and $\phi_{in} \simeq 11 M_{pl}$ one fits COBE. We will not discuss reheating.

The effective potential

Inflation is driven by a real scalar field with potential

$$V(\phi) = \mu^3 \phi + b\mu^3 f \cos\left(\frac{\phi}{f}\right)$$

- $b < 1 \Rightarrow$ monotonic potential
- $\phi \gg M_{pl}$ gives large-field inflation. With $\mu = 6 \cdot 10^{-4} M_{pl}$ and $\phi_{in} \simeq 11 M_{pl}$ one fits COBE. We will not discuss reheating.
- $f \ll M_{pl}$ many short ripples. Different from the superplanckian case that seems to be hard to achieve in string theory.

  [Banks et al. 03]

Background evolution

We solve the e.o.m. perturbatively in b:

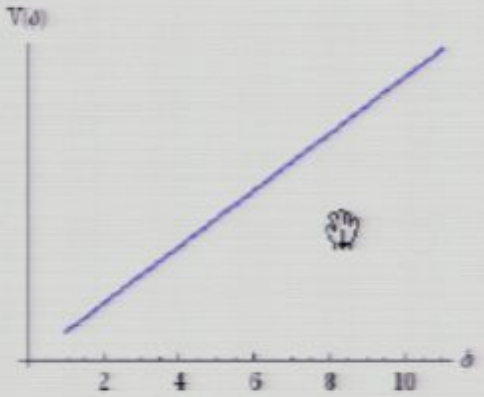

zeroth order

$$\phi_0 = \left(\phi_{in}^{3/2} - \frac{\sqrt{3}}{2} \mu^{3/2} t \right)^{2/3}$$

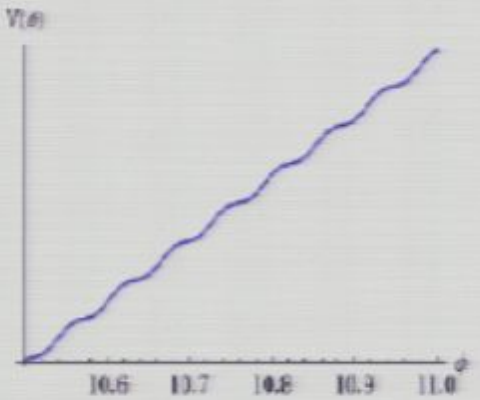

first order

$$\phi_1 \simeq -3bf^2\phi_0 \sin\left(\frac{\phi_0}{f}\right)$$

Background oscillations

The (Hubble) slow-roll parameters oscillate

$$\epsilon \equiv -\frac{\dot{H}}{H^2} \simeq \epsilon_0 + \epsilon_{osci} \cos\left(\frac{\phi_0}{f}\right)$$

$$\simeq \frac{1}{2\phi_0^2} + \frac{3bf}{\phi_{in}} \cos\left(\frac{\phi_0}{f}\right)$$

$$\eta \equiv \frac{\dot{\epsilon}}{\epsilon H} \simeq \eta_0 + \eta_{osci} \sin\left(\frac{\phi_0}{f}\right)$$

$$\simeq 0 + 6b \sin\left(\frac{\phi_0}{f}\right)$$

and can resonate with the perturbations ζ.

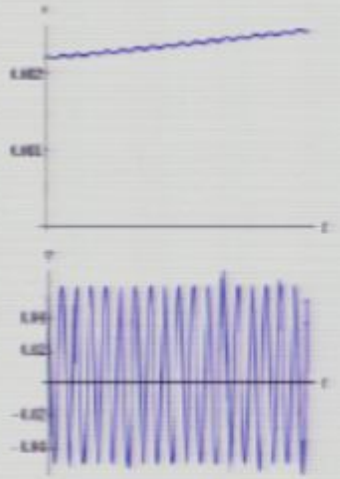

Background oscillations

The (Hubble) slow-roll parameters oscillate

$$\epsilon \equiv -\frac{\dot{H}}{H^2} \simeq \epsilon_0 + \epsilon_{osci}\cos\left(\frac{\phi_0}{f}\right)$$

$$\simeq \frac{1}{2\phi_0^2} + \frac{3bf}{\phi_{in}}\cos\left(\frac{\phi_0}{f}\right)$$

$$\eta \equiv \frac{\dot{\epsilon}}{\epsilon H} \simeq \eta_0 + \eta_{osci}\sin\left(\frac{\phi_0}{f}\right)$$

$$\simeq 0 + 6b\sin\left(\frac{\phi_0}{f}\right)$$

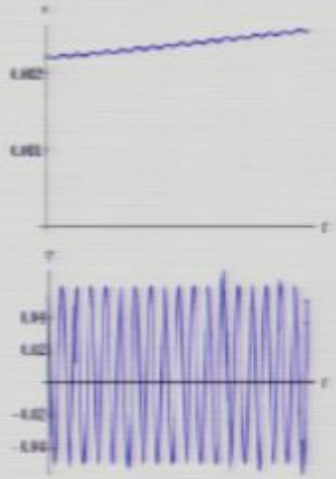

and can resonate with the perturbations ζ.

Notice that $\dot{\eta} \gg \epsilon$ so one can not use slow-roll formulae to compute the perturbations.

Spectrum of scalar perturbations

The oscillations in the potential induce oscillations in the spectrum:

$$P_s(k) = A_s \left(\frac{k}{k_*}\right)^{n_s-1} \left[1 + \delta n_s \cos\left(\frac{\phi_k}{f}\right)\right]$$

$$\Rightarrow A_s \left(\frac{k}{k_*}\right)^{n_s-1+\frac{\delta n_s}{\ln(k/k_*)}\cos\left(\frac{\varphi_k}{f}\right)}$$

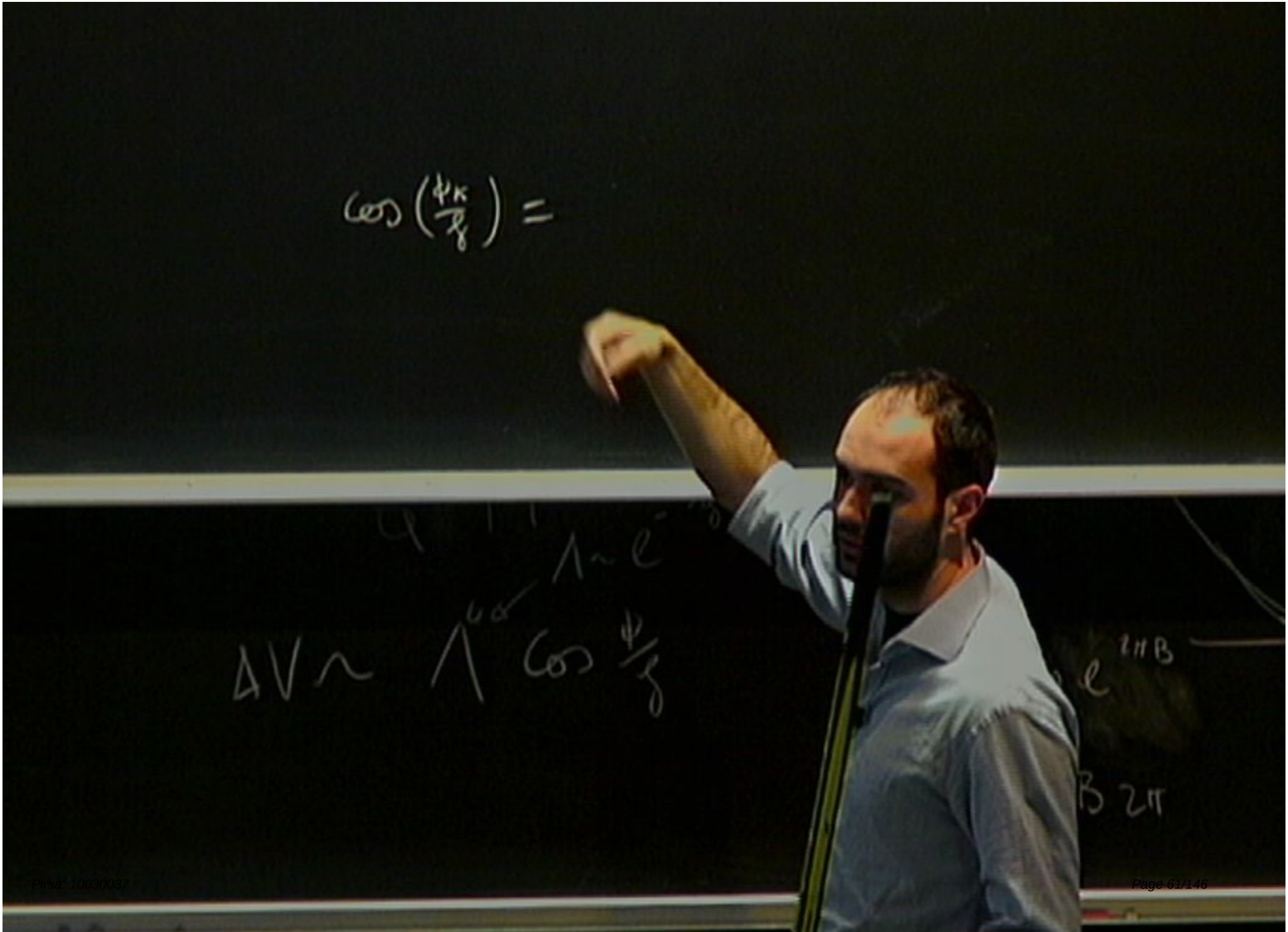
$\cos\left(\frac{\Psi_K}{2}\right) =$
$\Delta V \sim \Lambda^{\alpha} \cos\frac{\Psi}{2}$
$e^{i\pi B}$
$B\,2\pi$

$$\cos\left(\frac{\Psi_K}{g}\right) = \cos\left(\frac{\log_q K}{g}\right)$$

$$\Delta V \sim \Lambda^{\alpha} \cos\frac{\Psi}{g}$$

$$\sum_n \int C_4 \wedge e^{2\pi i B}$$

$$\int C_4 \wedge B \, 2\pi$$

Cosmological perturbation theory

- During single-field inflation, there is a single scalar degree of freedom after fixing the gauge (diffeomorphisms).
- We choose to have in the metric, i.e. the uniform density gauge $\delta\phi = 0$ and we are left with $\zeta(x)$ in

$$g_{ij} = a^2 \delta_{ij}[1 + 2\zeta(x)]$$

- The background inflationary solution is quasi de Sitter, i.e.

$$a(t) = a_0 e^{tH}$$

with slowly changing Hubble parameter.

- The action expanded to quadratic order around this classical background leads to the Mukhanov-Sasaki equation for the curvature perturbation $\zeta(x)$

Cosmological perturbation theory

- During single-field inflation, there is a single scalar degree of freedom after fixing the gauge (diffeomorphisms).
- We choose to have in the metric, i.e. the uniform density gauge $\delta\phi = 0$ and we are left with $\zeta(x)$ in

$$g_{ij} = a^2 \delta_{ij}[1 + 2\zeta(x)]$$

- The background inflationary solution is quasi de Sitter, i.e.

$$a(t) = a_0 e^{tH}$$

with slowly changing Hubble parameter.

- The action expanded to quadratic order around this classical background leads to the Mukhanov-Sasaki equation for the curvature perturbation $\zeta(x)$

The Mukhanov-Sasaki equation

Mukhanov-Sasaki equation leads to the power spectrum

- Slow roll is not enough because ϵ and δ are not approximatively constant, in fact oscillate fast.

$$\frac{d^2\zeta_k}{dx^2} - \frac{2(1+2\epsilon+\delta)}{x}\frac{d\zeta_k}{dx} + \zeta_k = 0\,,$$

where $x \equiv -k\tau$ and τ is the conformal time $ad\tau \equiv dt$

The Mukhanov-Sasaki equation

Mukhanov-Sasaki equation leads to the power spectrum

- Slow roll is not enough because ϵ and δ are not approximatively constant, in fact oscillate fast.

$$\frac{d^2\zeta_k}{dx^2} - \frac{2(1+2\epsilon+\delta)}{x}\frac{d\zeta_k}{dx} + \zeta_k = 0\,,$$

  where $x \equiv -k\tau$ and τ is the conformal time $ad\tau \equiv dt$

- We solve perturbatively in b.
- There is a resonance between ζ and δ at $x_{res} = 1/(2f\phi)$.

The Mukhanov-Sasaki equation

Mukhanov-Sasaki equation leads to the power spectrum

- Slow roll is not enough because ϵ and δ are not approximatively constant, in fact oscillate fast.

$$\frac{d^2\zeta_k}{dx^2} - \frac{2(1+2\epsilon+\delta)}{x}\frac{d\zeta_k}{dx} + \zeta_k = 0\,,$$

  where $x \equiv -k\tau$ and τ is the conformal time $ad\tau \equiv dt$

- We solve perturbatively in b.
- There is a resonance between ζ and δ at $x_{res} = 1/(2f\phi)$.
- Across the resonance a mode gets excited

$$\zeta_k(x) \simeq i\sqrt{\frac{\pi}{2}}x^{3/2}H^{(1)}_{3/2}(x) - c_k^- i\sqrt{\frac{\pi}{2}}x^{3/2}H^{(2)}_{3/2}(x)\,.$$

The Mukhanov-Sasaki equation

Mukhanov-Sasaki equation leads to the power spectrum

- Slow roll is not enough because ϵ and δ are not approximatively constant, in fact oscillate fast.

$$\frac{d^2\zeta_k}{dx^2} - \frac{2(1+2\epsilon+\delta)}{x}\frac{d\zeta_k}{dx} + \zeta_k = 0\,,$$

  where $x \equiv -k\tau$ and τ is the conformal time $ad\tau \equiv dt$

- We solve perturbatively in b.
- There is a resonance between ζ and δ at $x_{res} = 1/(2f\phi)$.
- Across the resonance a mode gets excited

$$\zeta_k(x) \simeq i\sqrt{\frac{\pi}{2}}x^{3/2}H^{(1)}_{3/2}(x) - c^-_k(x)\,i\sqrt{\frac{\pi}{2}}x^{3/2}H^{(2)}_{3/2}(x)\,,$$

The effect of the resonance on the modes

- The equation for $c_k^-(x)$ can be solved exactly

$$c_k^-(x) \sim bf\dot{\phi}_* e^{-i\frac{\log k}{f}} \Gamma\left[1 - \frac{i}{f\dot{\phi}_*}, -2ix\right]$$

- the resonance is seen numerically and anaytically

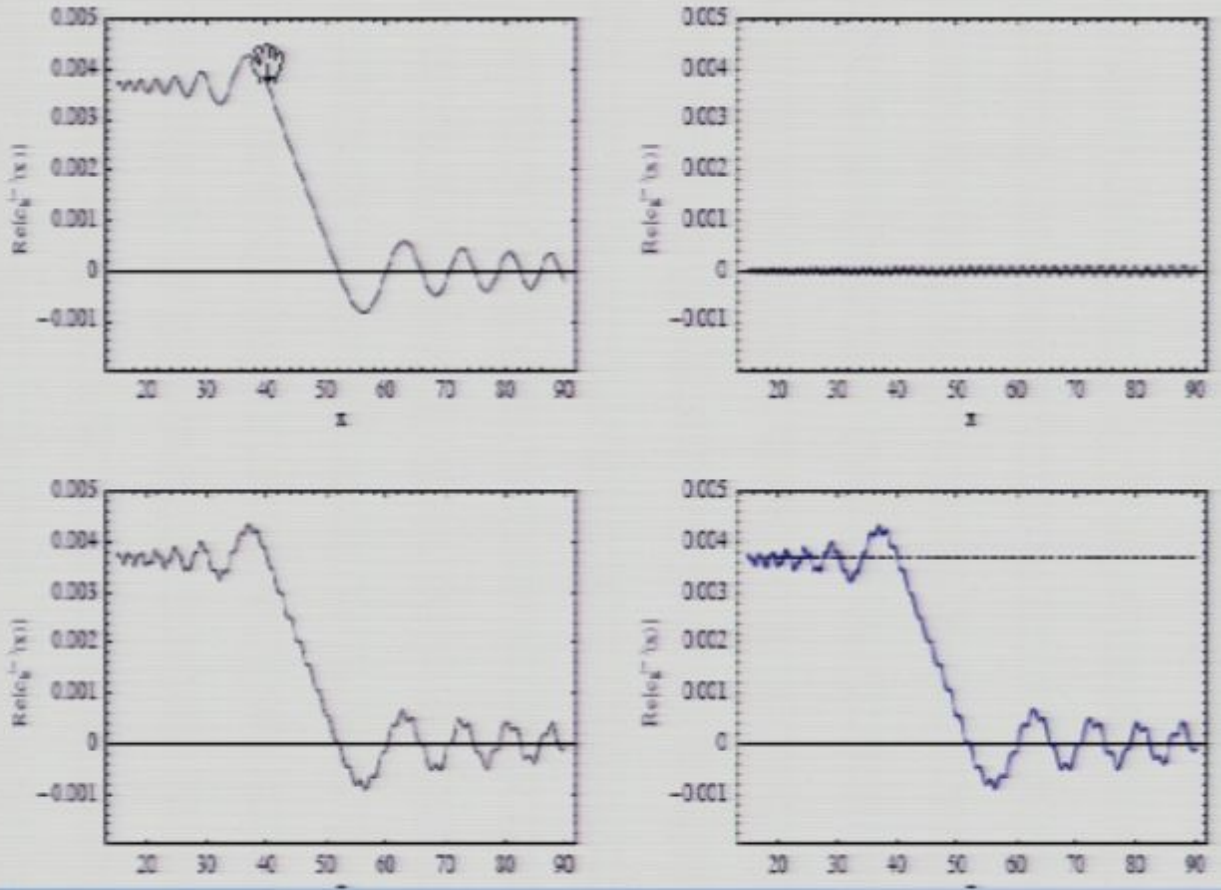

The effect of the resonance on the modes

- The equation for $c_k^-(x)$ can be solved exactly

$$c_k^-(x) \sim bf\dot{\phi}_* e^{-i\frac{\log k}{f}} \Gamma\left[1 - \frac{i}{f\dot{\phi}_*}, -2ix\right]$$

The effect of the resonance on the modes

- The equation for $c_k^-(x)$ can be solved exactly

$$c_k^-(x) \sim bf\dot{\phi}_* e^{-i\frac{\log k}{f}} \Gamma\left[1 - \frac{i}{f\dot{\phi}_*}, -2ix\right]$$

- the resonance is seen numerically and anaytically

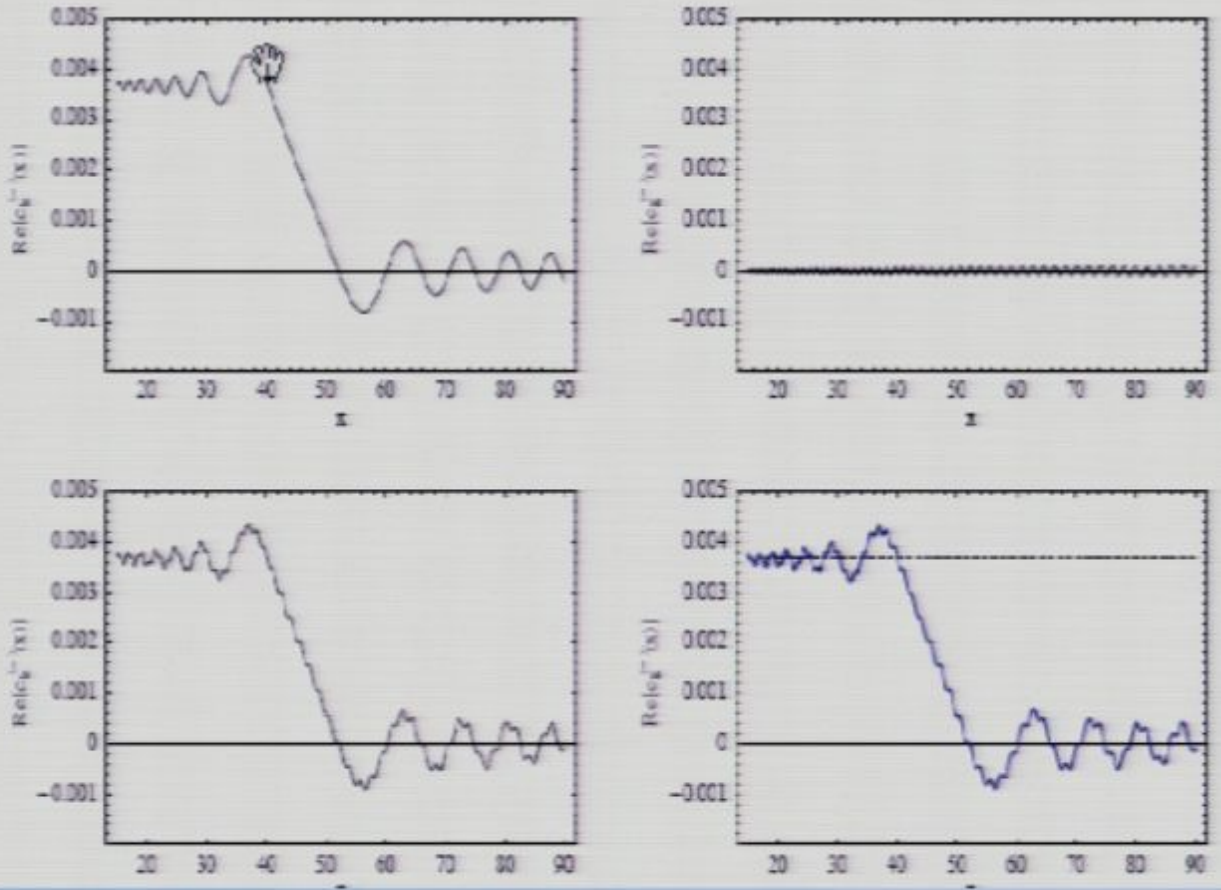

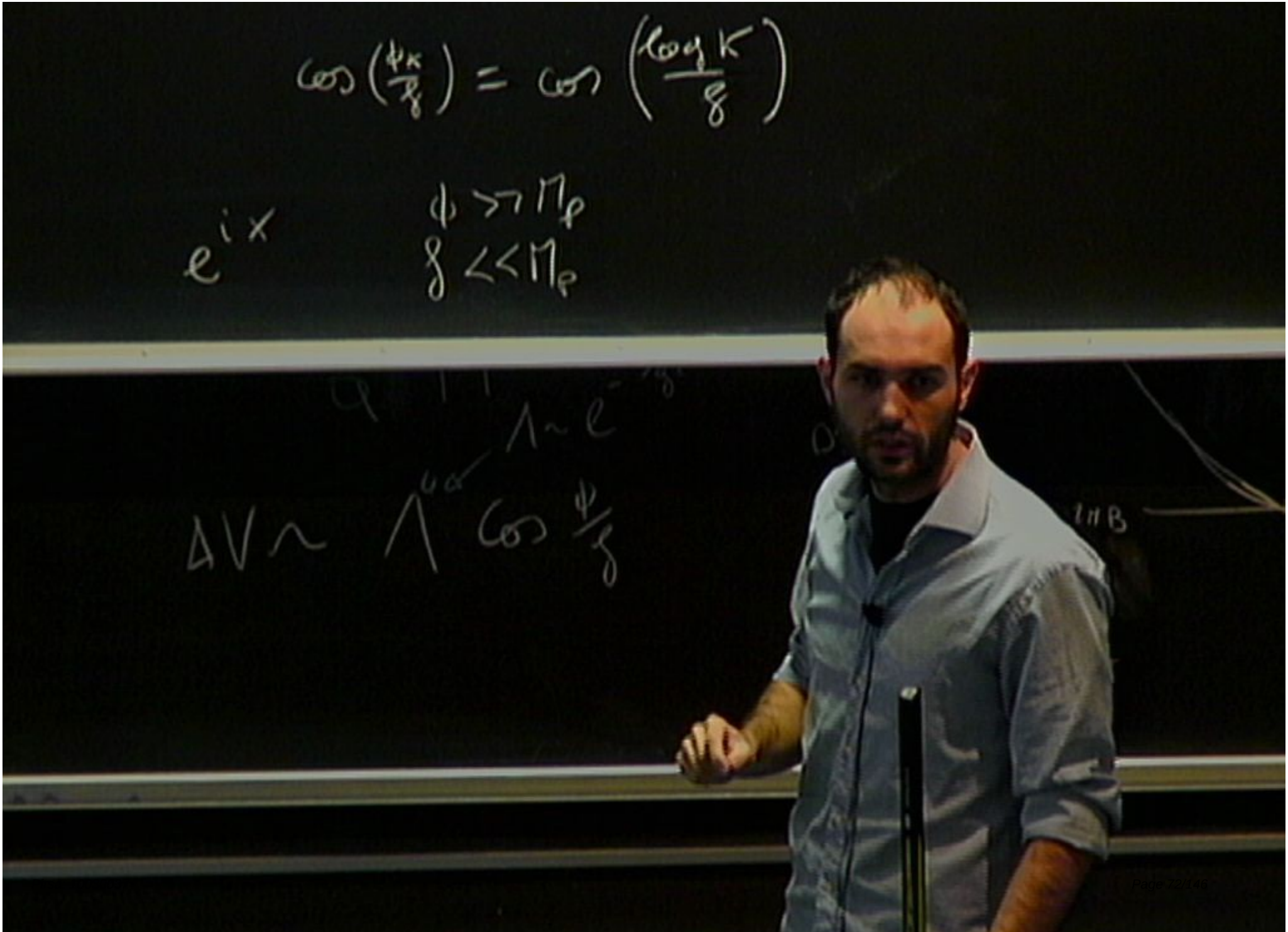
$\cos\left(\frac{\psi_K}{f}\right) = \cos\left(\frac{\log K}{f}\right)$
e^{ix}
$\phi >> M_p$
$f << M_p$
$\Delta V \sim \Lambda^4 \cos\frac{\psi}{f}$
1HB

The effect of the resonance on the modes

- The equation for $c_k^-(x)$ can be solved exactly

$$c_k^-(x) \sim bf\dot{\phi}_* e^{-i\frac{\log k}{f}} \Gamma\left[1 - \frac{i}{f\dot{\phi}_*}, -2ix\right]$$

- the resonance is seen numerically and anaytically

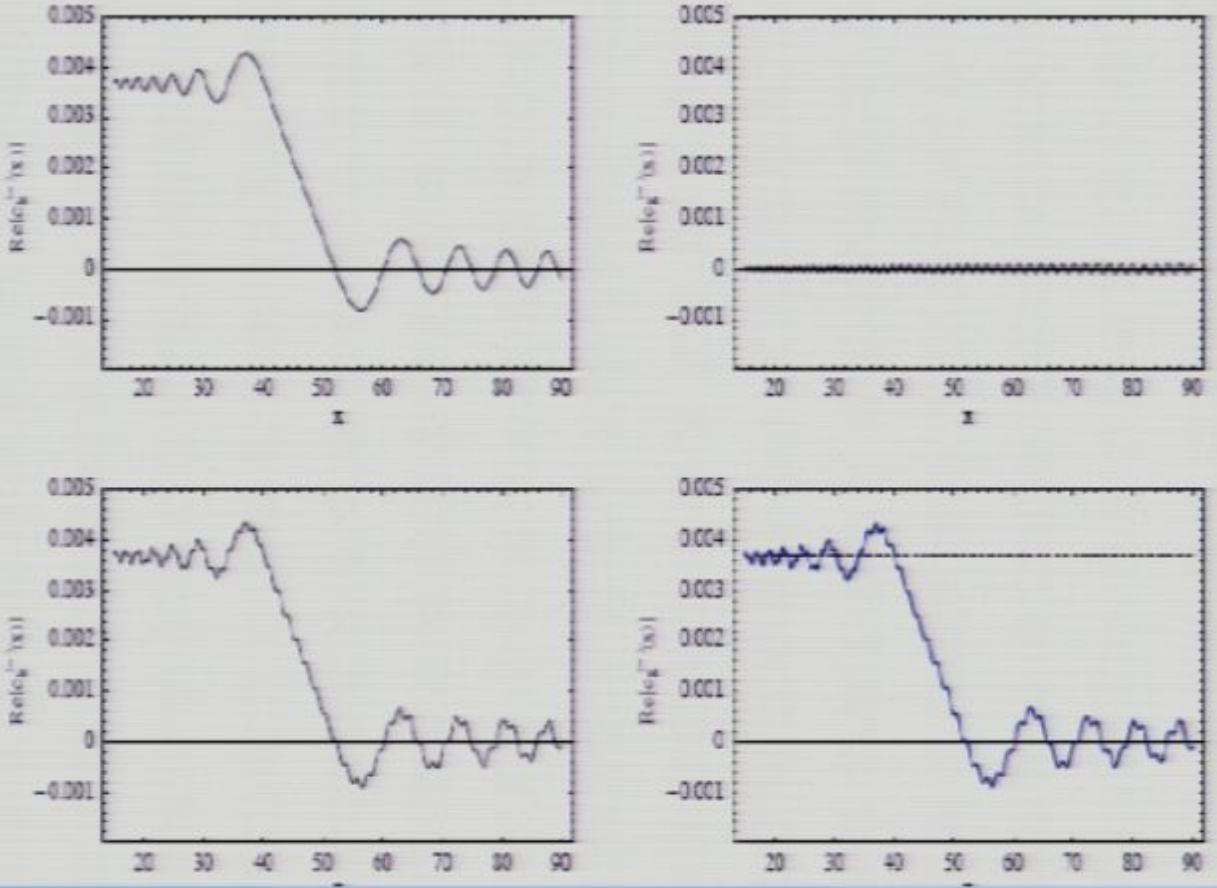

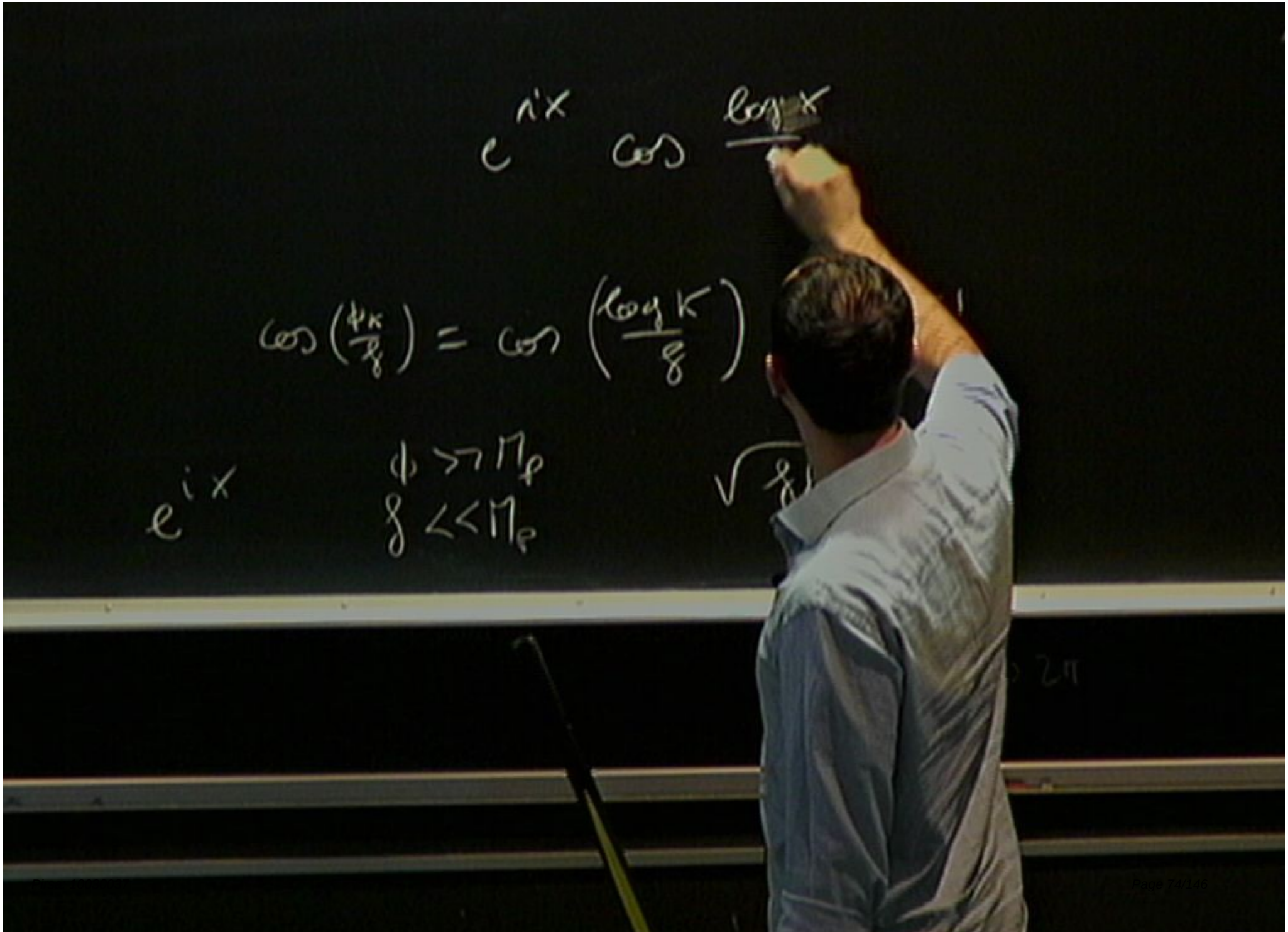
e^{ix}
$\cos\left(\frac{\psi_K}{\beta}\right) = \cos\left(\frac{\log K}{\beta}\right)$
e^{ix}
$\phi \gg M_p$
$\beta \ll M_p$

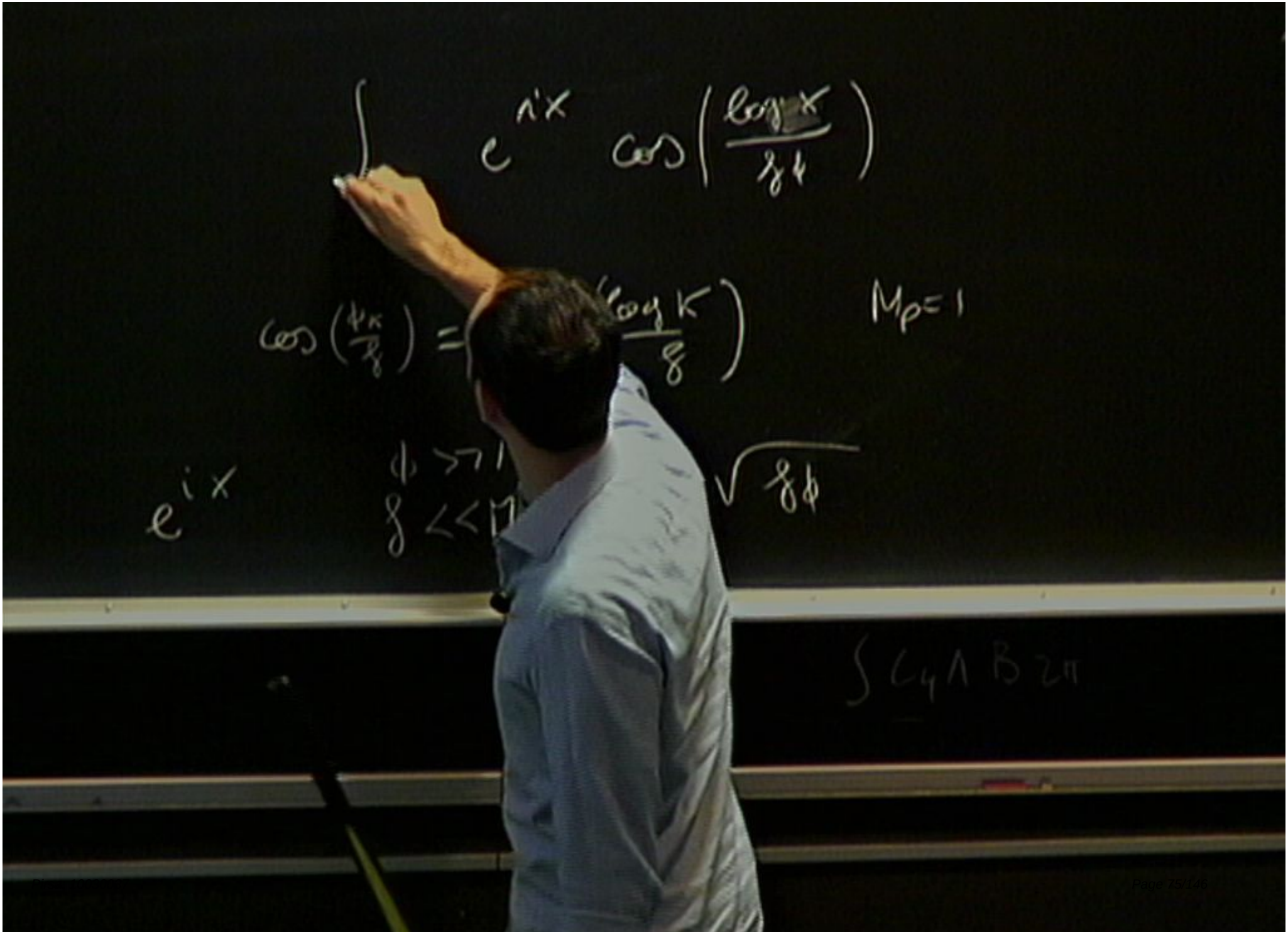
$\int e^{ix} \cos\left(\frac{\log x}{g\phi}\right)$
$\cos\left(\frac{\psi x}{g}\right) = \left(\frac{\log K}{g}\right)$
$M_p = 1$
e^{ix}
$\phi > 7$
$g << 1$
$\sqrt{g\phi}$
$S_{CA} B_{21}$

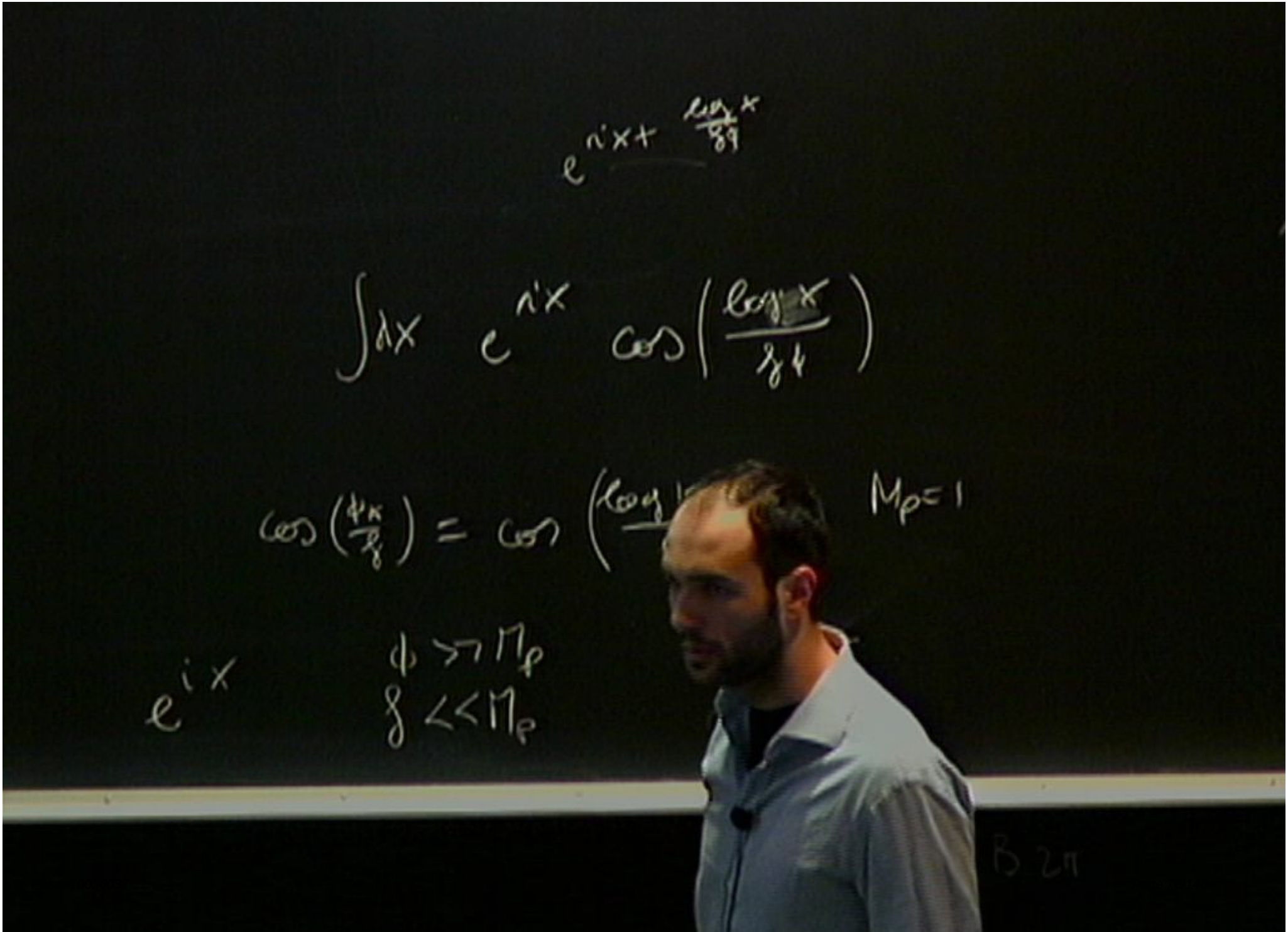
$e^{i\lambda x + \frac{\log x}{8\eta}x}$
$\int d\lambda \; e^{i\lambda x} \cos\left(\frac{\log x}{8\eta}\right)$
$\cos\left(\frac{\psi x}{8}\right) = \cos\left($
$M_p = 1$
e^{ix}
$\phi \gg M_p$
$8 \ll M_p$

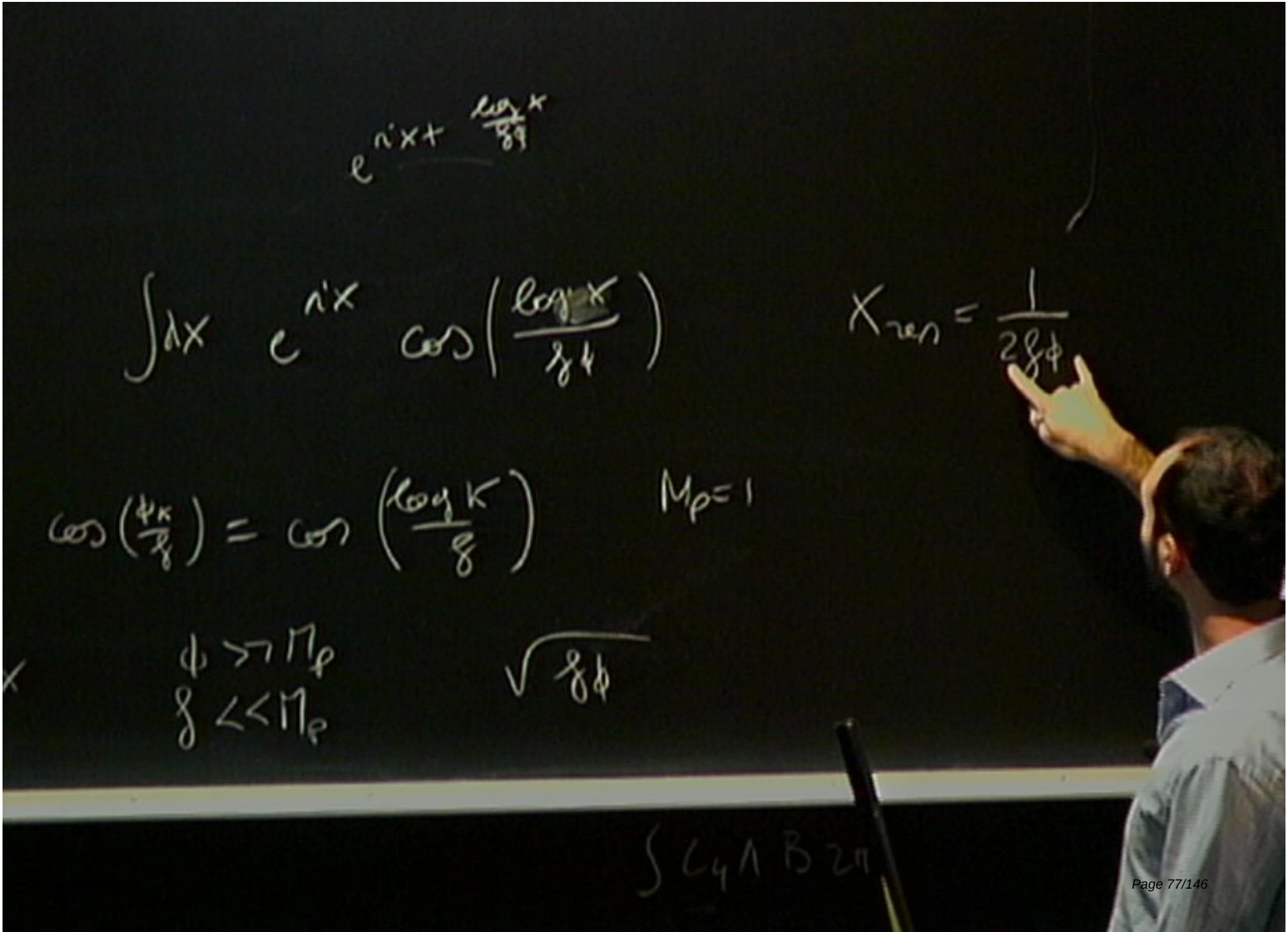
$e^{ikx + \frac{\log x}{g\phi} x}$
$\int dx \; e^{ikx} \cos\left(\frac{\log x}{g\phi}\right)$
$x_{zero} = \frac{1}{2g\phi}$
$\cos\left(\frac{\psi_K}{g}\right) = \cos\left(\frac{\log K}{g}\right)$
$M_p = 1$
$\phi \gg M_p$
$g \ll M_p$
$\sqrt{g\phi}$

$$e^{i\lambda x + \frac{\log x}{g\phi} x}$$

$$\int d\lambda \; e^{i\lambda x} \cos\left(\frac{\log x}{g\phi}\right) \qquad x_{zero} = \frac{1}{2g\phi}$$

$$\cos\left(\frac{\psi_K}{g}\right) = \cos\left(\frac{\log K}{g}\right) \qquad M_p = 1$$

$\phi \gg M_p$
$g \ll M_p$

$$\sqrt{g\phi}$$

$$\int C_4 \wedge B \, 2\pi$$

Solution of the Mukhanov-Sasaki equation

The amplitude of oscillations in the spectrum is then

$$\delta n_s = -12b\sqrt{\frac{\frac{\pi}{8}\coth\left(\frac{\pi}{2f\phi}\right)f\phi}{(1+(3f\phi)^2)}} \sim 3b\sqrt{2\pi f\phi},$$

valid for $\phi \gg M_{pl}$, $f \ll M_{pl}$ and $b \ll 1$.Excellent agreement with the numerics.

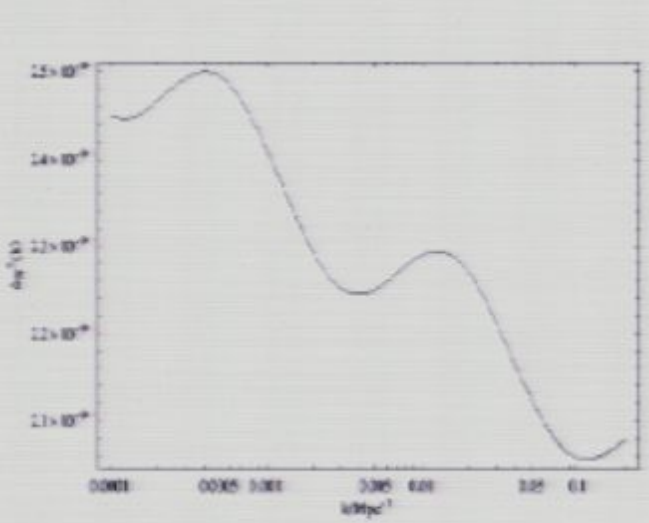

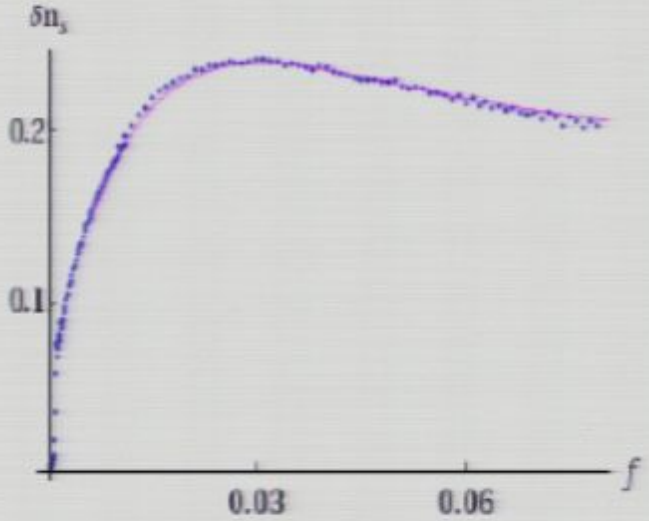

Solution of the Mukhanov-Sasaki equation

The amplitude of oscillations in the spectrum is then

$$\delta n_s = -12b\sqrt{\frac{\frac{\pi}{8}\coth\left(\frac{\pi}{2f\phi}\right)f\phi}{(1+(3f\phi)^2)}} \sim 3b\sqrt{2\pi f\phi},$$

valid for $\phi \gg M_{pl}$, $f \ll M_{pl}$ and $b \ll 1$.Excellent agreement with the numerics.

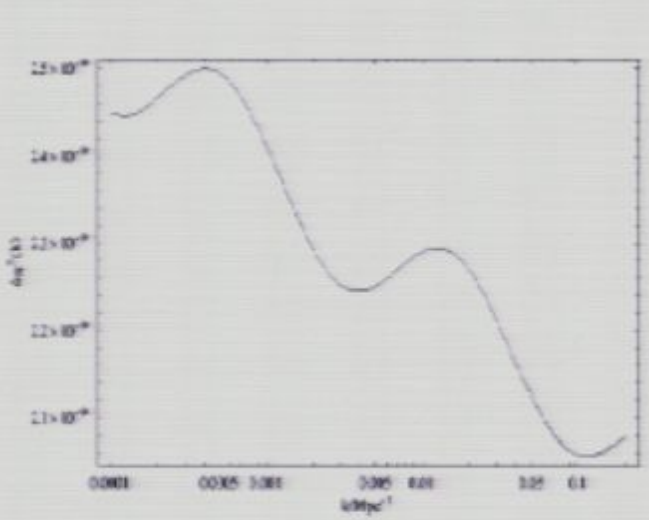

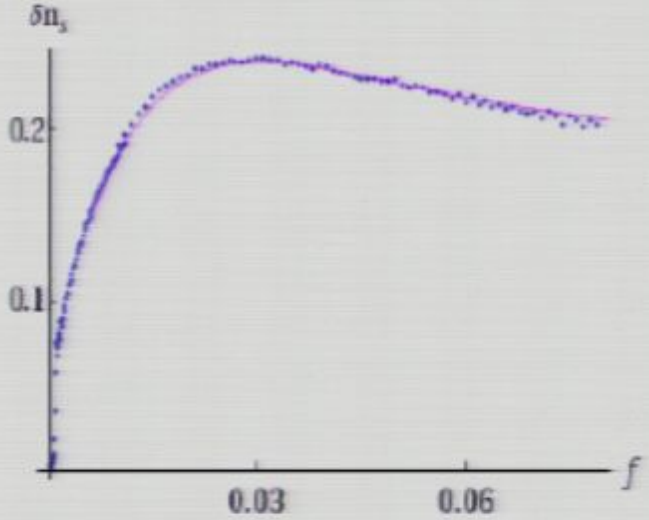

Observational constraints on the spectrum

We have evolved this signlat with CAMB and compared it with WMAP5. The one- and two-sigma exclusion contours are

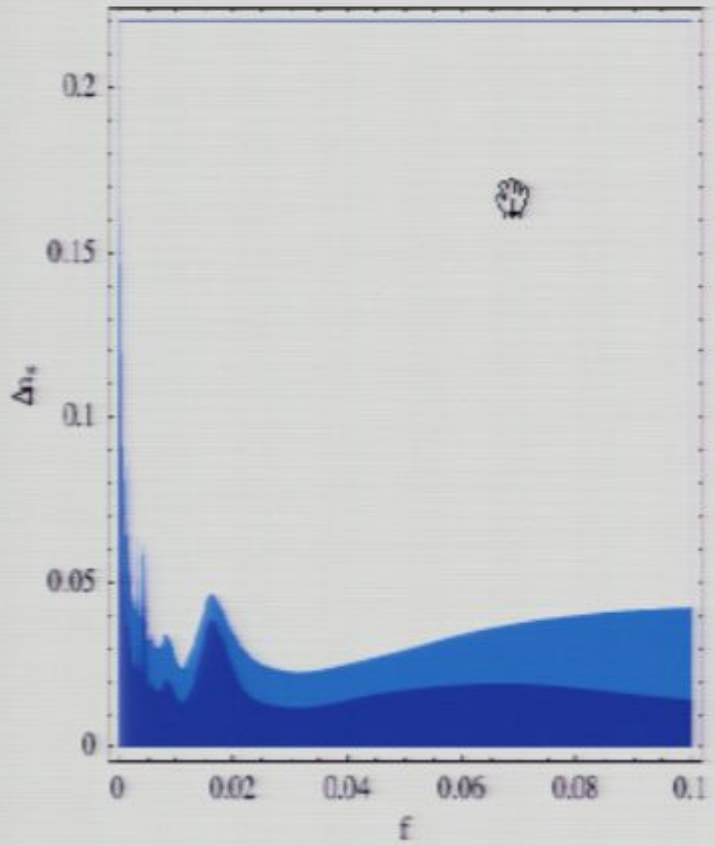

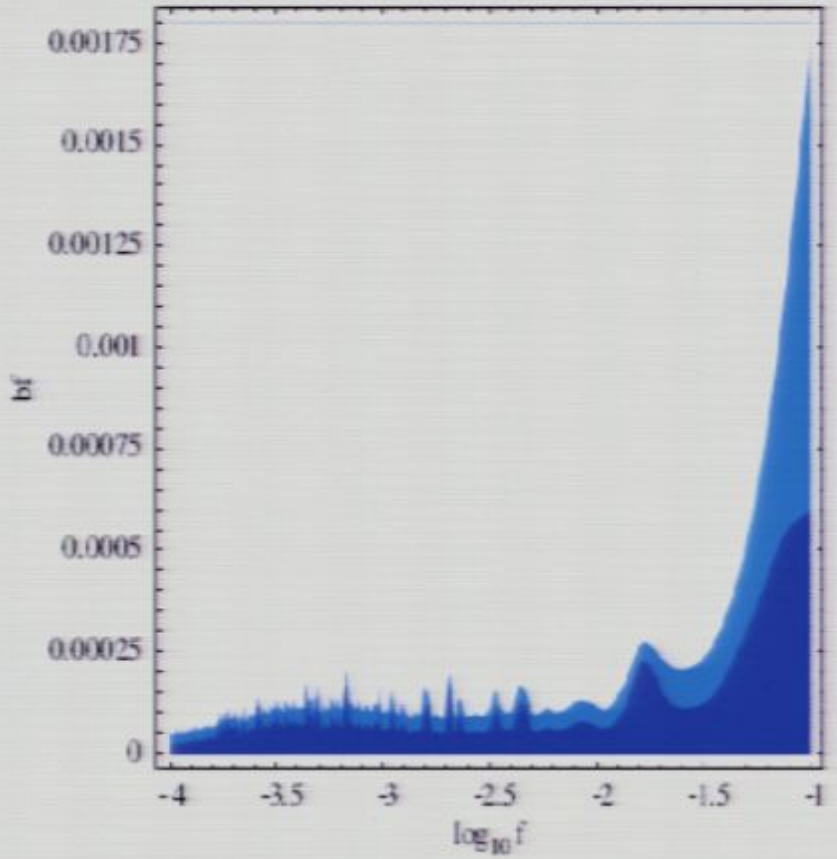

Solution of the Mukhanov-Sasaki equation

The amplitude of oscillations in the spectrum is then

$$\delta n_s = -12b\sqrt{\frac{\frac{\pi}{8}\coth\left(\frac{\pi}{2f\phi}\right)f\phi}{(1+(3f\phi)^2)}} \sim 3b\sqrt{2\pi f\phi},$$

valid for $\phi \gg M_{pl}$, $f \ll M_{pl}$ and $b \ll 1$.Excellent agreement with the numerics.

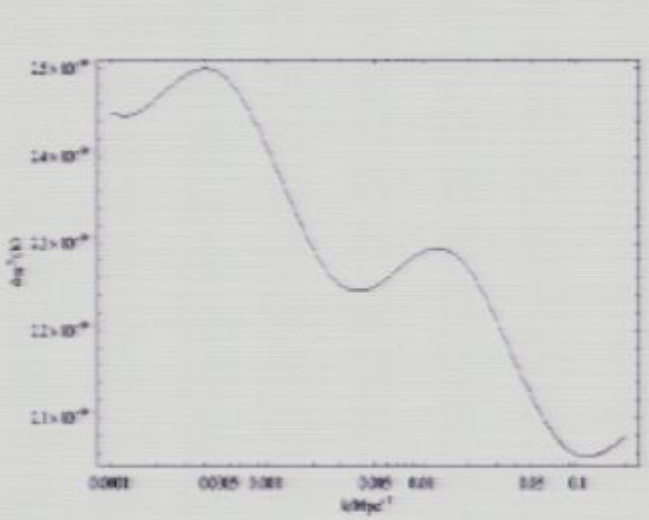

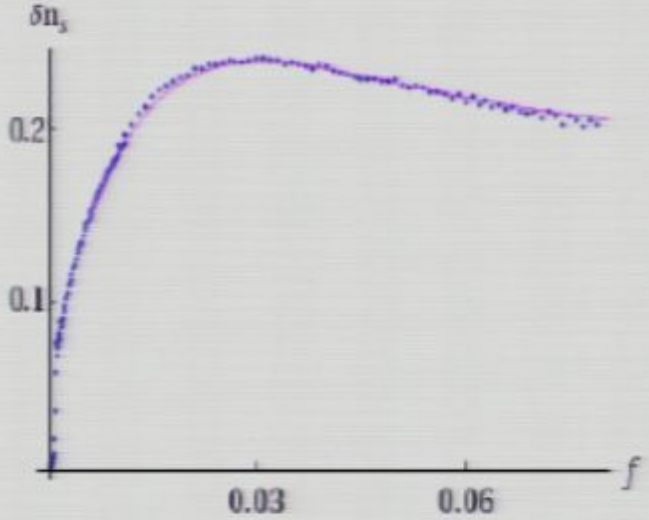

Observational constraints on the spectrum

We have evolved this signlat with CAMB and compared it with WMAP5. The one- and two-sigma exclusion contours are

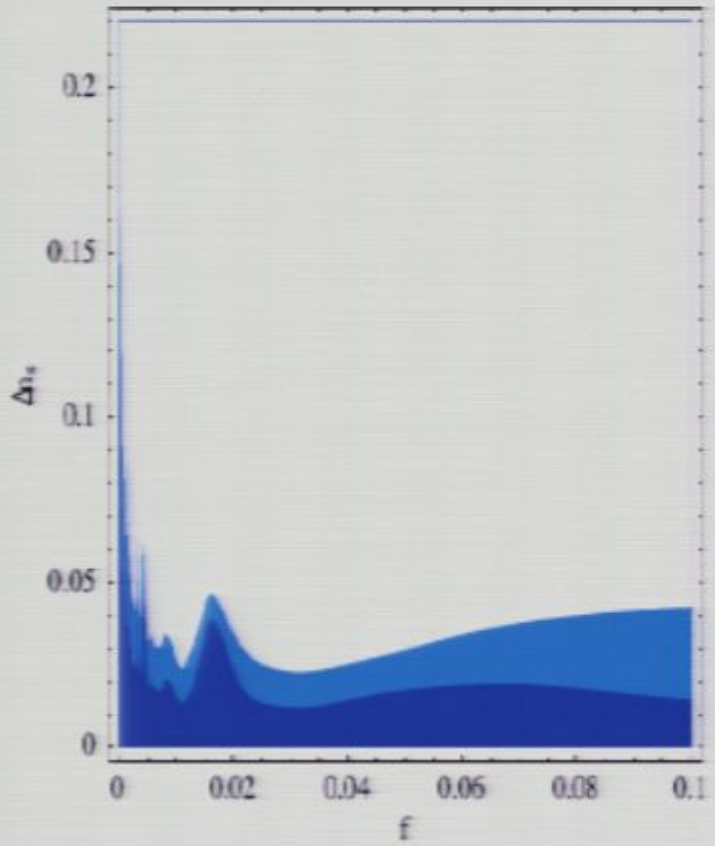

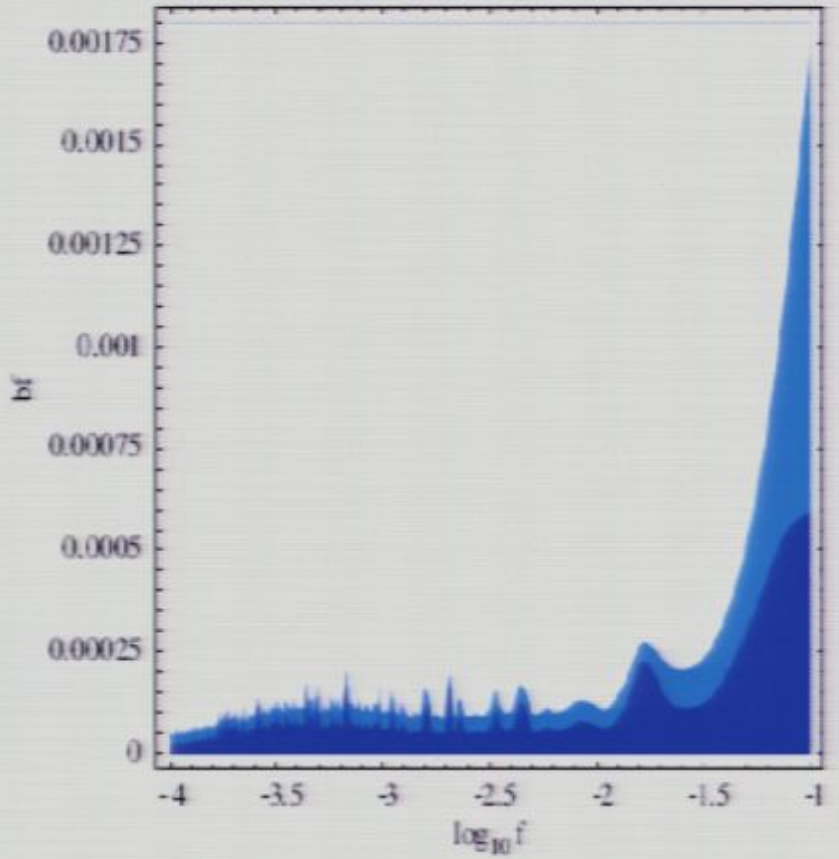

Observational constraints on the spectrum

We have evolved this signlat with CAMB and compared it with WMAP5. The one- and two-sigma exclusion contours are

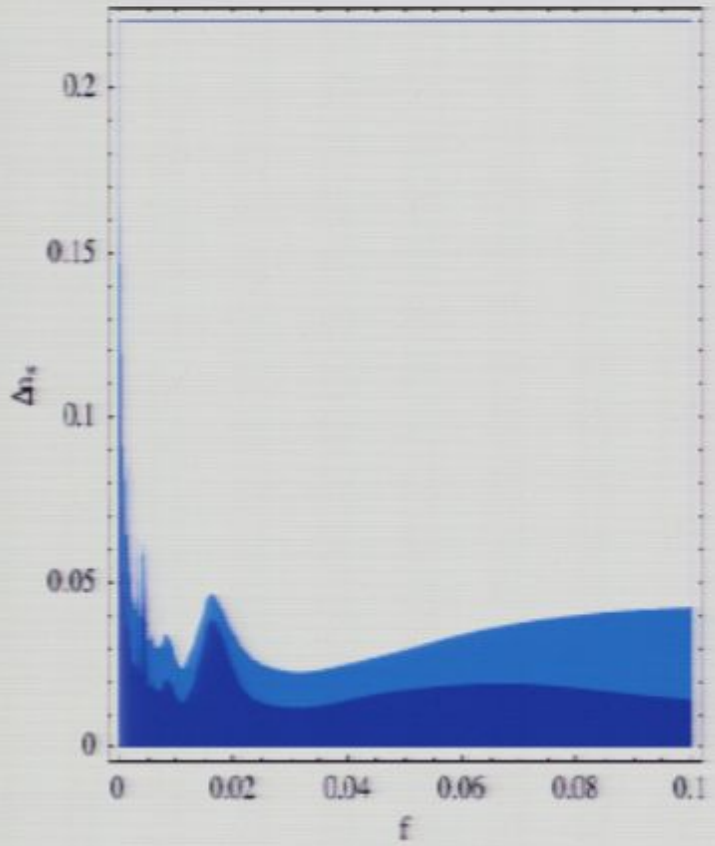

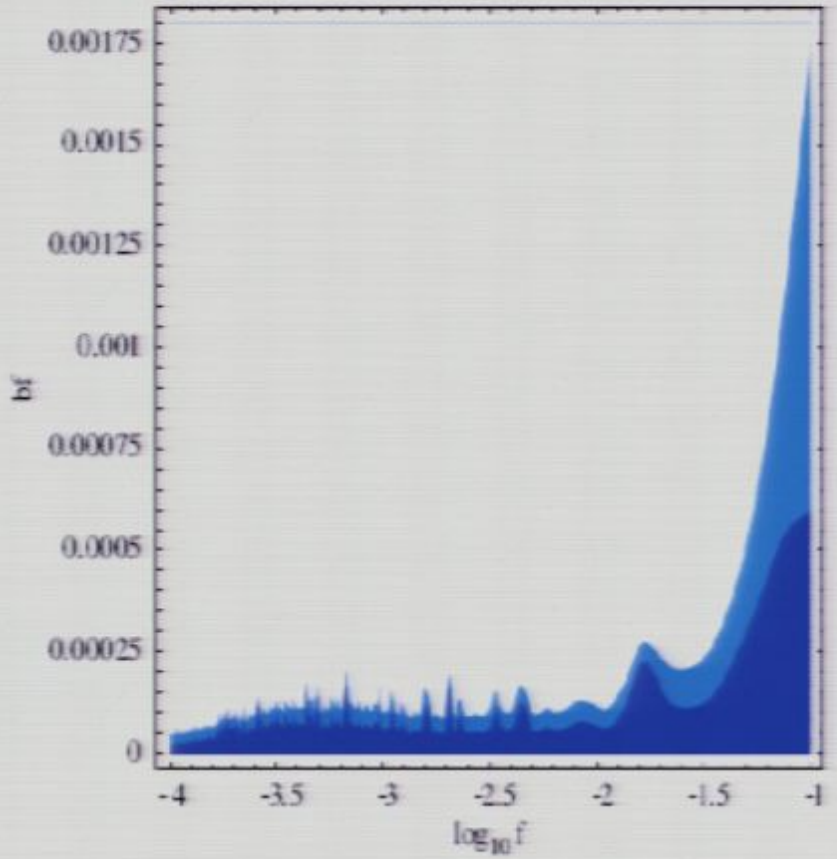

g, b 200 - 199

$b < \frac{10^{-4}}{g}$

$$\int dx \, e^{ix} \cos\left(\frac{\log x}{g\phi}\right) \qquad X_{ren} =$$

$$\cos\left(\frac{\phi_x}{g}\right) = \cos\left(\frac{\log x}{g}\right) \qquad M_p = 1$$

e^{ix} $\phi >> M_p$, $g << M_p$ $\sqrt{g\phi}$

Observational constraints on the spectrum

We have evolved this signlat with CAMB and compared it with WMAP5. The one- and two-sigma exclusion contours are

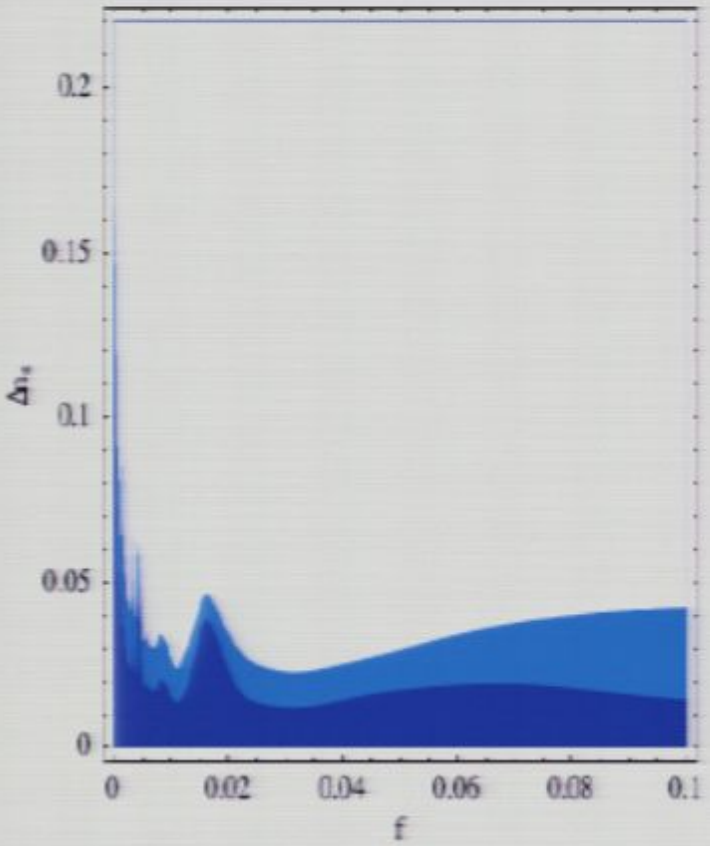

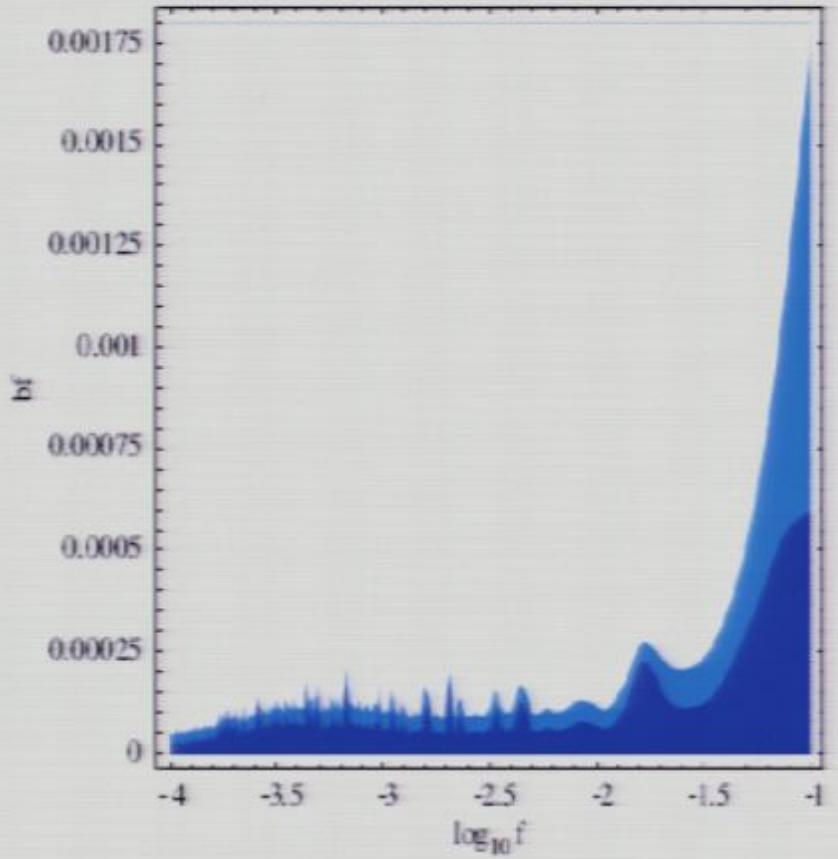

Observational constraints on the spectrum

- The best fit next to the unbinned WMAP5 data looks like

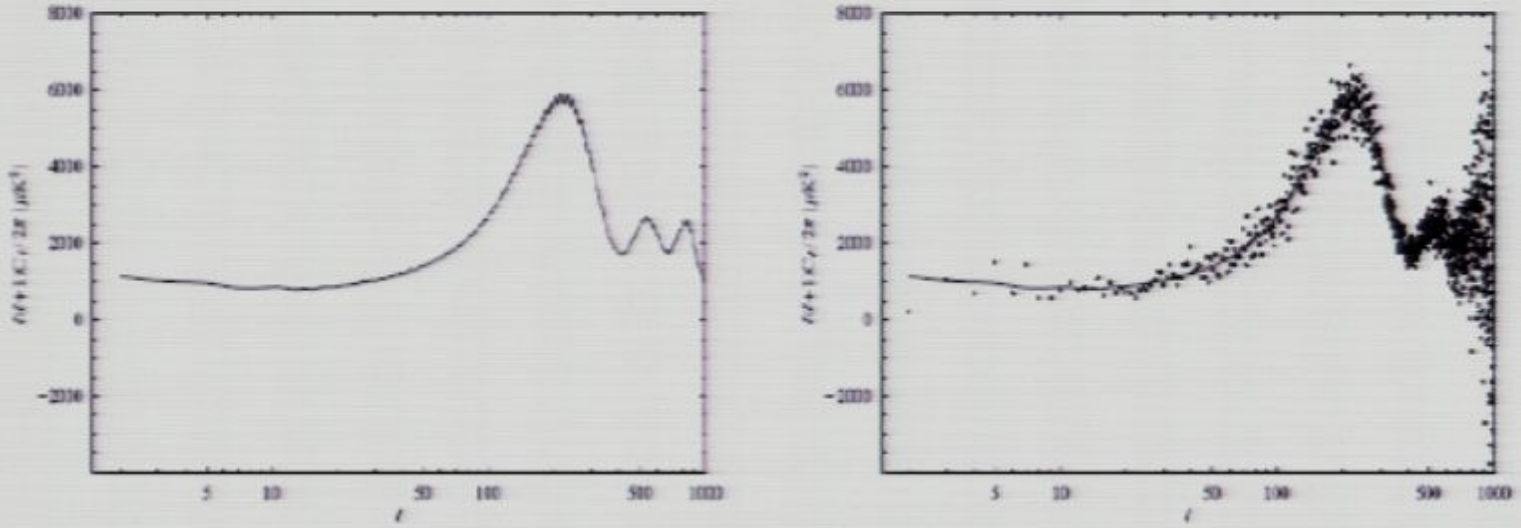

- The improvement of the fit is not statistically significant.

Observational constraints on the spectrum

- The best fit next to the unbinned WMAP5 data looks like

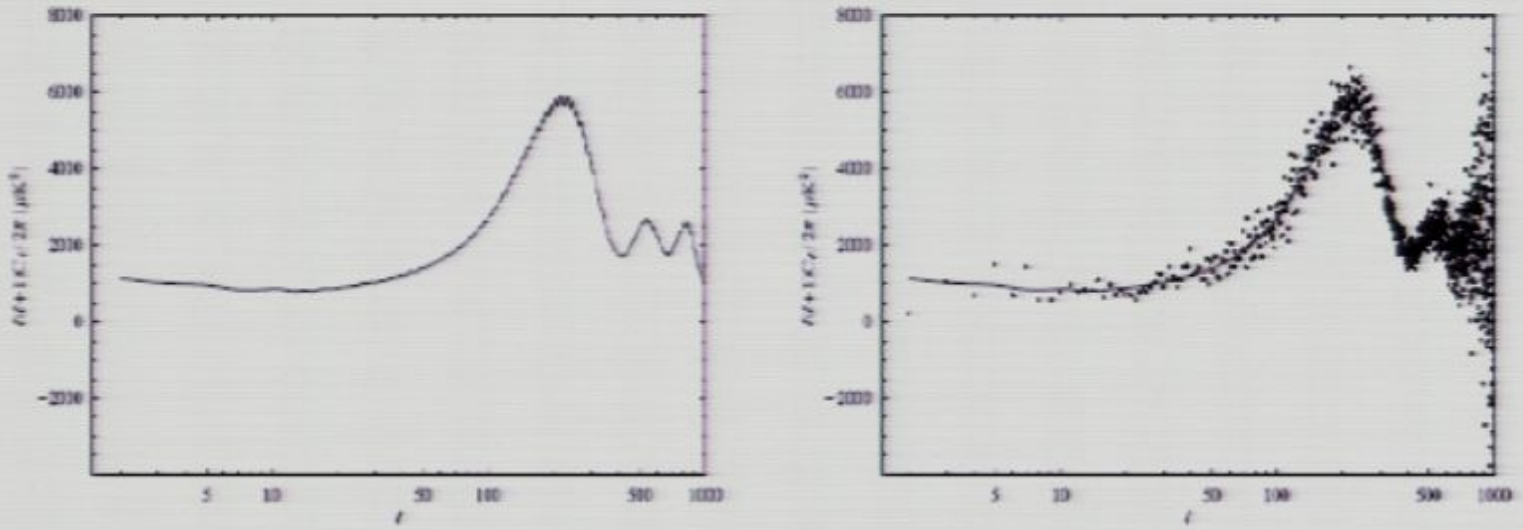

- The improvement of the fit is not statistically significant.

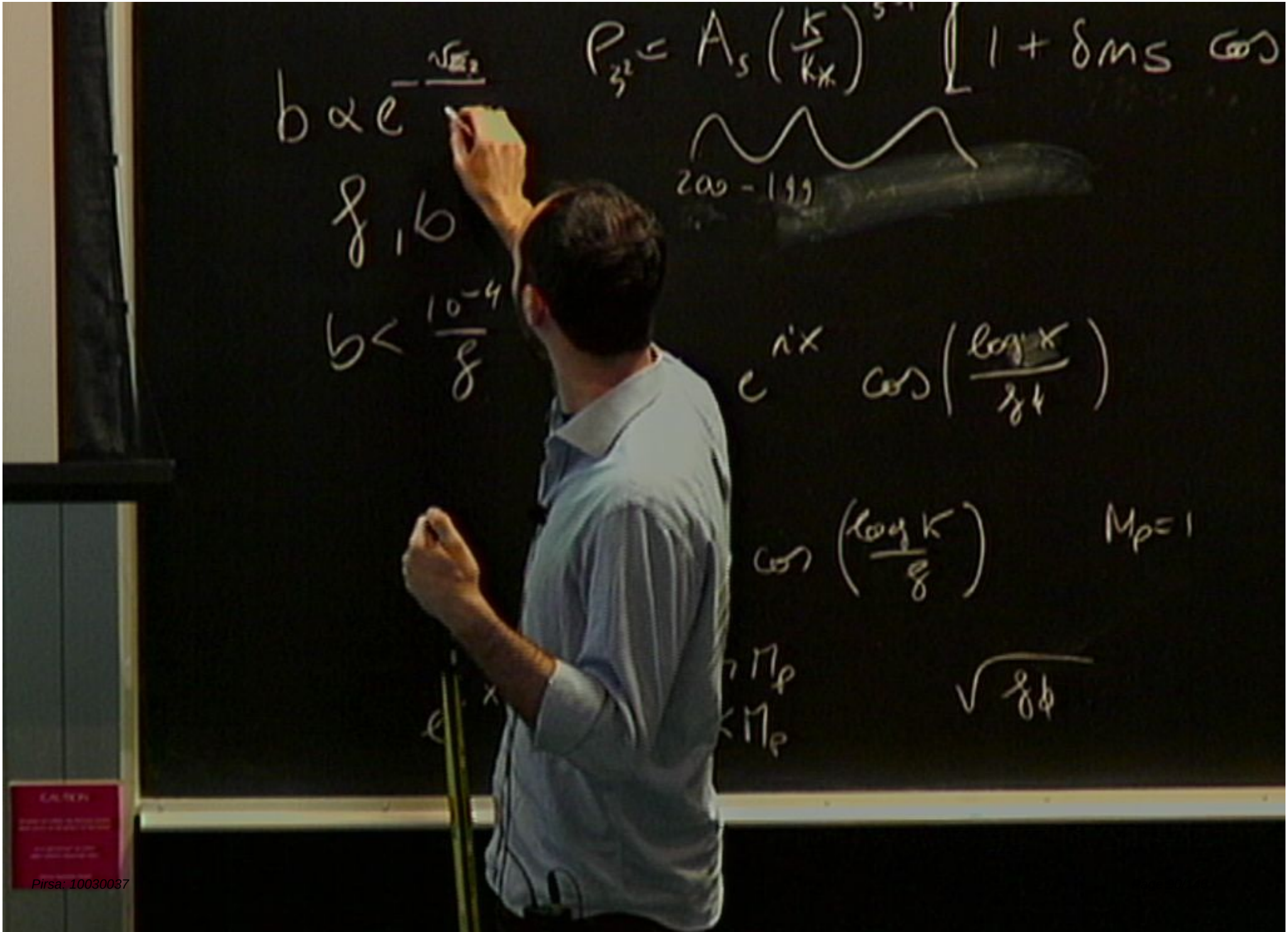

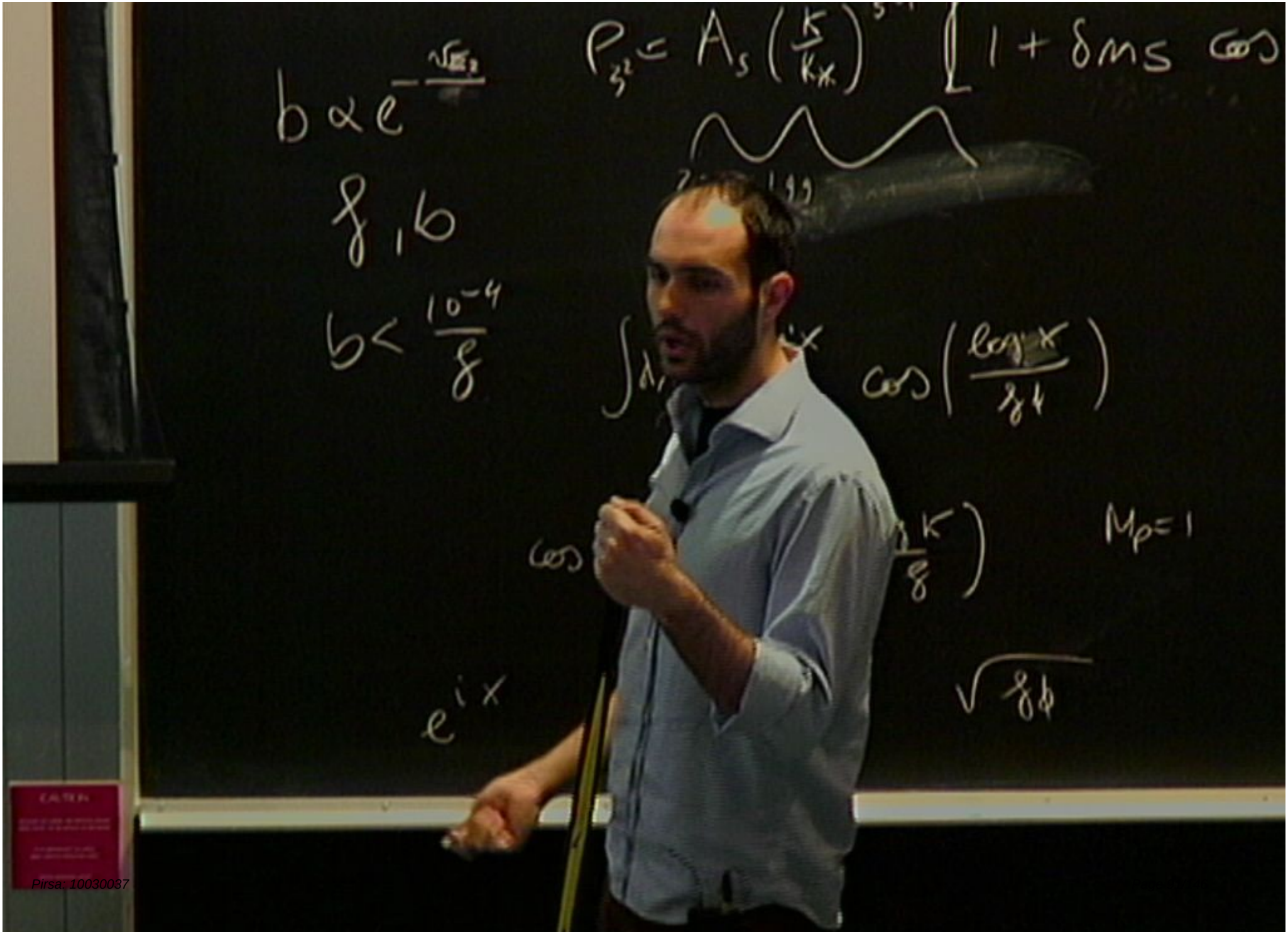

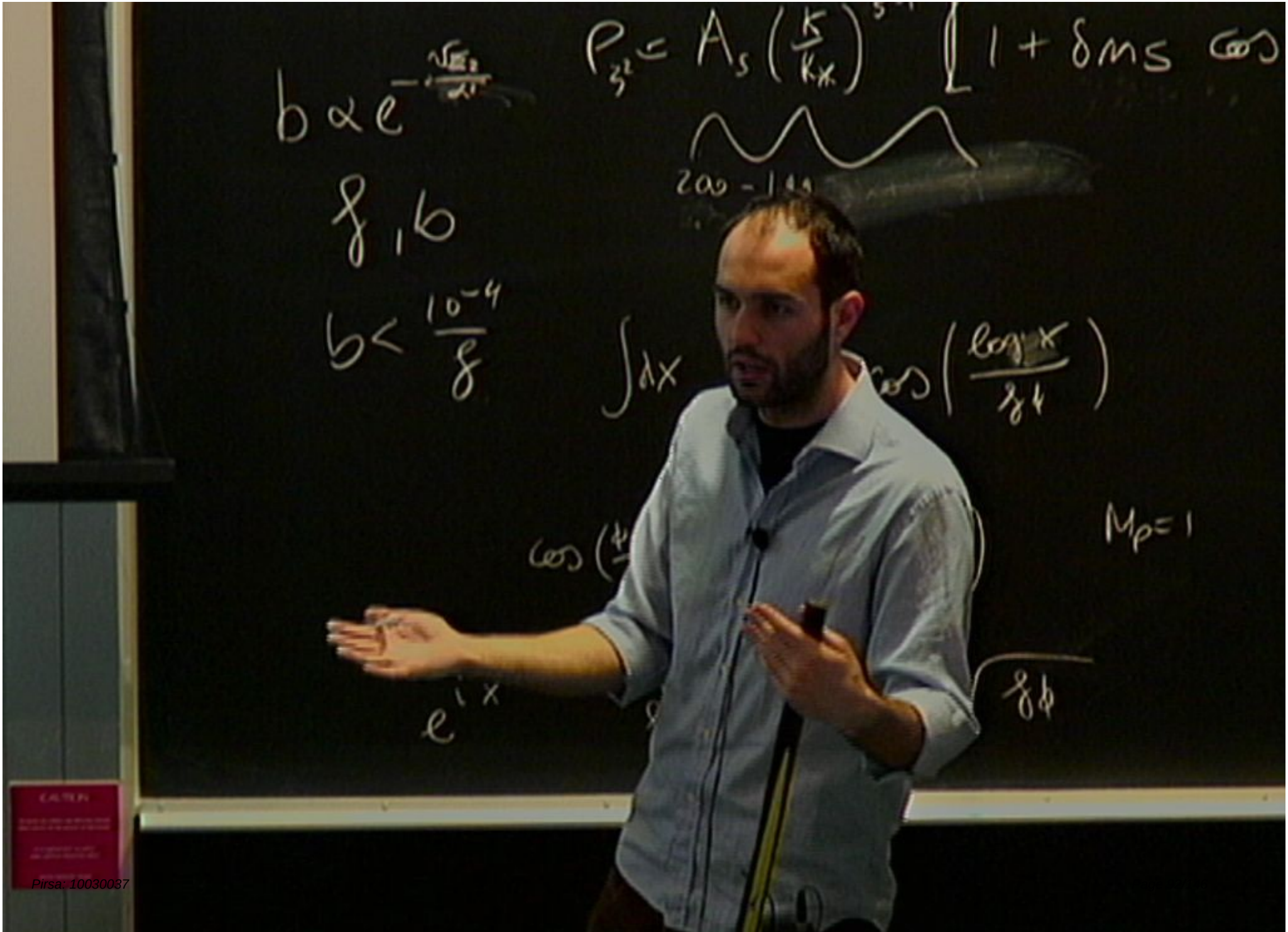

Observational constraints on the spectrum

- The best fit next to the unbinned WMAP5 data looks like

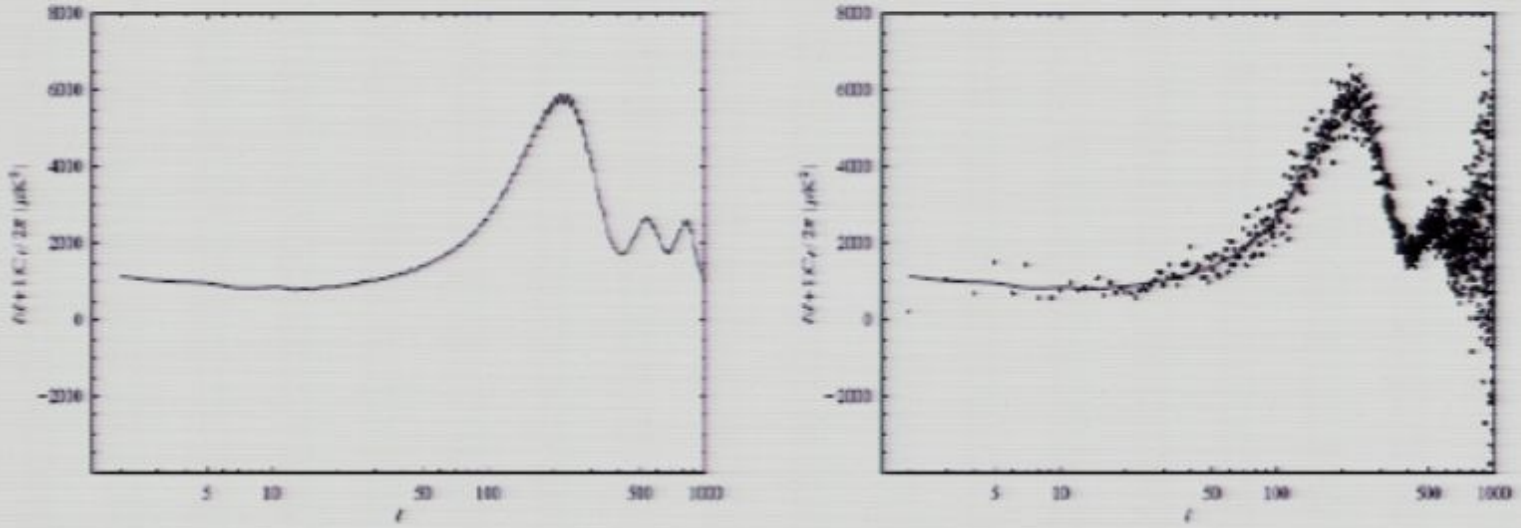

- The improvement of the fit is not statistically significant.
- The bound of WMAP5 data on the parameters of the model is roughly $fb < 10^{-4}$

Observational constraints on the spectrum

- The best fit next to the unbinned WMAP5 data looks like

Observational constraints on the spectrum

We have evolved this signlat with CAMB and compared it with WMAP5. The one- and two-sigma exclusion contours are

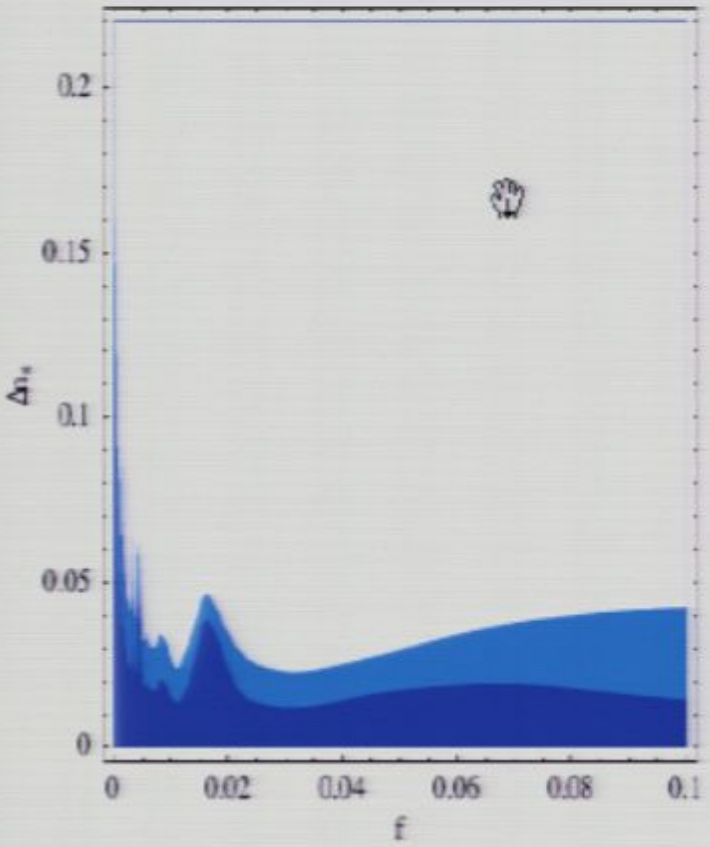

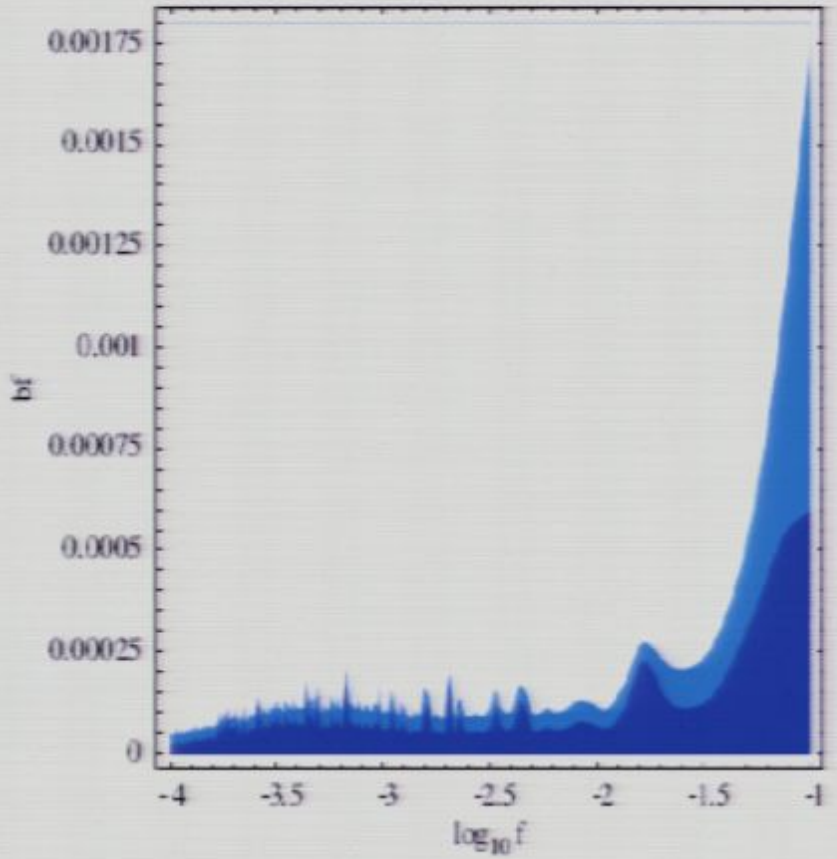

Observational constraints on the spectrum

We have evolved this signlat with CAMB and compared it with WMAP5. The one- and two-sigma exclusion contours are

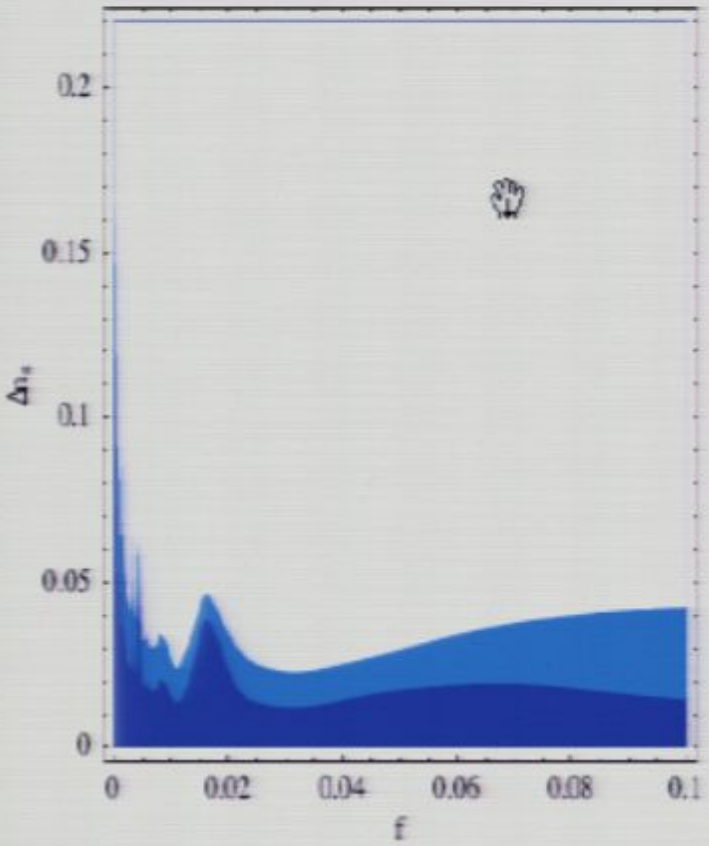

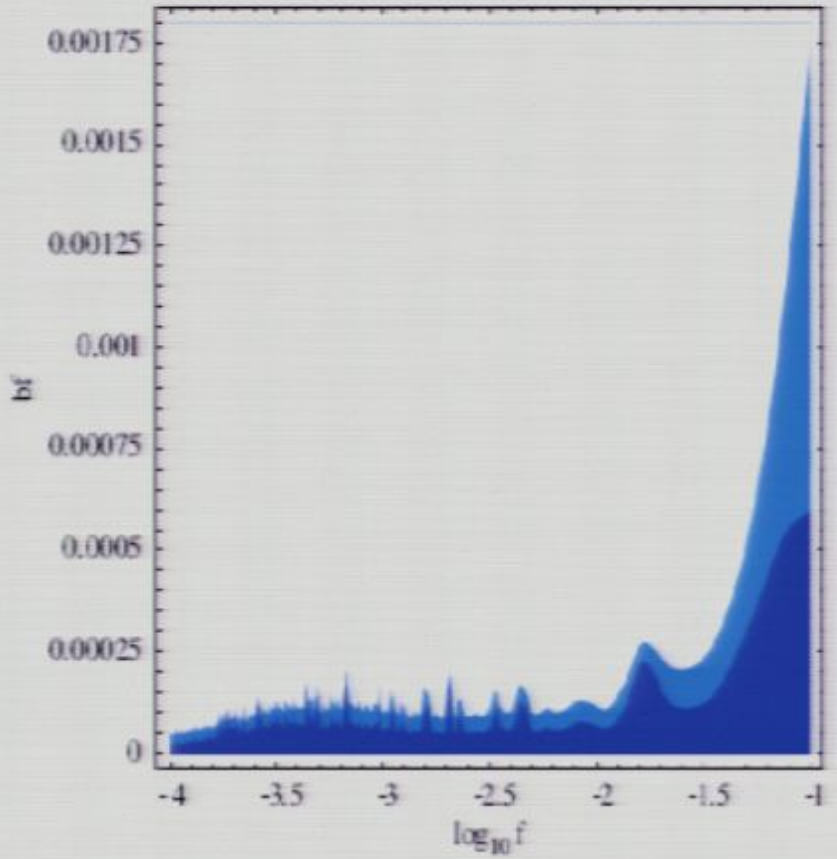

Observational constraints on the spectrum

- The best fit next to the unbinned WMAP5 data looks like

Observational constraints on the spectrum

- The best fit next to the unbinned WMAP5 data looks like

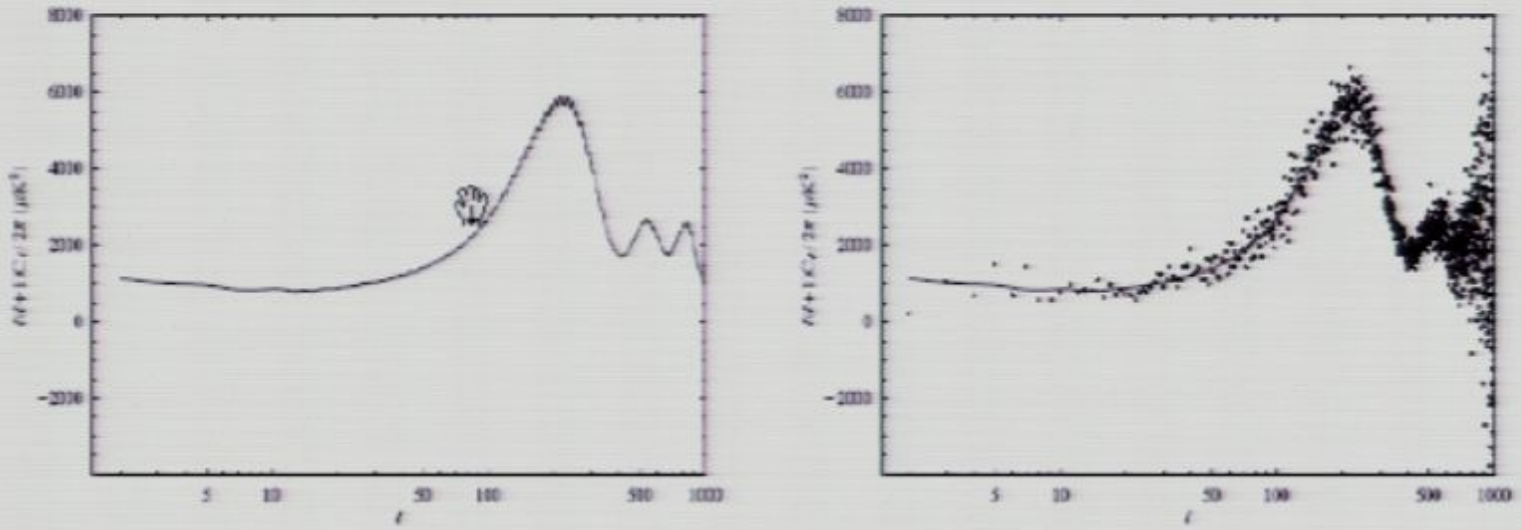

- The improvement of the fit is not statistically significant.

Observational constraints on the spectrum

- The best fit next to the unbinned WMAP5 data looks like

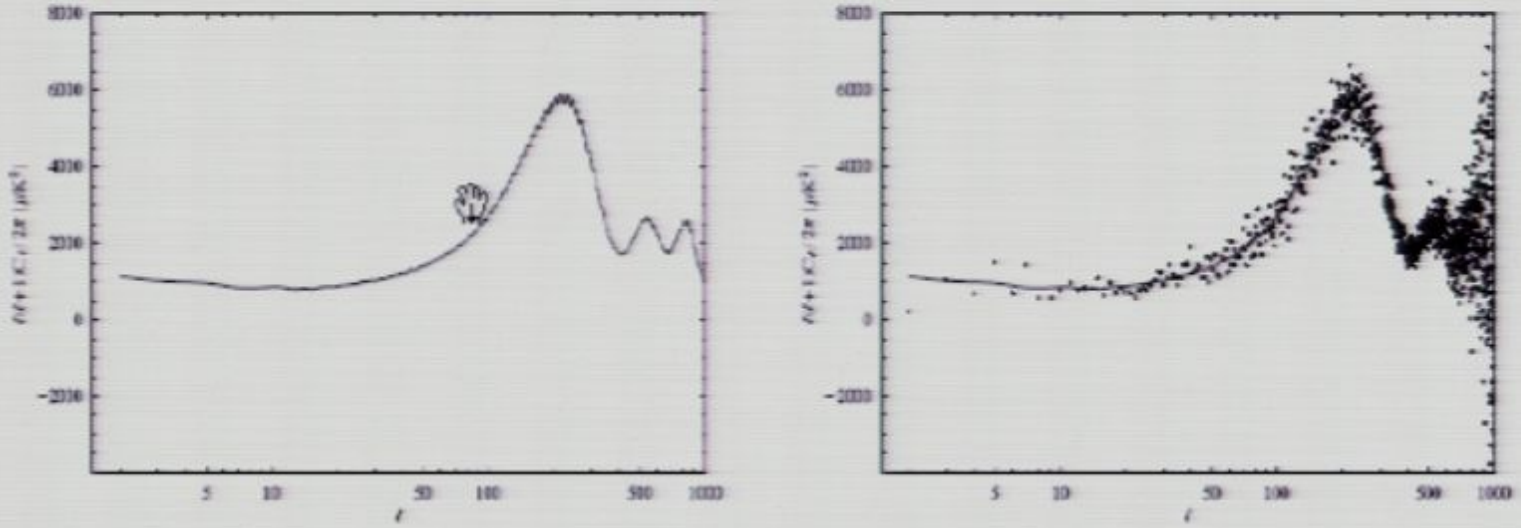

- The improvement of the fit is not statistically significant.
- The bound of WMAP5 data on the parameters of the model is roughly $fb < 10^{-4}$

Tensor modes

Our original motivation was to construc a large-field model in string theory $\Rightarrow$ detectable tensor modes

For $b = 0$ and using slow roll

$$r \simeq 0.07$$

This is within Planck sensitivity!

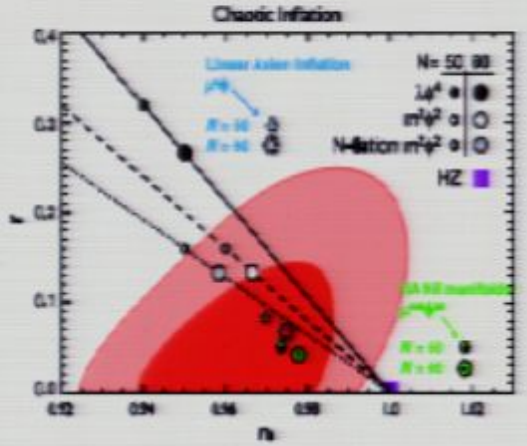

Tensor modes

Our original motivation was to construc a large-field model in string theory $\Rightarrow$ detectable tensor modes

For $b = 0$ and using slow roll

$$r \simeq 0.07$$

This is within Planck sensitivity!

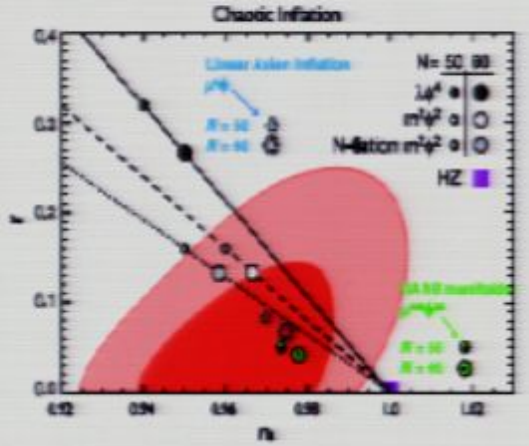

Tensor modes

Our original motivation was to construc a large-field model in string theory $\Rightarrow$ detectable tensor modes

For $b = 0$ and using slow roll

$$r \simeq 0.07$$

This is within Planck sensitivity!

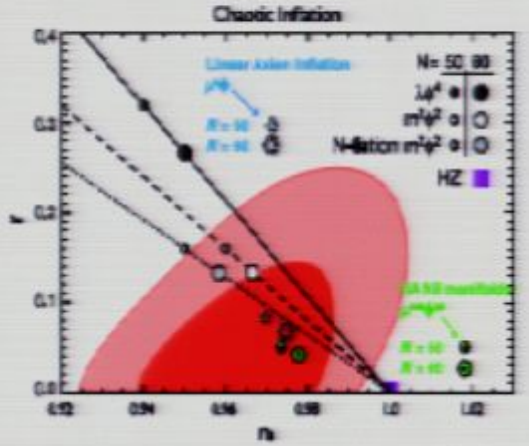

Oscillations

Oscillations in the tensor spectrum are suppressed w.r.t. those in the scalar spectrum due to a hierachy in the slow-roll parameters

$$\epsilon \sim \epsilon_0 + \epsilon_{osci} \cos(\phi/f)$$
$$\eta \sim \eta_0 + \eta_{osci} \sin(\phi/f)$$
$$\eta_{osci} \sim \epsilon_{osci}\, \phi/f$$

Outline

1. Motivations
2. The model: inflation from axion monodromy
3. Non-Gaussianity in the bispectrum
4. Summary and conclusions

Can you tell Gaussianity from non-Gaussianity?

Looking at a distribution is hard to detect small deviations from Gaussianity

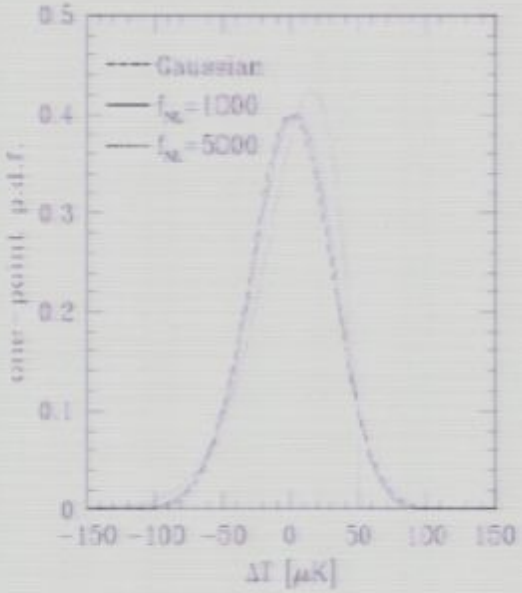

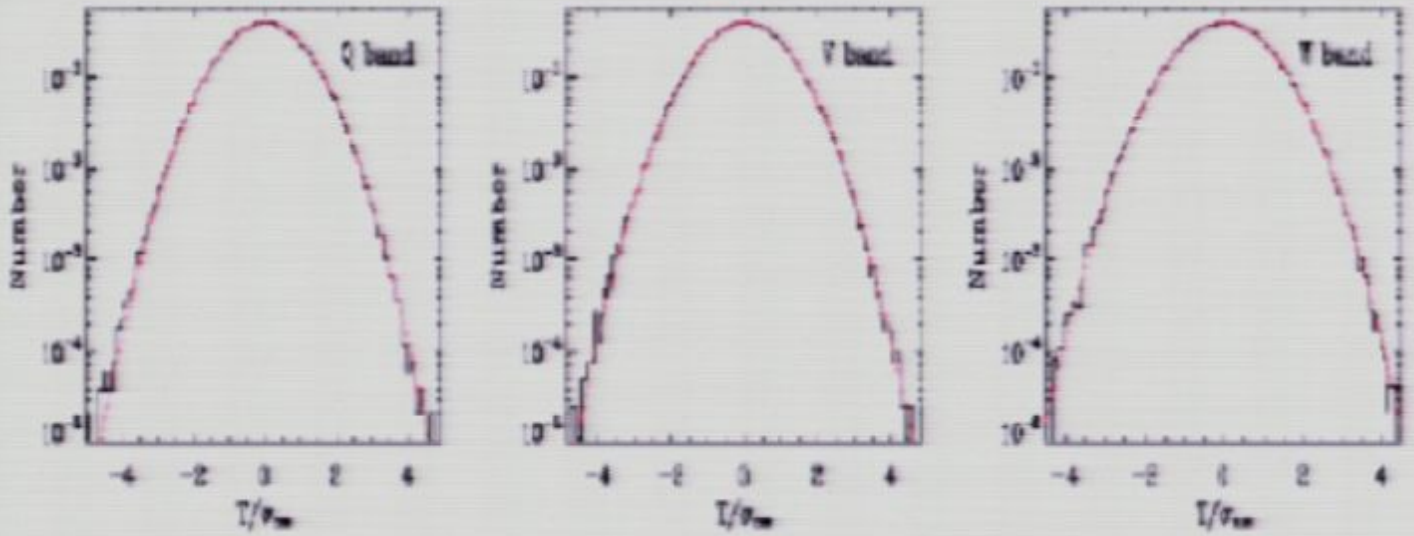

n-point functions

- For a Gaussian distributed varible ζ

$$\langle \zeta^{2n+1} \rangle = 0,$$
$$\langle \zeta^{2n} \rangle \propto \langle \zeta^2 \rangle^n$$

The three-point function $\langle \zeta^3 \rangle$, or bispectrum is the best observable to detect non-Gaussianity.

Computing the bispectrum

Primordial perturbations from inflation are computed using the in-in formalism [Maldacena 03] :

$$< \zeta_{k_1}(t)\zeta_{k_2}(t)\zeta_{k_3}(t) >= -i \int_{t_0}^{t} dt' < \left[\zeta_{k_1}(t)\zeta_{k_2}(t)\zeta_{k_3}(t), H_I(t')\right] >$$

where the intaraction Hamiltonian at order ζ^3 is obtained expanding around an inflationary solution

$$\begin{aligned} H_I &= \int a\epsilon^2\zeta\zeta'^2 + a\epsilon^2\zeta(\partial\zeta)^2 - 2\epsilon\zeta'(\partial\zeta)(\partial\chi) \\ &\quad + \frac{a}{2}\epsilon\dot{\eta}\zeta^2\zeta' + \frac{\epsilon}{2a}(\partial\zeta)(\partial\chi)(\partial^2\chi) + \frac{\epsilon}{4a}(\partial^2\zeta)(\partial\chi)^2, \\ \chi &\equiv a^2\epsilon\partial^{-2}\dot{\zeta} \end{aligned}$$

Computing the bispectrum

Primordial perturbations from inflation are computed using the in-in formalism [Maldacena 03] :

$$< \zeta_{k_1}(t)\zeta_{k_2}(t)\zeta_{k_3}(t) >= -i \int_{t_0}^{t} dt' < \left[\zeta_{k_1}(t)\zeta_{k_2}(t)\zeta_{k_3}(t), H_I(t')\right] >$$

where the intaraction Hamiltonian at order ζ^3 is obtained expanding around an inflationary solution

$$\begin{aligned} H_I &= \int a\epsilon^2\zeta\zeta'^2 + a\epsilon^2\zeta(\partial\zeta)^2 - 2\epsilon\zeta'(\partial\zeta)(\partial\chi) \\ &\quad + \frac{a}{2}\epsilon\dot{\eta}\zeta^2\zeta' + \frac{\epsilon}{2a}(\partial\zeta)(\partial\chi)(\partial^2\chi) + \frac{\epsilon}{4a}(\partial^2\zeta)(\partial\chi)^2, \\ \chi &\equiv a^2\epsilon\partial^{-2}\dot{\zeta} \end{aligned}$$

Symmetries, sizes and shapes

A priori, $\langle \zeta^3 \rangle$ depends on three momenta $\mathbf{k}_1, \mathbf{k}_2, \mathbf{k}_3$, 9 real numbers.

- Rotational invariance fixes 3 numbers (6 scalar products $\mathbf{k}_i \cdot \mathbf{k}_j$).

Symmetries, sizes and shapes

A priori, $\langle\zeta^3\rangle$ depends on three momenta $\mathbf{k}_1, \mathbf{k}_2, \mathbf{k}_3$, 9 real numbers.

- Rotational invariance fixes 3 numbers (6 scalar products $\mathbf{k}_i \cdot \mathbf{k}_j$).
- Conservation of momentum fixes 3 numbers

$$\langle\zeta^3\rangle \equiv (2\pi)^3 f_{NL} F(k_1, k_2, k_3)\delta^3(\mathbf{k}_1 + \mathbf{k}_2 + \mathbf{k}_3)$$

  $\mathbf{k}_1, \mathbf{k}_2$ and $\mathbf{k}_3$ form a triangle.
- f_{NL} gives the size and the normalized $F(k_1, k_2, k_3)$ gives the shape.

Symmetries, sizes and shapes

A priori, $\langle\zeta^3\rangle$ depends on three momenta $\mathbf{k}_1, \mathbf{k}_2, \mathbf{k}_3$, 9 real numbers.

- Rotational invariance fixes 3 numbers (6 scalar products $\mathbf{k}_i \cdot \mathbf{k}_j$).
- Conservation of momentum fixes 3 numbers

$$\langle\zeta^3\rangle \equiv (2\pi)^3 f_{NL} F(k_1, k_2, k_3)\delta^3(\mathbf{k}_1 + \mathbf{k}_2 + \mathbf{k}_3)$$

$\mathbf{k}_1, \mathbf{k}_2$ and $\mathbf{k}_3$ form a triangle.

- f_{NL} gives the size and the normalized $F(k_1, k_2, k_3)$ gives the shape.

$\langle\zeta^3\rangle$ and $F(k_1, k_2, k_3)$ depend on 3 numbers: two angles and one side.

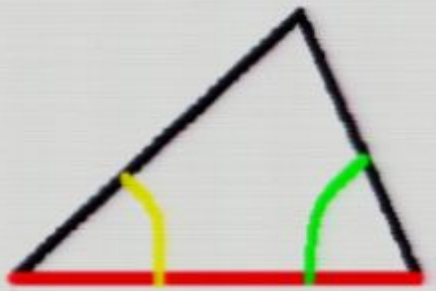

From primordial perturbations to the CMB

- The 2D temperature fluctuations decomposed in spherical harmonics

$$\frac{\Delta T}{T}(\hat{n}) = \sum_{lm} a_{lm} Y_{lm}(\hat{n}) \, .$$

From primordial perturbations to the CMB

- The 2D temperature fluctuations decomposed in spherical harmonics

$$\frac{\Delta T}{T}(\hat{n}) = \sum_{lm} a_{lm} Y_{lm}(\hat{n}) \, .$$

- The three-point correlation function of the CMB

$$\langle a_{l_1 m_1} a_{l_2 m_2} a_{l_3 m_3} \rangle \propto \int \frac{d^3\vec{k}_1}{(2\pi)^3} \frac{d^3\vec{k}_2}{(2\pi)^3} \frac{d^3\vec{k}_3}{(2\pi)^3} Y^*_{l_1 m_1}(\hat{k}_1) Y^*_{l_2 m_2}(\hat{k}_2) Y^*_{l_3 m_3}(\hat{k}_3)$$

$$\times \delta^3 \left(\sum_i \mathbf{k}_i \right) F(k_1, k_2, k_3) \Delta^T_{l_1}(k_1) \Delta^T_{l_2}(k_2) \Delta^T_{l_3}(k_3) \, .$$

From primordial perturbations to the CMB

- The 2D temperature fluctuations decomposed in spherical harmonics

$$\frac{\Delta T}{T}(\hat{n}) = \sum_{lm} a_{lm} Y_{lm}(\hat{n}) \, .$$

- The three-point correlation function of the CMB

$$\langle a_{l_1 m_1} a_{l_2 m_2} a_{l_3 m_3} \rangle \propto \int \frac{d^3\vec{k}_1}{(2\pi)^3} \frac{d^3\vec{k}_2}{(2\pi)^3} \frac{d^3\vec{k}_3}{(2\pi)^3} Y^*_{l_1 m_1}(\hat{k}_1) Y^*_{l_2 m_2}(\hat{k}_2) Y^*_{l_3 m_3}(\hat{k}_3)$$
$$\times \delta^3 \left(\sum_i \mathbf{k}_i \right) F(k_1, k_2, k_3) \Delta^T_{l_1}(k_1) \Delta^T_{l_2}(k_2) \Delta^T_{l_3}(k_3) \, .$$

- $Y_{l,m}$ and the radiation transfer function Δ^T_l oscillate fast.

From primordial perturbations to the CMB

- The 2D temperature fluctuations decomposed in spherical harmonics

$$\frac{\Delta T}{T}(\hat{n}) = \sum_{lm} a_{lm} Y_{lm}(\hat{n}) \, .$$

- The three-point correlation function of the CMB

$$\langle a_{l_1 m_1} a_{l_2 m_2} a_{l_3 m_3} \rangle \propto \int \frac{d^3\vec{k}_1}{(2\pi)^3} \frac{d^3\vec{k}_2}{(2\pi)^3} \frac{d^3\vec{k}_3}{(2\pi)^3} Y^*_{l_1 m_1}(\hat{k}_1) Y^*_{l_2 m_2}(\hat{k}_2) Y^*_{l_3 m_3}(\hat{k}_3)$$
$$\times \delta^3 \left(\sum_i \mathbf{k}_i \right) F(k_1, k_2, k_3) \Delta^T_{l_1}(k_1) \Delta^T_{l_2}(k_2) \Delta^T_{l_3}(k_3) \, .$$

- $Y_{l,m}$ and the radiation transfer function Δ^T_l oscillate fast.
- Number of operations: $l^3_{max} \sim 10^9$ integrals with 10^{10} operations each.
- 10^{19} operatons, numerically very challenging!

The cosine of shapes

How can we look for any non-Gaussian signal when even a single one requires computational superpowers? This is an open problem...

The cosine of shapes

How can we look for any non-Gaussian signal when even a single one requires computational superpowers? This is an open problem...

- If we define a scalar product between 3D shapes, we can use the cosine

$$C(F, F') \equiv \frac{F \cdot F'}{\sqrt{(F \cdot F)\,(F' \cdot F')}}$$

The cosine of shapes

How can we look for any non-Gaussian signal when even a single one requires computational superpowers? This is an open problem...

- If we define a scalar product between 3D shapes, we can use the cosine

$$C(F, F') \equiv \frac{F \cdot F'}{\sqrt{(F \cdot F)\,(F' \cdot F')}}$$

- The cosine is close to ± 1, the two shapes are similar.

The cosine of shapes

How can we look for any non-Gaussian signal when even a single one requires computational superpowers? This is an open problem...

- If we define a scalar product between 3D shapes, we can use the cosine

$$C(F, F') \equiv \frac{F \cdot F'}{\sqrt{(F \cdot F)\,(F' \cdot F')}}$$

- The cosine is close to ± 1, the two shapes are similar.
- The observational constraints on one apply to the other as well [Babich et al. 04] .

The scalar product

- Following [Fergusson & Shellard] , we chose the scalar product

$$F \cdot F' \equiv \int \frac{dk_1 dk_2 dk_3}{k_1 + k_2 + k_3} F(k_1, k_2, k_3) F'(k_1, k_2, k_3)$$

which has the same scaling as the optimal CMB estimator.

The state of the art

Ruling out the "simplest" model of inflation?

Single-field slow-roll inflation with canonical kinetic term, i.e. vanilla inflation, leads to undetectable non-Gaussianity.

The state of the art

Ruling out the "simplest" model of inflation?

Single-field slow-roll inflation with canonical kinetic term, i.e. vanilla inflation, leads to undetectable non-Gaussianity.

On the other hand, models with large non-Gaussianity (various shapes):

- non-canonical kinetic terms (e.g. DBI)
- extra light spectator fields (e.g. curvaton)
- multifields
- violations of slow roll.

Only a few shapes have been constrained by observations [WMAP7, Smith et al. 09] . They are all scale invariant.

Observational constraints

Observational constraints [WMAP7] on three different shapes:

Local	Orthogonal	Equilateral
$-10 < f^{loc} < 74$	$-410 < f^{ort} < 6$	$-214 < f^{equi} < 266$

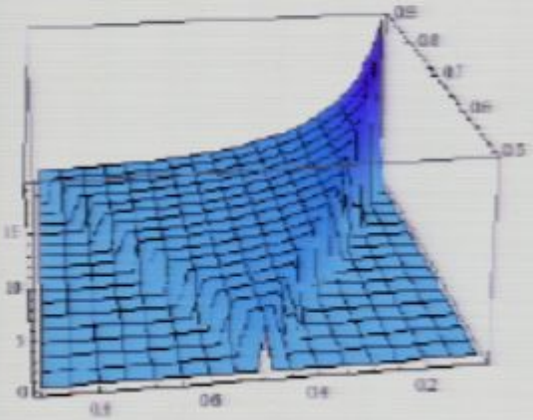

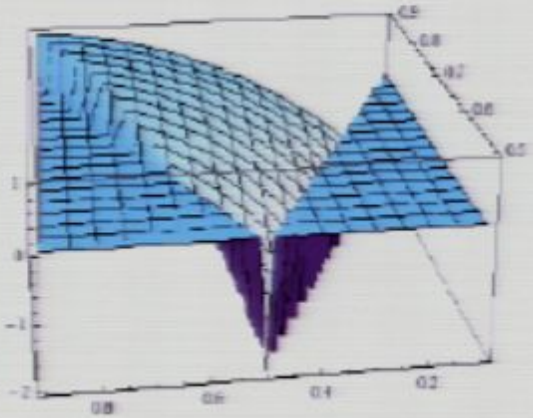

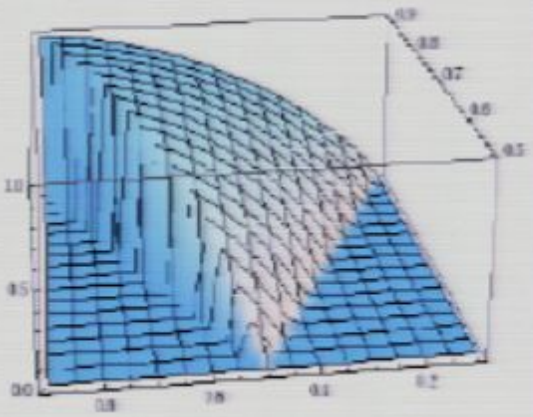

Resonant non-Gaussianity

Large non-Gaussianity from modulations

Modulations on the potential violate slow roll and can induce large non-Gaussianity.

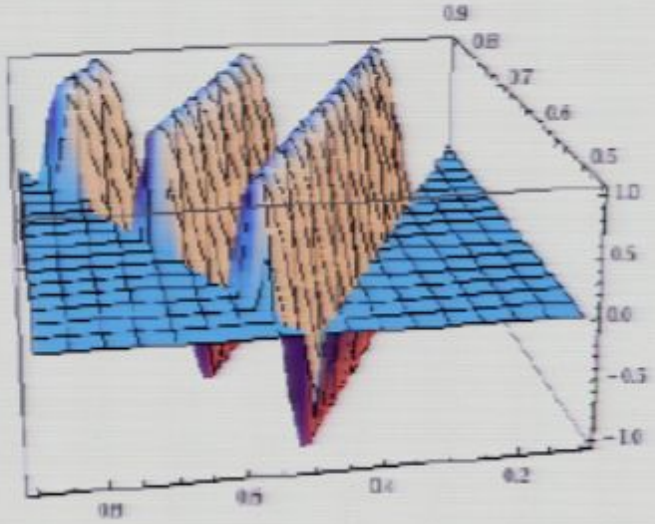

- We now present resonant non-Gaussianity.

Calculation of resonant of non-Gaussianity

Schematically [Chen et al 08, Flauger & E.P. 10]

$$\langle \zeta_{\mathbf{k}_1} \zeta_{\mathbf{k}_2} \zeta_{\mathbf{k}_3} \rangle \simeq (2\pi)^3 \delta^3(\mathbf{k}_1 + \mathbf{k}_2 + \mathbf{k}_3) \zeta_{k_1} \zeta_{k_2} \zeta_{k_3} \times \int dt' 2a^3 \epsilon \dot{\delta} \left[\zeta^*_{k_1} \zeta^*_{k_2} \dot{\zeta}^*_{k_3} + 2\, perm. \right] + c.c.,$$

$$\zeta_k \sim x^{3/2} H^{(1)}(x) \sim e^{ix}$$

$$\dot{\delta} \sim \sin\left(\frac{\log x}{f\dot{\phi}}\right)$$

Calculation of resonant of non-Gaussianity

Schematically [Chen et al 08, Flauger & E.P. 10]

$$\begin{aligned}
\langle \zeta_{\mathbf{k}_1} \zeta_{\mathbf{k}_2} \zeta_{\mathbf{k}_3} \rangle &\simeq (2\pi)^3 \delta^3(\mathbf{k}_1 + \mathbf{k}_2 + \mathbf{k}_3) \zeta_{k_1} \zeta_{k_2} \zeta_{k_3} \times \\
&\int dt' 2a^3 \epsilon \dot{\delta} \left[\zeta^*_{k_1} \zeta^*_{k_2} \dot{\zeta}^*_{k_3} + 2\, perm. \right] + c.c.\,, \\
\zeta_k &\sim x^{3/2} H^{(1)}(x) \sim e^{ix} \\
\dot{\delta} &\sim \sin\left(\frac{\log x}{f\dot{\phi}} \right)
\end{aligned}$$

The frequency of ζ_k is stretched by the expansion from M_{pl} to H when it exits the horizon.

Necessary condition

$$H < \omega < M_{pl} \quad \Rightarrow \quad f\dot{\phi} \ll M_{pl}^2 \text{ and } f \ll M_{pl}$$

where ω is the frequency of background oscillations.

Calculation of resonant of non-Gaussianity

The integral can be computed exactly. The final result is [Flauger & E.P.]

$$\langle \zeta_{\mathbf{k}_1} \zeta_{\mathbf{k}_2} \zeta_{\mathbf{k}_3} \rangle = (2\pi)^7 \Delta_\zeta^4 \frac{\delta^3(\mathbf{k}_1 + \mathbf{k}_2 + \mathbf{k}_3)}{k_1^2 k_2^2 k_3^2} f^{res} \times$$

$$\left[\sin\left(\frac{\log K/k_*}{f\phi_*} \right) + f\phi_* \sum_{i,j} \frac{k_i}{k_j} \cos\left(\frac{\log K/k_*}{f\phi_*} \right) \right],$$

$$f^{res} \equiv \frac{3\sqrt{2\pi} b}{8(f\phi_*)^{3/2}}.$$

Resonant enhancement of non-Gaussianity

- The size of the resonant non-Gaussianity is

$$f_{res} \simeq \frac{3\sqrt{2\pi}}{8} \frac{b}{(f\dot{\phi})^{3/2}}$$

Resonant enhancement of non-Gaussianity

- The size of the resonant non-Gaussianity is

$$f_{res} \simeq \frac{3\sqrt{2\pi}}{8} \frac{b}{(f\phi)^{3/2}}$$

Large resonant non-Gaussianity

The non Gaussian signal is

- Liner in b as for the spectrum

Resonant enhancement of non-Gaussianity

- The size of the resonant non-Gaussianity is

$$f_{res} \simeq \frac{3\sqrt{2\pi}}{8}\frac{b}{(f\dot{\phi})^{3/2}}$$

Large resonant non-Gaussianity

The non Gaussian signal is

- Liner in b as for the spectrum
- Fixing b, one finds $f_{res} \propto f^{-3/2}$. Remember that $\delta n_s \propto f^{1/2}$. Both spectrum and bispectrum are potential observables.
- Non-scale-invariant due to the sinusoidal oscillation. It is scale invariant if avareged over the period

Oscillations in the spectrum and bispectrum

These are the observational constraints from the spectrum together with a contour plot of f^{res} as functions of f and b.

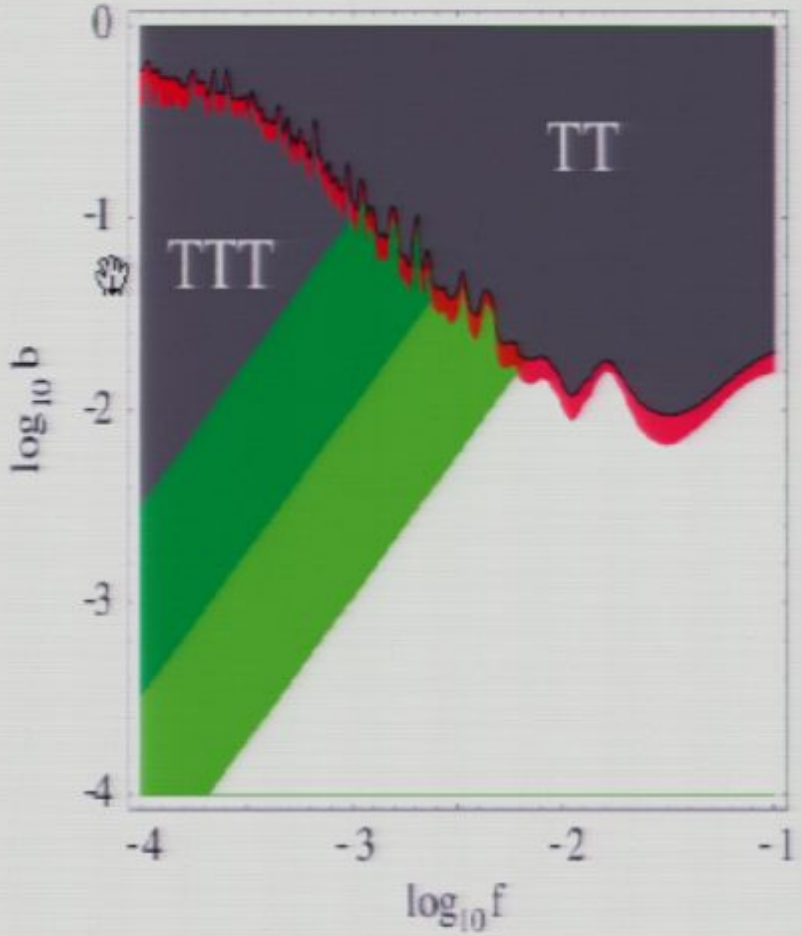

- For small f the bispectrum is the most relevant observable.

Correlation with other shapes: numerics

- Numerical computation of the cosine between resonant non-Gaussianity and local, equilateral and orthogonal shapes gives

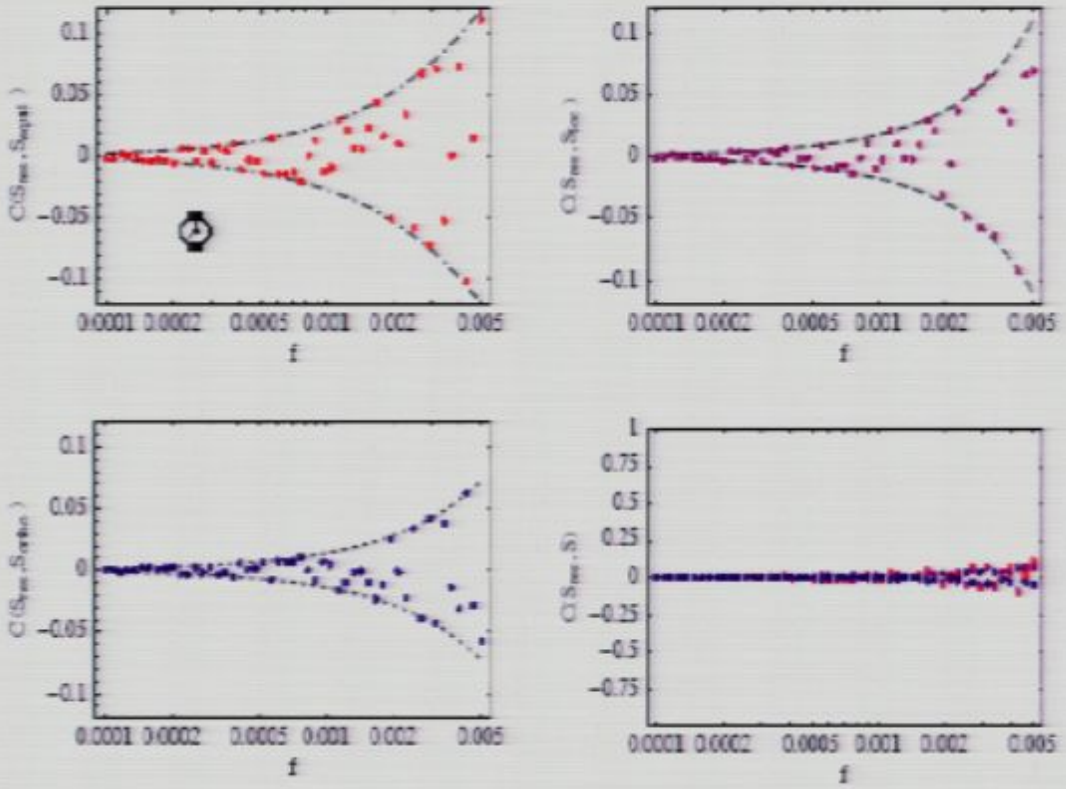

Oscillations in the spectrum and bispectrum

These are the observational constraints from the spectrum together with a contour plot of f^{res} as functions of f and b.

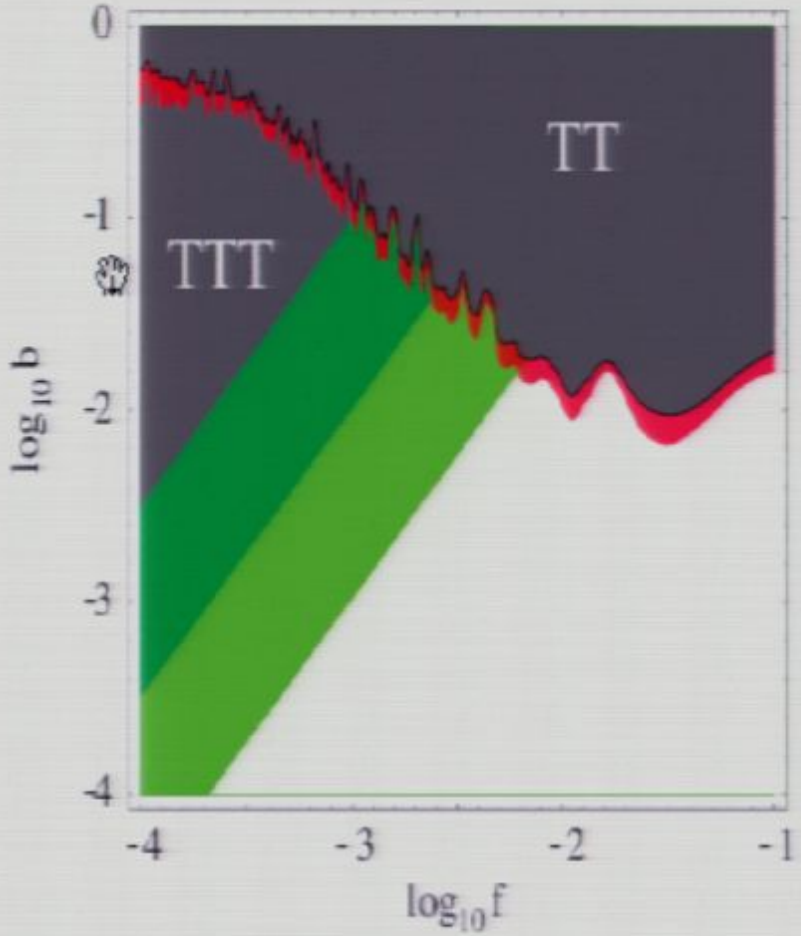

- For small f the bispectrum is the most relevant observable.

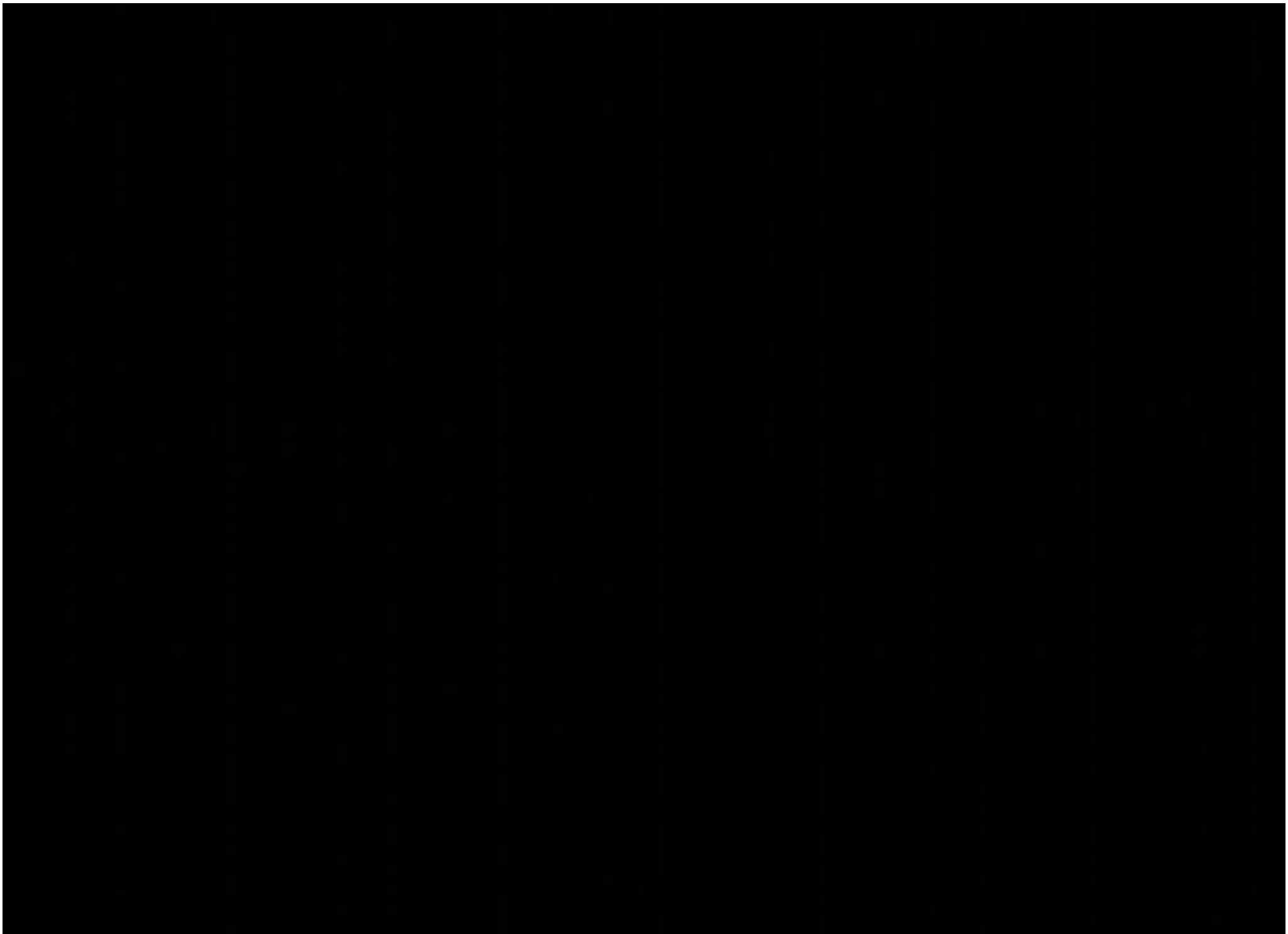

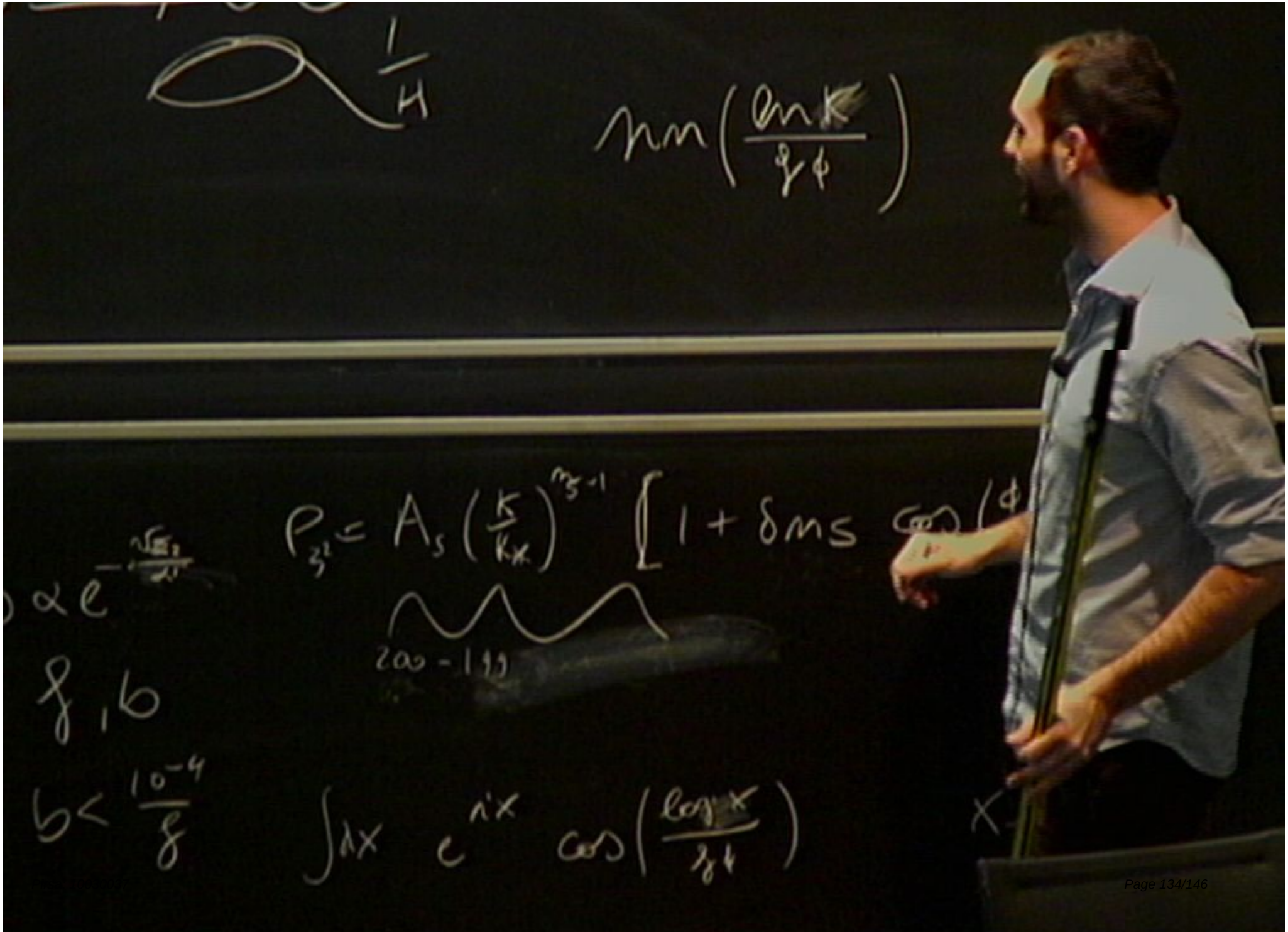
$\frac{1}{H}$
$\ln\left(\frac{\partial \ln k}{\partial \phi}\right)$
$P_{\zeta} = A_s \left(\frac{k}{k_*}\right)^{n_s - 1}$
200 - 199
$\int dx \; e^{ix} \cos\left(\frac{\log x}{\partial \phi}\right)$

Correlation with other shapes: heuristic

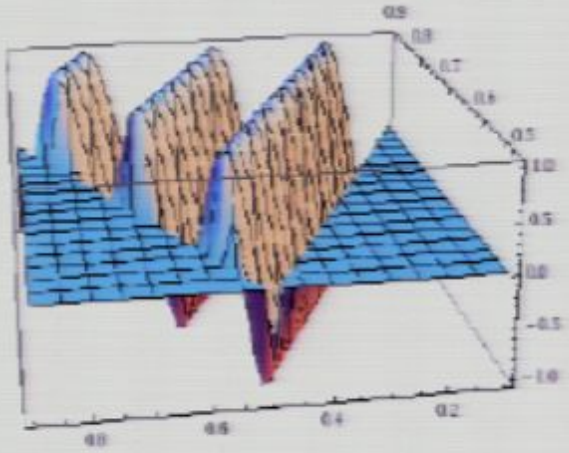

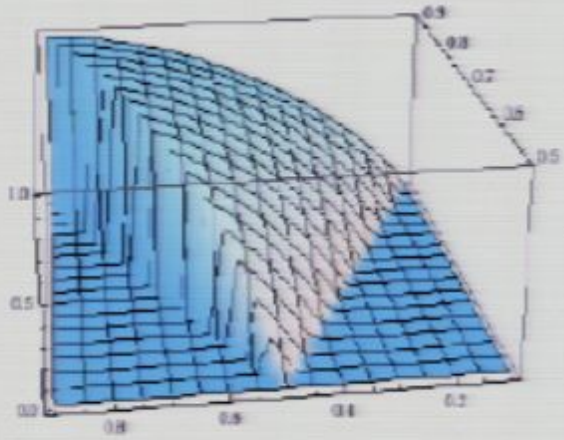

- The resonant shape oscillates as

$$F^{res}(k_1, k_2, k_3) \propto \cos\left(\frac{\log K}{f\phi}\right)$$

Outline

1. Motivations
2. The model: inflation from axion monodromy
3. Non-Gaussianity in the bispectrum
4. Summary and conclusions

Summary

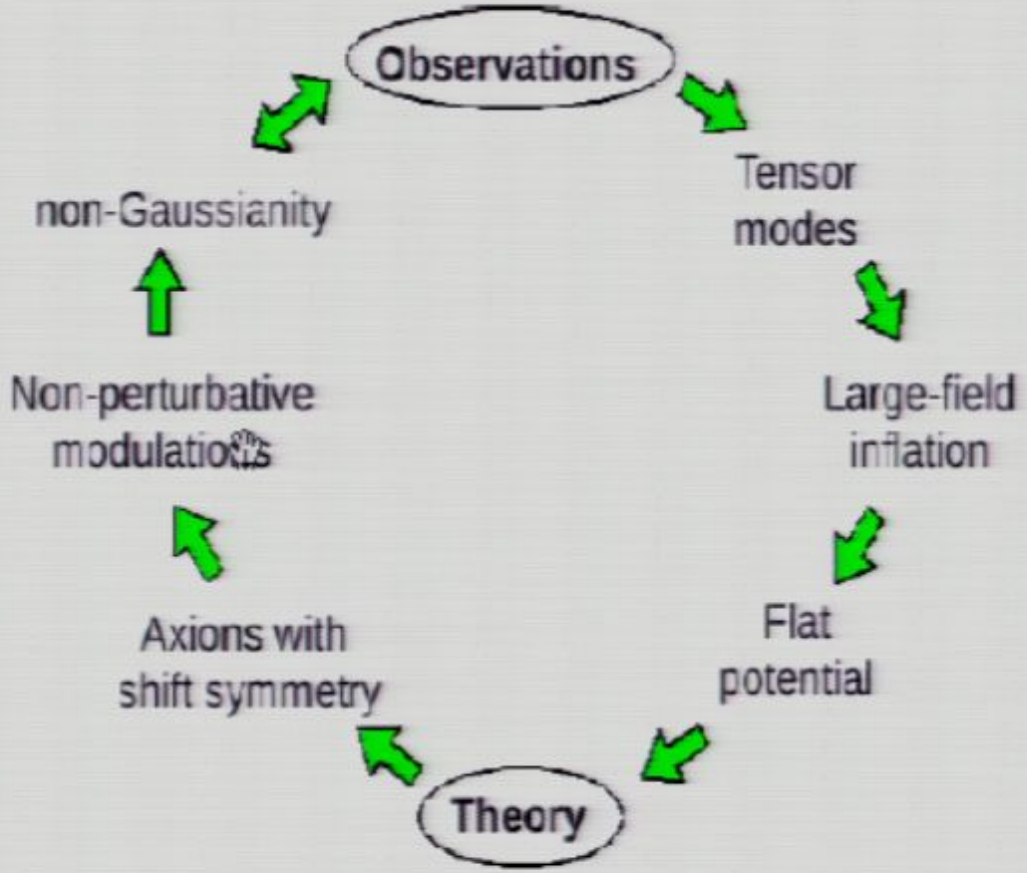
Observations
Tensor modes
Large-field inflation
Flat potential
Theory
Axions with shift symmetry
Non-perturbative modulations
non-Gaussianity

Summary

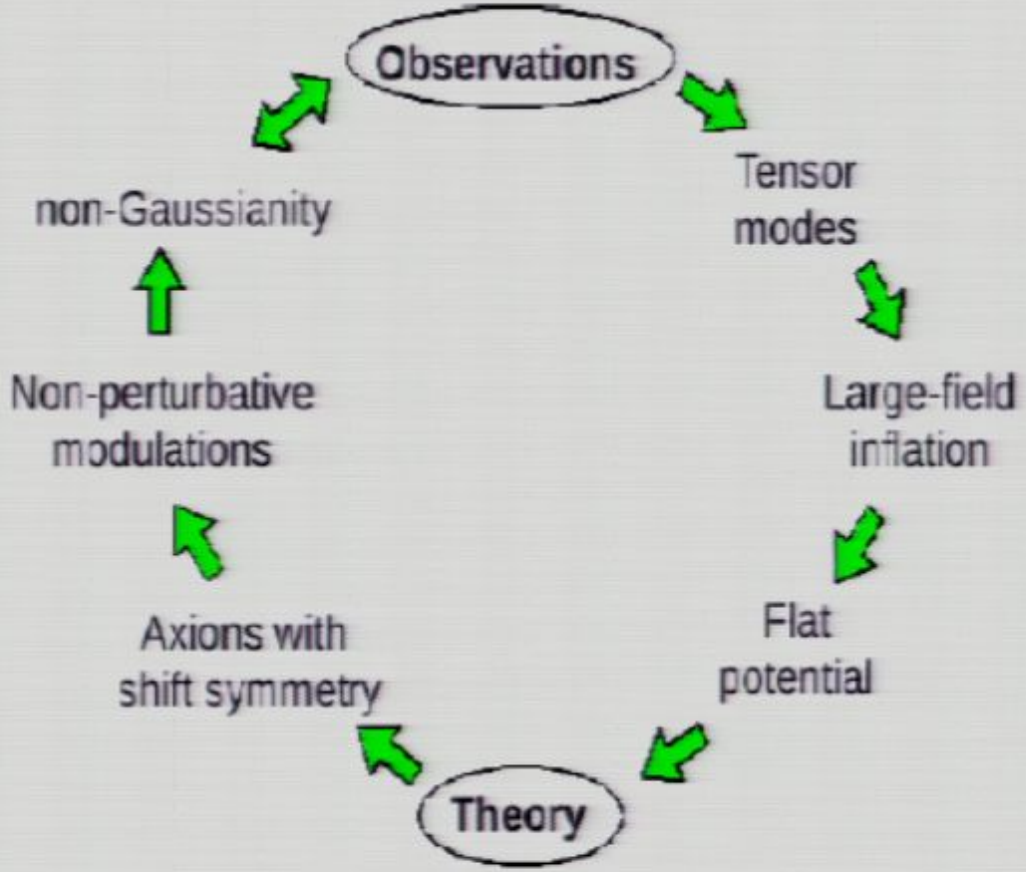
Observations
Tensor modes
Large-field inflation
Flat potential
Theory
Axions with shift symmetry
Non-perturbative modulations
non-Gaussianity


Thanks!

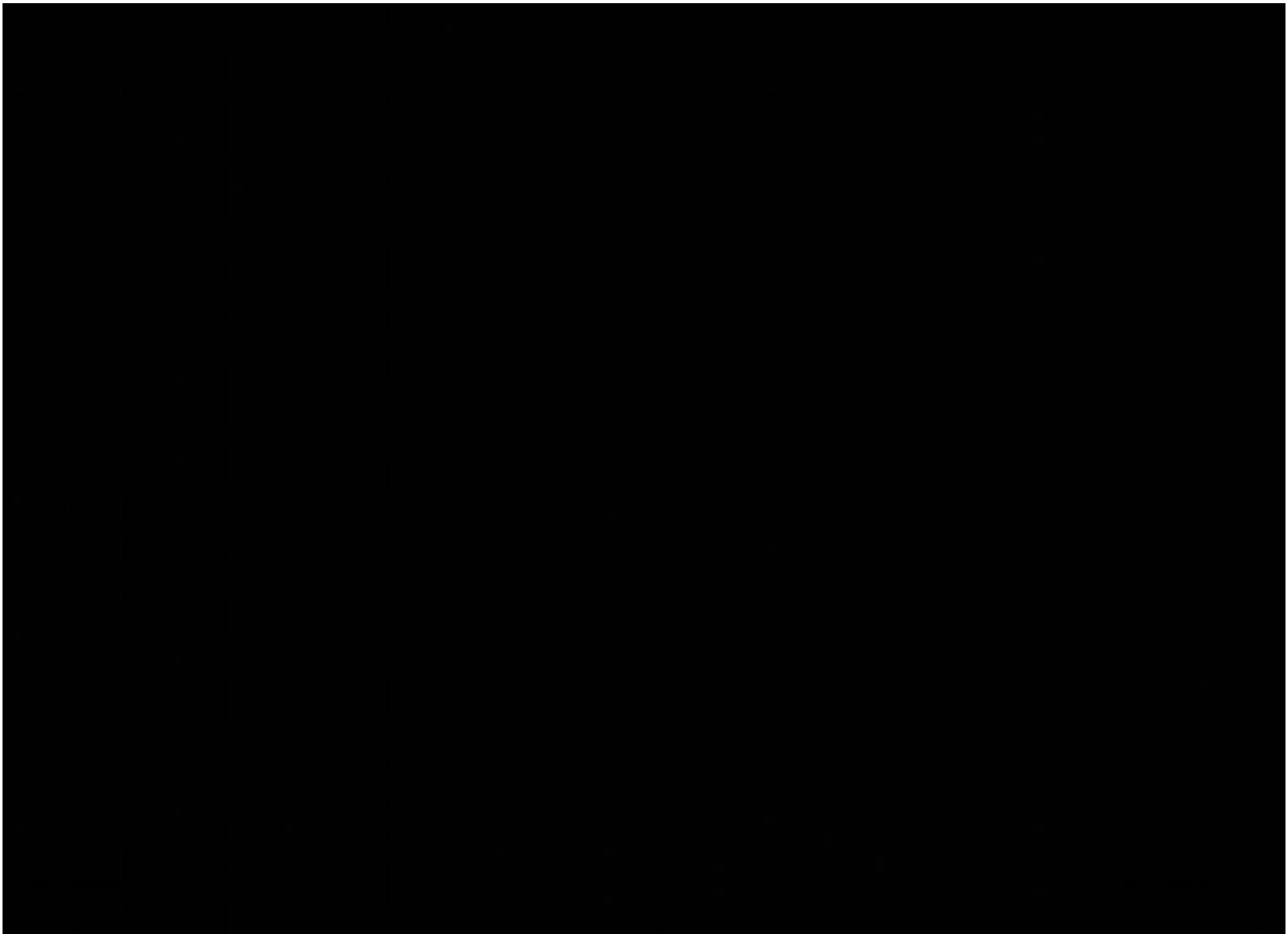

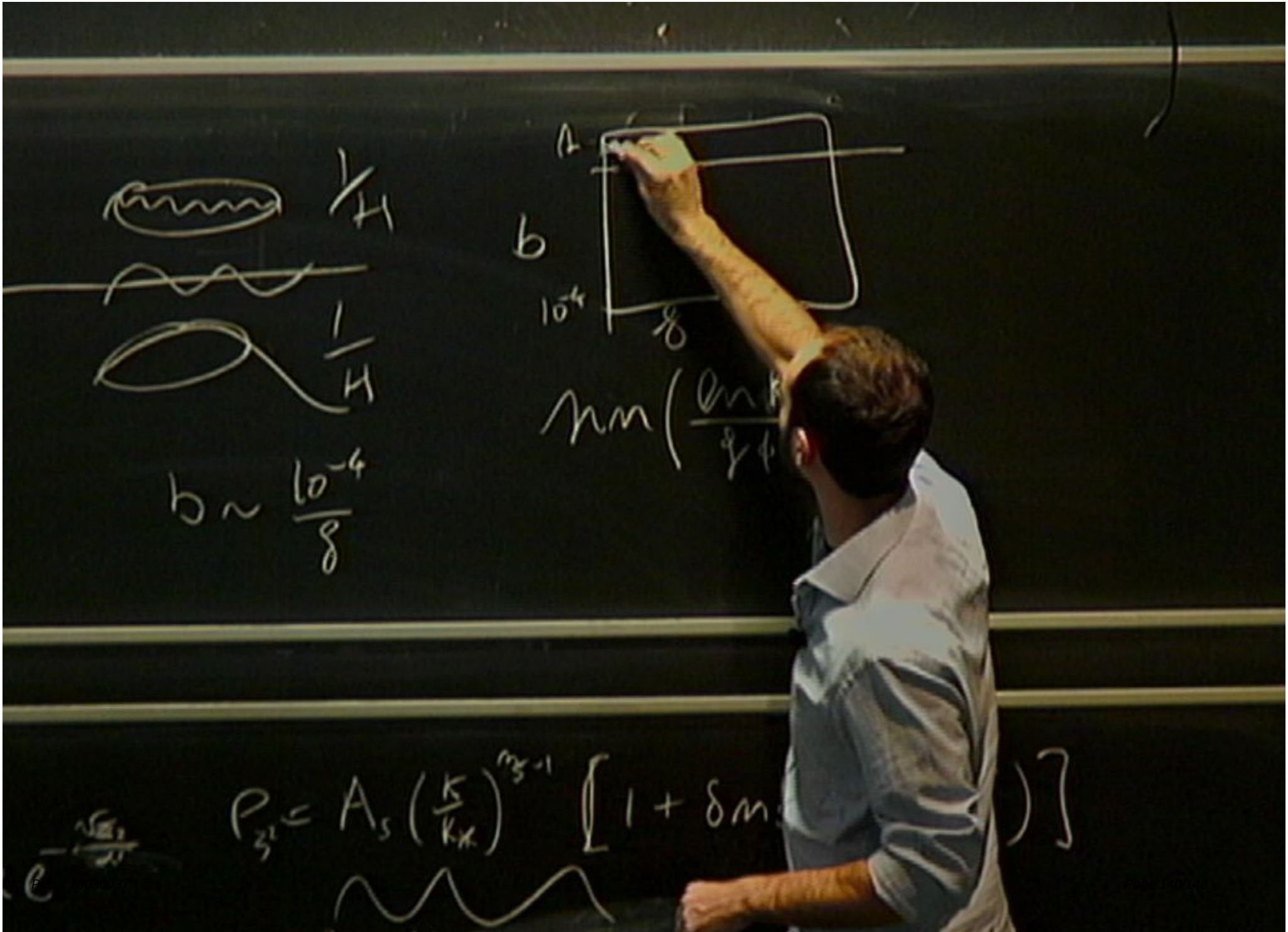
1/H
1/H
b ~ 10^-4 / 8
b
10^-4
8

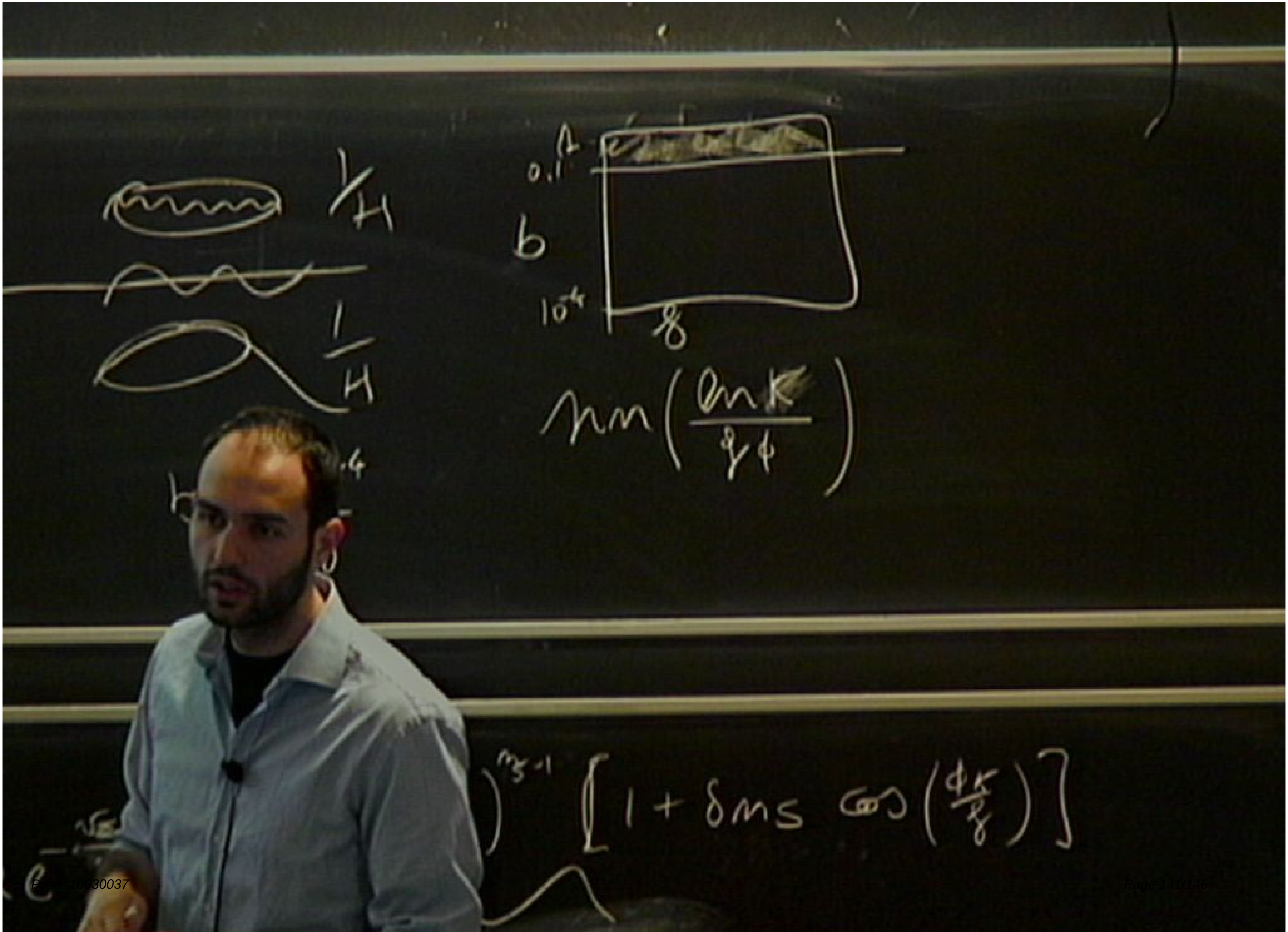

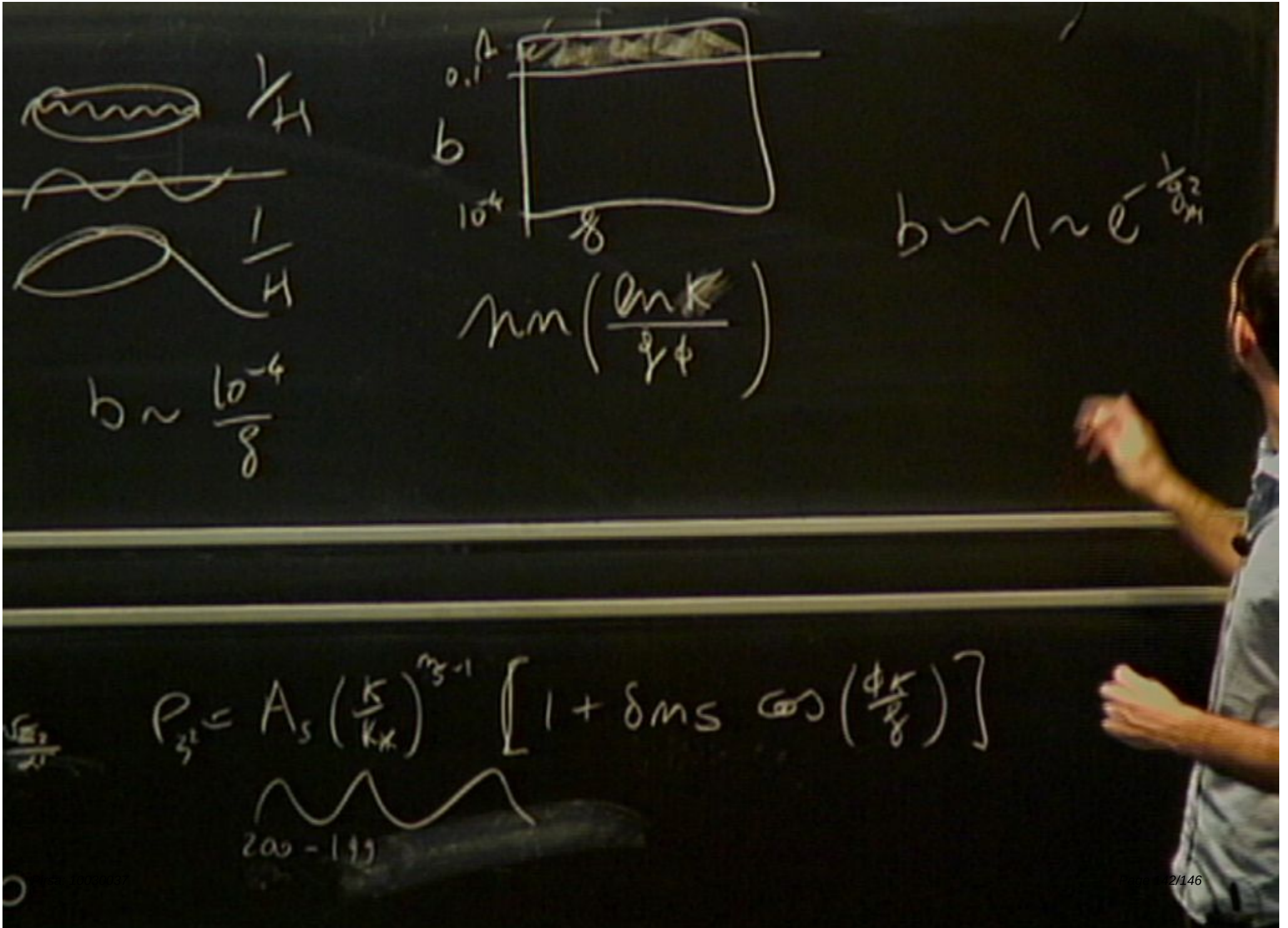
1/H
1/H
b ~ 10^-4 / δ
0.1
b
10^-4
δ
ln m (φ_m K / φ_4)
b ~ Λ ~ e^(-1/δ_H^2)
P_ζ = A_s (K/K_*)^(n_s - 1) [1 + δn_s cos(φ/δ)]
200 - 199

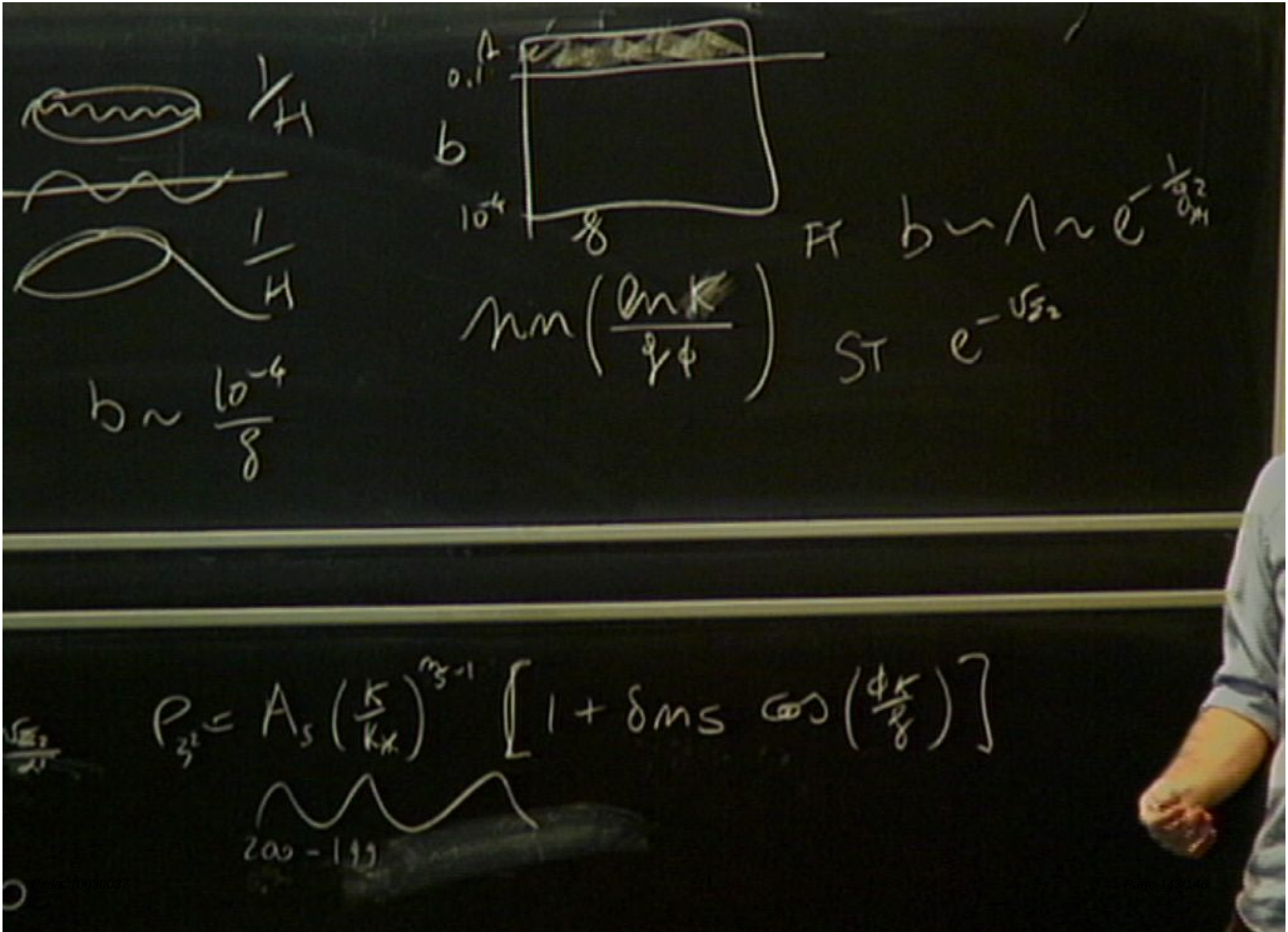
1/H
1/H
0.1
b
10^-4
g
b ~ 10^-4 / g
FT b ~ Λ ~ e^-1/g^2
ST e^-√gs
P = A_s (k/k*)^(n_s-1) [1 + δ n_s cos(φk/g)]
200 - 199

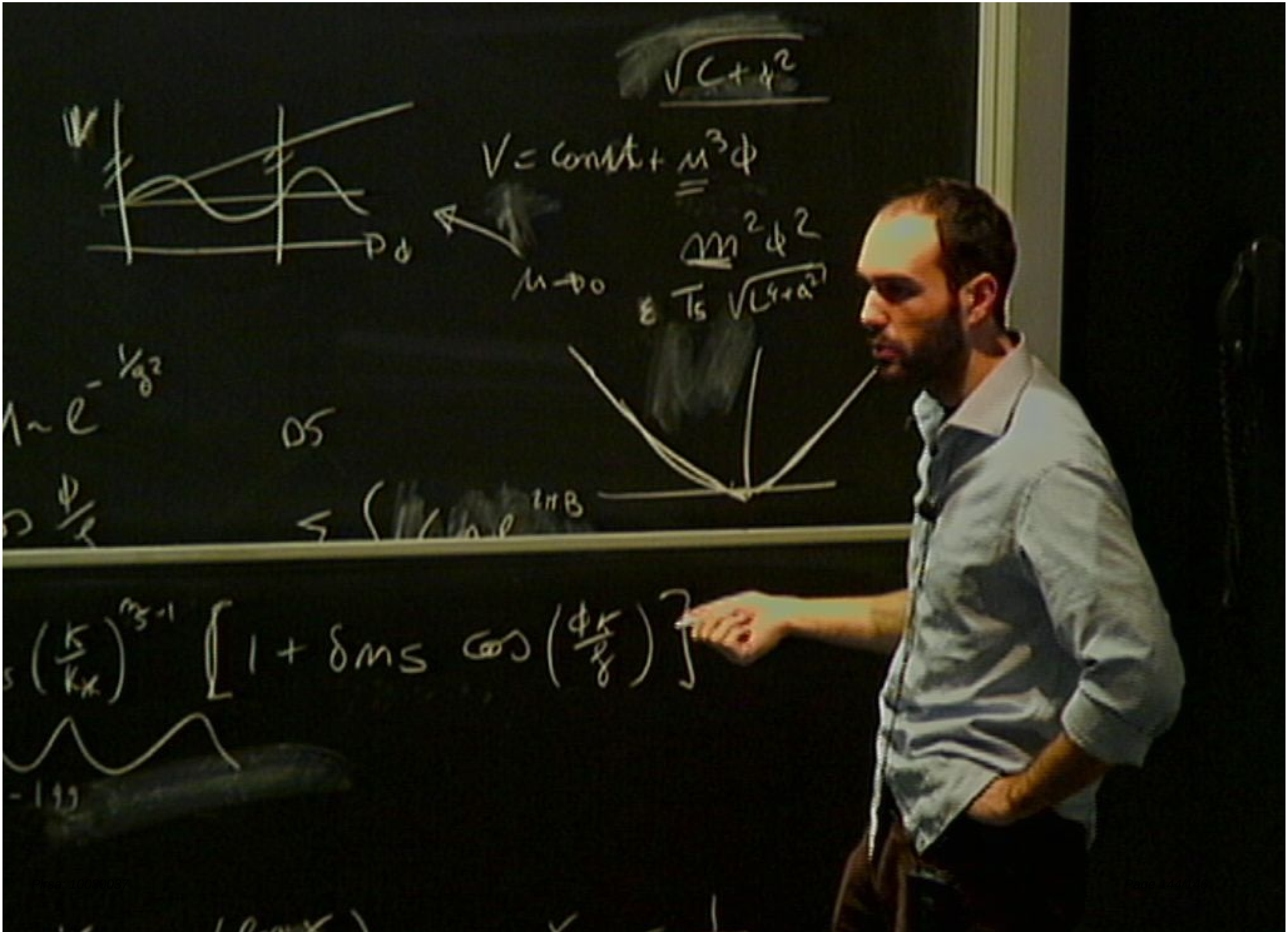
V = const + μ³φ
m²φ²
D5
1 + δms cos

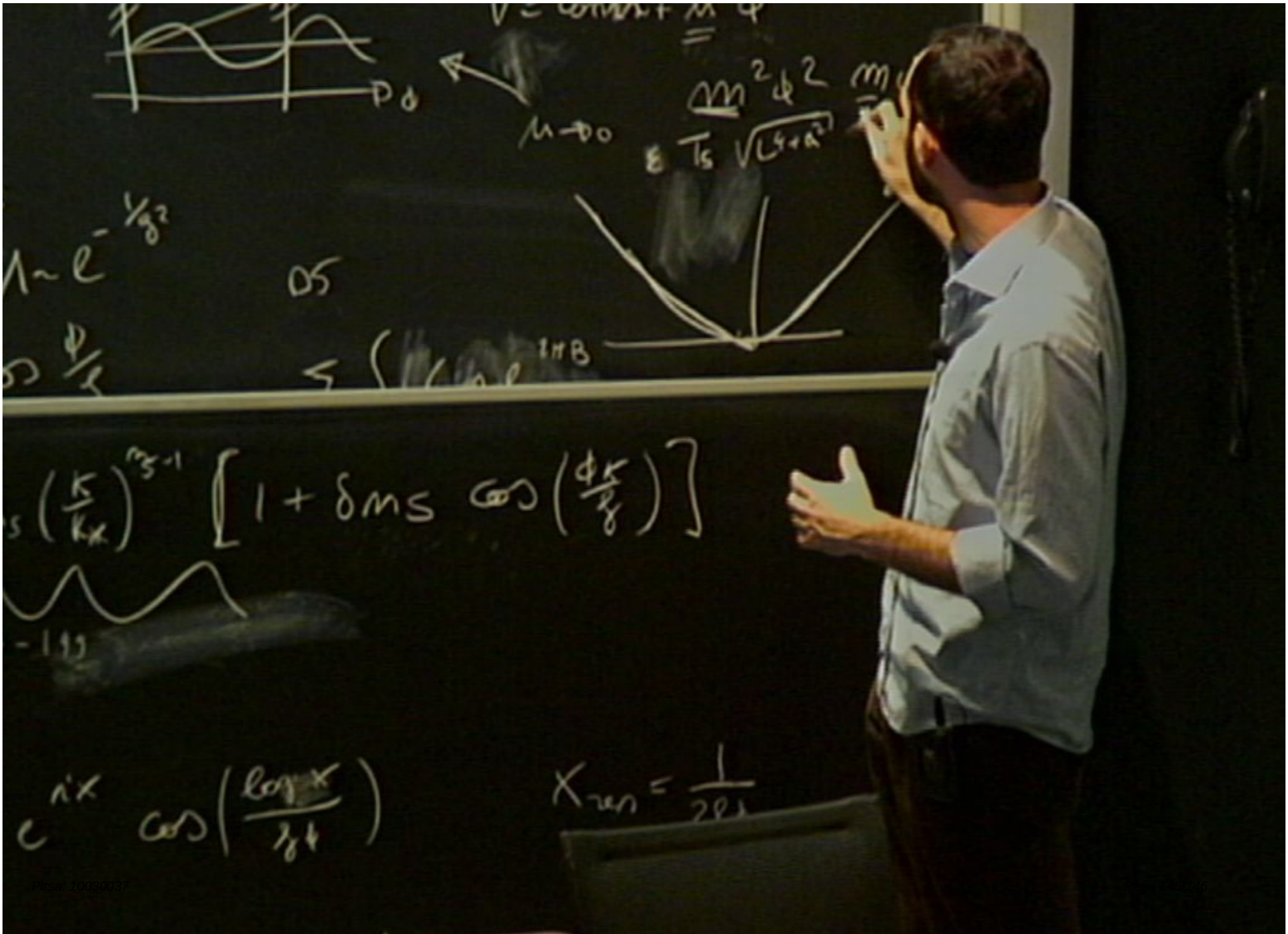

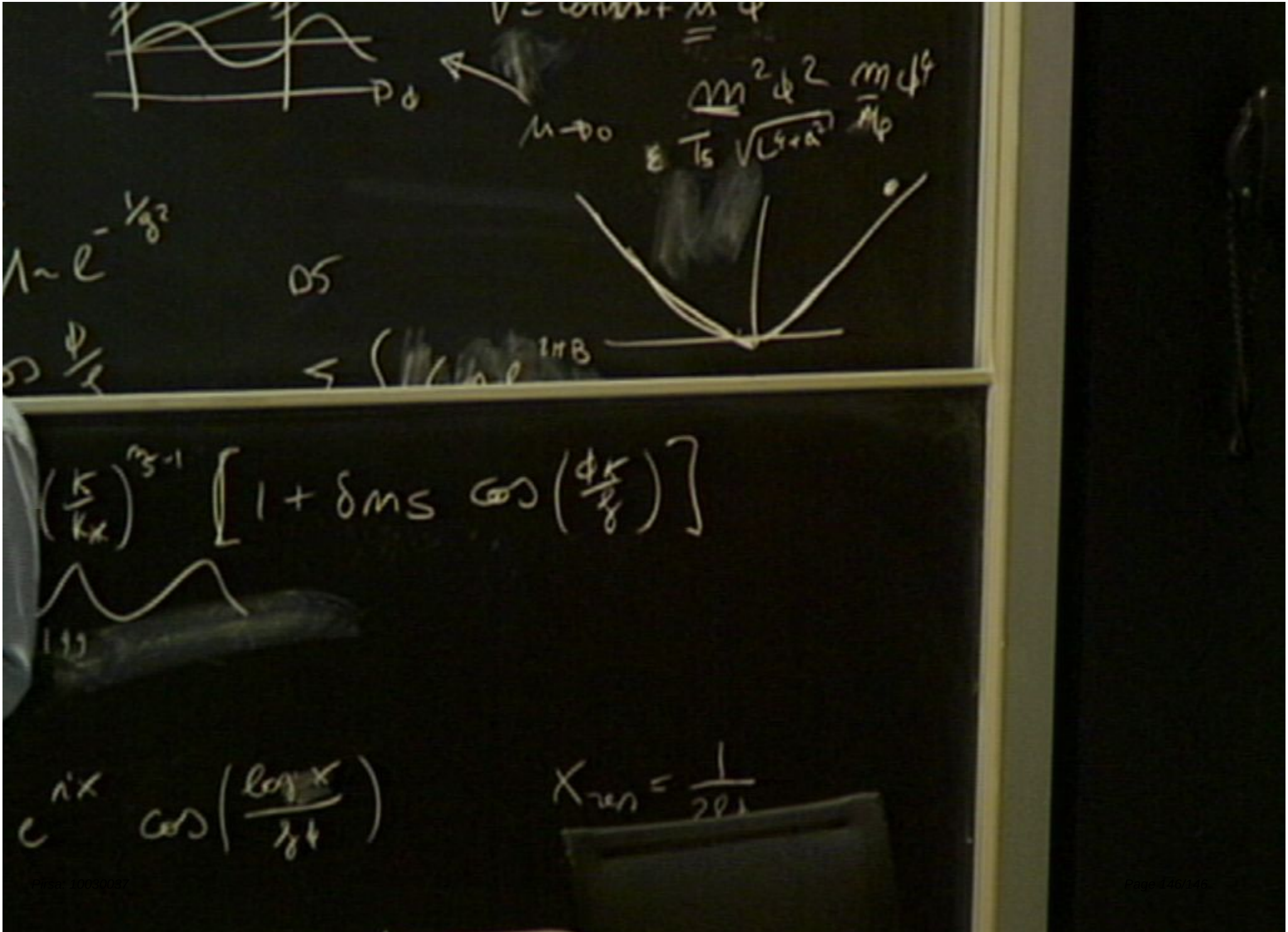
$\mu \to 0$
$\left(\frac{k}{k_{FS}}\right)^{m-1}\left[1+\delta m s \cos\left(\frac{\phi_k}{s}\right)\right]$
$e^{ikx}\cos\left(\frac{\log x}{\gamma_4}\right)$
$x_{rm} = \frac{1}{2\beta_1}$